



DISSERTATION

Thermal, acoustical, and visual performance aspects of traditional bath buildings

ausgeführt zum Zwecke der Erlangung des akademischen Grades eines
Doktors der technischen Wissenschaften

unter der Leitung von
Univ. Prof. Dipl.-Ing. Dr. techn. A. Mahdavi
E 259-3 Abteilung für Bauphysik und Bauökologie
Institut für Architekturwissenschaften

eingereicht an der
Technischen Universität Wien
Fakultät für Architektur

von
DI Kristina Orehounig

Matrikelnr. 0050007
Fasanstraße 13, 2362 Biedermannsdorf

Wien, im März 2009

Zusammenfassung

Die Stärken traditioneller Architektur basieren meist auf qualitativen Beschreibungen von verschiedenen Entwurfsplanungen und Bauelementen. Nur selten können diese mit empirischen Daten hinterlegt werden. Die hier vorliegende Arbeit ist Teil eines multidisziplinären Forschungsprojekts (Hammam 2008), mit dem Fokus auf die thermischen, akustischen und visuellen Eigenschaften einer bestimmten Klasse von traditionellen Bauten, nämlich öffentlicher islamischer Bäder - „Hammams“, - welche über mehrere Jahrhunderte ein etablierter Bautyp islamischer Bautradition war und ist (Grotzfeld 1970, Dow 1996).

Über die Dauer von einem Jahr wurden Innen- und Außen-Klimaparameter (Temperatur, rel. Luftfeuchtigkeit, Solarstrahlung, Windgeschwindigkeit und Windrichtung) für fünf dieser Bauten in Ägypten, Türkei, Marokko, Syrien und Algerien gesammelt. Weiters wurden Akustik- und Lichtmessungen in einiger dieser Gebäude ausgeführt.

Die Resultate können für eine objektive Beurteilung der aktuellen Performance dieser Gebäude verwendet werden, und geben Auskunft über deren Stärken und Schwächen. Mithilfe von Datenvisualisierung und Performanceanalyse ist es möglich die entwurfsrelevanten Parameter (wie Layout, Zonierung, Thermische Masse, Eigenschaften der Gebäudehülle, der Öffnungen und der Innenoberflächen, sowie dem Energiesystem) zu identifizieren und deren Auswirkung auf Gesundheit und Komfort zu eruieren.

Zusätzlich zur Evaluation und Interpretation von Innen- und Außenklimadaten, wurden diese zur Kalibrierung von numerischen Simulationsmodellen verwendet. Es wurden drei thermische Simulationsmodelle von Hammams in Kairo, Ankara und Constantine und akustische Simulationsmodelle von 3 Objekten in Algerien erstellt. Diese kalibrierten Modelle wurden zur Analyse und Beschreibung bestehender Trends in den Messergebnissen, wie z.B. dem kritischen Hinterfragen und stellenweise auch Falsifizieren von Heizschemas verwendet, indem simulierte und gemessene Daten miteinander verglichen wurden. Weiters können Simulationsmodelle zur Vorhersage von Konsequenzen alternativer Optionen der Renovierung, Restaurierung, Umnutzung und Adaptierung verwendet werden. Demnach konnten Performanceimplikationen eingesetzter moderner Technologien und Produkte (z.B. Thermische Isolierung und akustische Absorptionsmaterialien) im kulturellen und historisch sensiblen Kontext traditioneller Bäder kritisch hinterfragt werden, bevor sie zum Einsatz kommen.

Summary

Most appraisals of the presumed strengths of traditional buildings are typically based on qualitative descriptions of some design strategies and features. In few instances, such appraisals are based on solid empirical data. This present contribution is part of a multidisciplinary research effort (Hammam 2008), which focuses on the thermal, acoustical, and visual performance of a certain class of traditional buildings in the Mediterranean region, namely public baths "hammams", which have been, for centuries, a hallmark of Islamic architecture (Dow 1996, Grotzfeld 1970).

Over a period of one year, indoor and outdoor climate data (air temperature and relative humidity, wind speed and direction, solar irradiance) for five such buildings in Egypt, Turkey, Morocco, Syria, and Algeria have been collected. Moreover, acoustical and light measurements were performed in a number of these buildings.

The monitoring results allow for an objective assessment of the actual performance of these buildings and evaluation of their strengths and weaknesses. Using data visualization and performance analysis, it is possible to identify those design-relevant parameters (such as space layout and zonal sequence, thermal mass distribution, envelope and apertures, indoor surface properties, energy systems) that contribute to (and explain) such strengths and weaknesses in view of the related health and comfort implications.

In addition, the monitored data was also used to calibrate digital performance simulation models of a number of the objects studied. Specifically, thermal performance simulation models were generated for three buildings in Cairo, Ankara, and Constantine. Likewise, acoustical performance simulation models were generated for three baths in Algeria. These calibrated models were applied in two complementary ways. First, detailed simulation runs allowed exploring possible reasons for certain trends in measured data. For example, available heating system information (e.g. heating schedule data) could be critically examined and partially falsified based on comparison of measured and simulated data. Second and more importantly, simulation runs made it possible to predict the consequences of alternative options for the renovation, restoration, reuse, and adaptation of these buildings. Thus, performance implications of the utilization of modern technologies and products (e.g. thermal insulation and acoustical absorption materials), in the culturally and historically sensitive context of traditional bath buildings, could be carefully scrutinized before such interventions would be actually carried out.

Acknowledgments

The research presented in this dissertation was supported, in part, by a European Union grant; project: "Hamam, Aspects and Multidisciplinary Methods of Analysis for the Mediterranean Region", European Commission's 6th Framework Programme Specific Targeted Research Projects FP6-2003-INCO-MPC-2 Contract No.: 517704 (Scientific coordinator: OIKODROM, Vienna, Austria).

Parts of the text in this dissertation are adopted from papers, written in relation to the project, and co-authored with Prof. Mahdavi and project-team members.

First and foremost, I would like to thank my advisor Prof. Ardeshir Mahdavi, for his generous support and guidance throughout my thesis work. He spent much time supporting me, giving suggestions, and reviewing the results.

I would also like to thank Prof. Jan Hensen for acting as the second examiner for this thesis.

Furthermore, my thanks go to a number of past and present colleagues at the Department of Building Physics and Building Ecology, including L. Lambeva, N. Mikats, B. Kainrath, and J. Lechleitner as well as the entire Hamam project research team.

Above all I am indebted to my parents, brothers, and friends, without whose constant encouragement and support this thesis would not have been possible.

for Renate, Peter, Andreas, and Mathias

1. INTRODUCTION.....	1
1.1. Objective	1
1.2. Motivation	2
1.3. Structure	2
2. BACKGROUND.....	3
2.1. Overview	3
2.2. Historic development of hammams.....	3
2.3. Hammam Tradition	4
2.4. Typology	6
2.4.1. General	6
2.4.2. A regional view of typology	8
2.4.2.1. Baths in Egypt	8
2.4.2.2. Baths in Turkey	9
2.4.2.3. Baths in Morocco	9
2.4.2.4. Baths in Syria	9
2.4.2.5. Baths in Algeria.....	10
2.5. Construction details	11
2.5.1. Materials	11
2.5.2. Lighting	12
2.6. Technical systems and equipment	14
3. METHOD	15
3.1. Overview	15
3.2. Selected buildings.....	16
3.2.1. Overview	16
3.2.2. Hammam Bab al-Bahr, Cairo, Egypt	18
3.2.2.1. General	18
3.2.2.2. Spatial organization	19
3.2.2.3. Technical details	20
3.2.3. Hammam Şengül, Ankara, Turkey	22
3.2.3.1. General	22
3.2.3.2. Spatial organization	23
3.2.3.3. Technical details	24

3.2.4.	Hammam Saffarin, Fez, Morocco	26
3.2.4.1.	General	26
3.2.4.2.	Spatial organization	26
3.2.4.3.	Technical details	28
3.2.5.	Hammam Ammouneh, Damascus, Syria	30
3.2.5.1.	General	30
3.2.5.2.	Spatial organization	31
3.2.5.3.	Technical details	32
3.2.6.	Hammam Suq al-Ghazal, Constantine, Algeria.....	34
3.2.6.1.	General	34
3.2.6.2.	Spatial organization	34
3.2.6.3.	Technical details	37
3.3.	Measurements	38
3.3.1.	Overview	38
3.3.2.	Thermal parameters.....	38
3.3.2.1.	External parameters	38
3.3.2.2.	Internal parameters	42
3.3.3.	Acoustical parameters.....	46
3.3.4.	Visual parameters.....	47
3.4.	Data Analysis	48
3.4.1.	Overview	48
3.4.2.	Thermal analysis.....	48
3.4.2.1.	Mean monthly values.....	48
3.4.2.2.	Relative temperature	48
3.4.2.3.	Temperature range	48
3.4.2.4.	Transition between spaces.....	48
3.4.2.5.	Thermal comfort.....	48
3.4.2.6.	Cumulative temperatures	49
3.4.3.	Acoustical analysis.....	49
3.4.4.	Visual analysis.....	49
3.5.	Simulations	50
3.5.1.	Overview	50

3.5.2.	Thermal simulations	50
3.5.2.1.	The method	50
3.5.2.2.	Simulation tool	51
3.5.2.3.	Cairo model	52
3.5.2.4.	Ankara model	55
3.5.2.5.	Constantine model	58
3.5.2.6.	Parametric studies.....	61
3.5.3.	Acoustic simulation	63
3.5.3.1.	Simulation tool	63
3.5.3.2.	Simulation models.....	64
3.5.3.3.	Improvement scenarios.....	65
4.	RESULTS.....	66
4.1.	Overview	66
4.2.	Hygro-thermal Indoor Conditions	66
4.2.1.	Cairo	66
4.2.1.1.	Hourly values for reference days	66
4.2.1.2.	Relative Temperature.....	70
4.2.1.3.	Temperature distribution.....	71
4.2.1.4.	Thermal Comfort conditions	72
4.2.2.	Ankara	73
4.2.2.1.	Hourly values for reference days	73
4.2.2.2.	Relative Temperature.....	78
4.2.2.3.	Temperature distribution.....	79
4.2.2.4.	Thermal Comfort conditions	80
4.2.3.	Fez	81
4.2.3.1.	Hourly values for reference days	81
4.2.3.2.	Relative temperature	88
4.2.3.3.	Temperature distribution.....	88
4.2.3.4.	Thermal Comfort conditions	90
4.2.4.	Damascus	91
4.2.4.1.	Hourly values for reference days	91
4.2.4.2.	Relative temperature	95

4.2.4.3.	Temperature distribution.....	96
4.2.5.	Constantine	97
4.2.5.1.	Hourly values for reference days	97
4.2.5.2.	Relative temperature	100
4.2.5.3.	Temperature distribution.....	101
4.2.5.4.	Thermal Comfort conditions	102
4.3.	Room acoustics.....	103
4.4.	Illumination	105
4.5.	Simulation.....	109
4.5.1.	Reproduction of measurements	109
4.5.1.1.	Thermal Simulation model of Bab al Bahr.....	109
4.5.1.2.	Thermal Simulation model of Şengül	113
4.5.1.3.	Thermal Simulation model of Suq al Ghazal	116
4.5.1.4.	Room Acoustic Simulation models.....	118
4.5.2.	Parametric simulation studies.....	119
4.5.2.1.	Thermal improvement options	119
4.5.2.2.	Inquiry into the thermal mass effect.....	120
4.5.2.3.	Acoustical improvement possibilities.....	121
5.	DISCUSSION	123
5.1.	Overview	123
5.2.	Thermal quality	123
5.2.1.	General	123
5.2.2.	Thermal comfort	124
5.2.3.	Thermal transition.....	125
5.2.4.	Hidden thermal patterns.....	126
5.3.	Acoustics.....	127
5.4.	Visual Aspects.....	128
5.5.	Simulation.....	129
6.	CONCLUSIONS.....	131
6.1.	Contributions.....	131
6.2.	Future research	131
6.3.	Publications	132

7. REFERENCES.....	134
7.1. Literature.....	134
7.2. Tables	137
7.3. Figures	139
7.4. Equations.....	150
8. APPENDIX	151
8.1. Measurement Equipment	151
8.1.1. External.....	151
8.1.1.1. Onset weather station.....	151
8.1.1.2. Driesen and Kern weather station	151
8.1.2. Internal sensors	152
8.1.2.1. Dataloggers from Onset	152
8.1.2.2. Dataloggers from E+E	152
8.2. Further Results	153
8.2.1. Cairo	153
8.2.1.1. Hygro-thermal indoor conditions.....	153
8.2.2. Ankara	156
8.2.2.1. Hygro-thermal indoor conditions.....	156
8.2.3. Fez	161
8.2.3.1. Hygro-thermal indoor conditions.....	161
8.2.4. Constantine	166
8.2.4.1. Hygro-thermal indoor conditions.....	166

1. Introduction

1.1. Objective

The overall objective of this work is to gain a deeper knowledge about traditional Islamic bath buildings ("hammams"). This study was conducted within a larger research project (Hammam, Aspects and Multidisciplinary Methods of Analysis for the Mediterranean Region) which was supported by the European Union (Hammam 2008). A principal goal of this study is to understand and evaluate the function, the concept, the technology and the rules for the running of a Hammam.

This work focuses in particular on the thermal, acoustical, and visual performance of these buildings. Within the framework of the project five cities in the Mediterranean region have been targeted namely Cairo (Egypt), Ankara (Turkey), Fez (Morocco), Damascus (Syria), and Constantine (Algeria). In each city a particular hammam was selected for which a detailed survey was carried out. During case study visits to the selected objects measurement equipment was installed to collect external as well as internal climatic data. The essence of this approach is the long-term data collection for a period spread over one year. Moreover acoustical and light measurements were carried out.

The main focus of the work lies in analysis, visualization and interpretation of collected data. Moreover thermal and acoustical simulation models were developed for a number of objects. The application of such simulation models can deepen the understanding of the environmental performance features of traditional architecture. Moreover, such digital models can facilitate the evaluation of alternative options for the improvement, restoration, and reuse of traditional buildings.

1.2. Motivation

The principal goal of this study is to gain a deeper understanding in the specific performance features of traditional bath buildings and to contribute in the conservation of this cultural heritage objects.

Most hammams can be considered as traditional buildings, which are believed to embody numerous intelligent design features, emerged and refined through the historical process of adjustment to local climatic conditions and social functions. To tap into this potentially rich source of design knowledge, a deeper understanding of the working of such environmentally adapted buildings is necessary. Towards this end, the typically available general qualitative descriptions of the respective design strategies are insufficient. Rather, detailed performance analyses are needed that are based on high-resolution empirical performance data. In this context, the present work is expected to contribute to a better technical understanding of building performance features of traditional hammams, based on high-resolution empirical performance measurements (Mahdavi 2007).

Furthermore hammams play a special role in the Islamic region and are considered as one of the three main building types besides the mosque and the suq. Despite the importance of ritual cleansing, hammams are a central place for social life, and for relaxation. It is one of the rare meeting places for women and provide place for religious, artistic, and ceremonial activities. However, the Islamic bathing tradition and hammams as an institution has been in decline since the 19th century, particularly with the process of urban development and the introduction of private bathrooms (Sibley 2006, Dow 1996). With the disappearance of Hammams, Islamic cities are about to lose a major feature of their cultural heritage with deteriorating consequences on the urbanistic, societal and architectural qualities.

1.3. Structure

This dissertation is structured in terms of eight sections. Section 2 provides general information regarding the tradition of hammam and the related typology. Section 3 describes the methodology underlying the dissertation. Section 4 includes the main results of the work, including the hygro-thermal, visual, and acoustical measurements, as well as the calibration and application of thermal and acoustical simulation models. Section 5 entails the discussion of the results and section 6 includes the conclusions.

2. Background

2.1. Overview

One of the first publications where Islamic bath buildings were mentioned was made by Alois Musil in the year 1907 (Musil 1907). His study focuses at the Ummayyad palaces and there hammams in the Syrian desert. Later in the 1930s Edmund Pauty authored the book "Les Hammams du Caire" which centers on the Architecture of Egyptian Hammams (Pauty 1933). Claude Ecochard and Michel Le Coeur studied the baths of Damascus and wrote the book "Les Bains de Damas" (Écochard and Le Coeur 1942). In 1970 the German book "Das Bad im arabisch-islamischen Mittelalter" was published by Heinz Grotzfeld, which offers a detailed survey about architectural details and the social history of Islamic bath buildings in medieval times (Grotzfeld 1970). A summary about bath buildings in Orient and Occident from the Antiquity till the late Barock period "Bäder und Badekultur in Orient und Okzident" was carried out by Ulrika Kiby in the year 1995 (Kiby 1995). The book "The Islamic Baths of Palestine" published by Martin Dow in the year 1996, offers a detailed description of hammams in Palestine (Dow 1996). Finally, several publications have been carried out with the EU-funded research project "Hammam, Aspects and Multidisciplinary Methods of Analysis for the Mediterranean Region" (Hammam 2008) in the years 2006 to 2008.

2.2. Historic development of hammams

Public bath buildings have already existed since the Hellenistic period and flourished during the Roman and Byzantine Empire (Sibley 2006, Dow 1996). The development of the Islamic bathing tradition started a few decades after the founding of the Islamic religion and still exists in the Mediterranean region. It is remarkable that the Hammam tradition remained almost unchanged during centuries, although it varies much from region to region.

The early Islamic hammams or steam baths, of which we know, are found in the Umayyad palaces in the Syrian and Jordanian desert (Sibley 2006). Qusair 'Amra (711-715 ac), a hunting lodge is one of the earliest historical building with a steam bath (Kiby 1995). Later on the tradition of bathing was established also in urban environment and spread out through the

Middle East. During the Arabic medieval times a main part of private and public life took place in hammams which were considered as one of the main building types in Islamic cities next to the mosque and the suq. Most of the hammams were built by private hand. Building a bath was considered a good deed appreciated by god and people.

Starting with the 12th century the hammam tradition flourished in the area of Damascus. The respective bath type remained unchanged till 15th century. In 17th century the room sequence changed slightly. In Cairo the Islamic bathing tradition started to develop in 8th and 9th century. Because of the small size of the hammams at this time, literature refers to them as "mouse baths" (Grotzfeld 1970). With the 13th century, the current Egyptian bath type started to develop. In 11th century, the Islamic bathing tradition was also brought to Spain, Morocco, Algeria, and Tunisia. The Anatolian bathing tradition started to develop in 11th century when Turkish people came to Asia and converted to Islam. Compared to the Arabic bath-type, the Turkish bathing tradition is very different.

However, the Islamic bathing tradition and hammams as an institution have been in decline since the 19th century, particularly with the process of urban development and the introduction of private bathrooms (Sibley 2006, 2).

2.3. Hammam Tradition

Ritual cleansing is very important in the Islamic religion, therefore culture and history was a major factor in the hammam development. In addition to ritual cleansing, hammams are also used for relaxation, before a wedding, after a journey or illness, and after a birth (Grotzfeld 1970). In the Islamic culture bathing in running water is obligatory. This is one of the main differences to the Roman bathing tradition. Grotzfeld writes in the book "Das Bad im arabisch-islamischen Mittelalter" that the four stages or rooms represent the four seasons and have a healing effect on the body (Grotzfeld 1970).

The typical hammam activity pattern includes 4 stages (Shehayeb 2006):

The **first stage** after entering the hammam is undressing. This occurs usually in the cool and dry area (changing room, mashlah or frigidarium). Women use in winter sometimes the more intermediate zones for undressing.

In the **second stage**, clients go usually wrapped in towels with slippers to the bait al-harara or caldarium where a three step process takes place including a steam bath, a scrub, and a shower or washing. Clients stay usually from 45 minutes up to 2 hours in this stage. This hot and humid zone consists of a central area where usually the scrubbing occurs, a

steam area which is either a hot steam bath as in Egypt the "maghtas" or a hot room with the hot water reservoir. The washing-facilities or showers are usually situated in small separate areas or chambers next to the central room. For the scrubbing, clients can use the service of a hammam employee which takes about 10 minutes followed sometimes by a short massage. For the last step, the washing, different habits have been developed. Small wash basins which are located at the walls of the hot area are common in Syria, Egypt and Turkey. Figure 1 shows this basin along the walls of the hot room of Hammam Ammouneh, Damascus, Syria. In some hammams showers have been installed recently. In the North African Islamic countries a bucket system is used where clients get their hot and cold water from the water reservoirs in buckets for washing.



Figure 1 Basins in hot room of Hammam Ammouneh



Figure 2 Bucket system in Hammam Saffarin (HAMMAM 2007c)

The main function of the third stage is to give body time for thermal transition between the hot wet zone and the cold and dry zone. This takes

place in the intermediate zone historically called the tepidarium. Associated activities may differ from hammam to hammam and from client to client. Women often use this stage for dressing up, talking, eating or waiting for friends to return from the bait al-harara. Men use this area after using the hot and steam area.

Stage four usually occurs in the changing room and involves getting dressed, resting, packing, paying, and allowing the body for adaptation. Further activities may differ by gender and involve eating and drinking tea or coffee. Clients either bring their own food from home or order in the hammam food from close by places. Women related activities include mainly beauty related activities. Men sometimes also use the mashlah for sleeping.

2.4. Typology

2.4.1. General

The early Islamic hammams of which we know consisted of a relatively large changing room and three successive bathing chambers, the latter two of which were heated. The designated room sequence was derived from the roman baths consisting of the apodyterium (changing room), the frigidarium (room with cold water pool), the tepidarium (room with warm water pool), the caldarium (room with hot water pool), and the sudatorium (sweating room).

The original type from the Umayyad period is not known, since most of the hammams have changed their layout. Starting with the Ayyubid period, a typical bath (for example Hammam el-Bzuriye 1154-1171) included the following rooms:

The first room after entering the hammam is the **changing room** "mashlah". It is usually the largest room and is used as a changing room mainly in summer time. People spend most of the time during their hammam visit in this room. It has various functions including changing clothes, relaxing, sleeping, chatting, drinking tea or eating. The mashlah has usually a quadratic floor plan covered with a high dome, and 4 adjacent iwans on each side, which add up to a cruciform layout. It is equipped with "mastabas" i.e., raised platforms made of stone or wood. The floor of the mastabas is covered with carpets or mats and along the walls benches made of wood or stone are situated. In the middle of the room is a stone basin located, which usually holds a fountain in the centre (see Figure 3). This fountain is the reason why it is said that the mashlah was derived from the Romans frigidarium and not from the apodyterium (Grotzfeld 1970). The floor is mostly made of marble - depending on the

location - in white, yellow, red or black color. In some hammams also the staircase to the terrace is located in the mashlah.



Figure 3 Mashlah, fountain in Hammam Fairouzi

The second room namely "Al-bait al awwal" or **cold room** is usually unheated, but due to the vicinity to the hot room this room holds a moderate temperature. In winter times when temperatures are low it is also used as a changing room. It consists usually of a slightly bigger main room and small adjacent rooms all covered by pierced domes. One of the side rooms was usually used for depilation. Sometimes water basins with a fountain either in the center of the room or next the wall are found in the cold room.

The third room is called "Al-bait al wastani" or **warm room**. It has either a quadratic or octagonal floor plan covered with a pierced dome and is enclosed by extensions, called iwans, equipped with small wash basins at the walls. In addition you can usually find adjoining rooms "maqasir" next to the main room, which are covered by two domes. Initially referred to as the main hot room, it gradually lost its importance and disappeared in some areas totally.

The last room is called the "Al-bait al harara" or **hot room**, which is covered by a mulden-dome. Adjacent to this room is the main hot water basin located which is the reason why the climate is hot and humid. Figure 4 shows the entrance to the hot water basin in a Hammam. In some areas it is also equipped with small water basins along the walls (Grotzfeld 1970).



Figure 4 Hot room of a hammam in Isfahan, Iran

Main difference between the Umayyad and Ayyubid periods is the change from harara to wastani as the main room. In 14th century, bait al harara became more important, the awwal acted than more as a transition space. In the 16th and 17th centuries wastani gradually lost its importance whereas bait al-harara became more and more important. During renovations some old bath houses were adapted in accordance with the prevailing tradition at that time (Grotzfeld 1970).

2.4.2. A regional view of typology

The following section provides a short overview regarding the hammam tradition and regional typology in the five countries which have been targeted within the study.

2.4.2.1. Baths in Egypt

The number of working hammams in Cairo has drastically declined, as in most African or Middle-east countries. Usually three main spaces can be found in Egyptian baths, the "maslakh" as the main changing room, the bait al-awwal, and the bait al-harara. The central room from the bait al-harara is usually surrounded by three to four iwans and two additional smaller rooms, from which one is called "maghtas". This elevated room holds an inserted hot water plunge pool. It became popular during the Mamluke period and can only be found in the Egyptian region. A further feature of Egyptian hammams is the additional function of the furnace for cooking "ful", a traditional Egyptian dish made of fava beans (HAMMAM 2006g).

2.4.2.2. Baths in Turkey

The Anatolian bathing tradition started to develop in 11th century when Turkish groups came to Asia and converted to Islam. Most of the Ottoman hammams are carried out as double baths or twin baths, which are usually rather large. Whereas the male entrance is usually decorated, the female entrance is more hidden (located in a side street). The changing room "sogukluk" is equipped with wooden cabins for more private undressing possibility than in other countries. Since the 16th or 17th century the Turkish baths offer, similar to the Egyptian baths, just two bathing spaces. The hot room has usually an octagonal floor plan with several iwans.

2.4.2.3. Baths in Morocco

"It was estimated that ninety-three hammams existed in Fez during the Almohades period in the 12th century. In the year 2000, 30 hammams were still operating" (Sibley 2006, 2). Hammams are usually well embedded in the urban fabric and are located in close proximity to the underground river channels. While the Mamluk and Ottoman public baths in Damascus tend to have a central organization of the bathing spaces, the hammams especially in Fez have maintained a linear and axial organization reminiscent of the first Umayyad public baths (Sibley 2006). Usually they consist of four sequential rooms: the changing room – (called mashlah or al-Ghelsa) used for undressing, resting and socializing, the cold room (called al-Barrani), the warm room (called al-Wasti), and the hot room (called al-Dakhli). Unlike in the Syrian, Turkish, and Egyptian water distribution tradition, in Morocco a bucket system is used. Clients don't get their water from wash basins, but rather take a number of buckets with cold and hot water to use it for washing.

2.4.2.4. Baths in Syria

In the 1940s 40 baths could be identified in the Damascus-area, in the year 2004 just 13 hammams were still operating (Sibley 2006). In Syria the layout of hammam spaces has changed over the years. Already in the Damascene baths of the 12th century the typical hypocaust system was replaced by a duct system (0.5 m-0.7 m width and 0.7 m-1.2 m height) which leads from the furnace to the hot room and finally to the chimneys from where the hot smoke can exhaust. The duct branches out into side chambers. Its presence was made evident by flat swellings, small platforms or colored stone tiling. Till 15th century the existing bath type remains without significant changes. In the following centuries bathing spaces and particularly the hot room became dominant over the other spaces. The hot room receives side chambers for separate washing, massage etc. which were originally took place in the warm room.

2.4.2.5. Baths in Algeria

Very typical for Algerian or North African hammams is the linear progression of the bathing spaces. In Algeria two additional rooms can be found namely an entrance lobby leading to the changing room called Skiffa and a small transition space between the cold and hot room called SAS. The changing room is usually made up of two floors whereas the first floor is based on a timber structure. The typical warm room is absent. As with the Moroccan hammams, the bucket system for water distribution is used.

2.5. Construction details

2.5.1. Materials

Similar construction techniques were used in various hammams. Generally they were built using the same method as for other local buildings. Masonries of hammam buildings are rather massive (see Figure 5) and are either made of stone (Limestone, Sandstone, or Rubble stone) or brick. Vaults and domes are usually built with brick. Lime was used for surface finish as well as for mortar in the constructions. The slaked lime was usually mixed with other materials such as ash or eggshells. This original plaster-system was highly water resistant and permeable.

In some areas (e.g., Egypt, Algeria) wood is used in the changing room for the second floor and roof structures.

Floors are tiled by marble, stone or ceramic tiles (see Figure 6) and in the changing room sometimes additionally covered by carpets.



Figure 5 Massive walls in Hammam Tambali, Cairo Egypt (picture by A. Mahdavi)



Figure 6 Floor in Hammam Fairouzi (Damascus, Syria)

2.5.2. Lighting

All typical hammams use the same method to bring daylight into the hot space. Numerous round, octagonal or stellar shaped openings are built into the dome overhead. These openings are usually covered by glass in either white or colored (Figure 7 and 8). The apertures are arranged in different patterns. In some hammams, some of these glass covers can be opened for increasing the ventilation. In the last couple of decades many of the openings have been blocked by mortar or cement due to restoration of the roof or to increase privacy. See for example blocked apertures in Hammam Suq al-Ghazal in Figure 9.

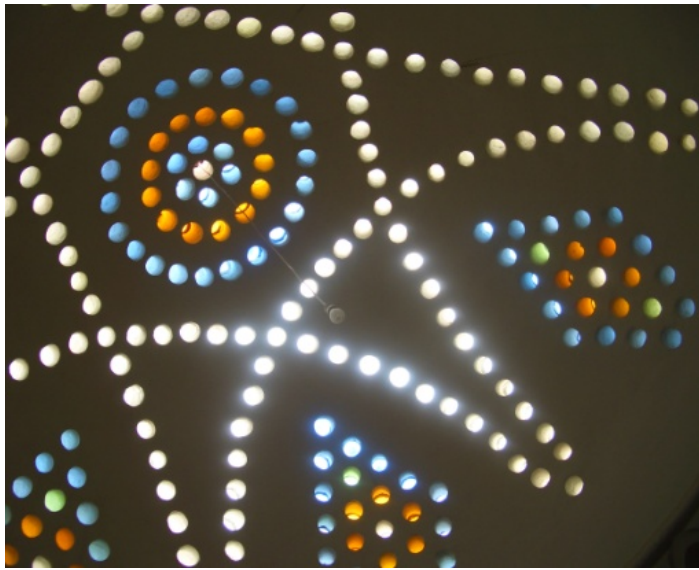


Figure 7 Typical openings in domes of hammam (Hammam Fairouzi)



Figure 8 Typical openings in domes of hammam, outside view (Hammam Fairouzi)



Figure 9 Blocked apertures of Hammam Suq al Ghazal, Algeria

2.6. Technical systems and equipment

Technical thermal systems include the boiler, the hot water reservoir, and the hypocaust system. The heating section or furnace of the hammam is located along a wall of the hot room. It is provided with a separate entrance and has no connection to the bathing spaces. The firing is located below the hot water reservoir which contains two or more cauldrons, whereas just one is directly above the firing. The cauldron is supplied with cold water from wells, cisterns or via subterranean ducts. After boiling, the hot water flows through a connecting tube to a smaller tank where it is kept at high temperature.

Warm and hot rooms are usually heated by a hypocaust system which was already used at roman times. Hypocausts are floor heating systems where the hot smoke from the furnace passes under the suspended floor in hot and warm room before rising up through a chimney in the wall. Additionally hot rooms are also heated by the use of hot water. The following drawing exemplifies a typical hypocaust system in the Hammam al-Basha (Dow 1996).

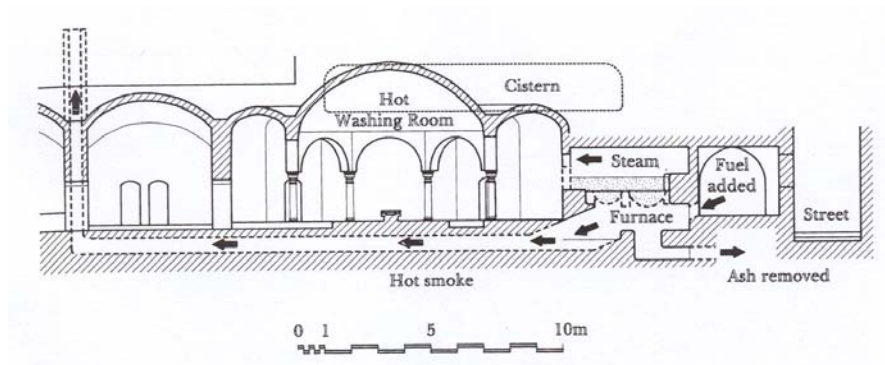


Figure 10 Section showing typical heating arrangements at Hammam al-Basha (Dow 1996)



Figure 11 Furnace of Hammam Saffarin (picture by Aisha Darwish)

3. Method

3.1. Overview

This study was conducted within an overall research effort concerning traditional Hammams in the Mediterranean region. The high-level objective of this interdisciplinary project was a comprehensive understanding of the technical and social aspects of hammams, including their current state, role, and functionality, as well as their future potential (Hammam 2008). Within the project five different hammams in five different North-African and Mediterranean countries have been targeted namely Egypt, Turkey, Morocco, Syria, and Algeria.

This work particularly addresses the thermal, visual, and acoustical performance of these thermal bath buildings. For an improved technical understanding of building performance features of traditional architecture, high-resolution empirical performance measurements are needed. Therefore, outdoor and indoor environmental parameters were monitored, which mainly relate to the thermal visual and acoustical performance of the objects studied. Furthermore data concerning the construction methods, building materials, and building systems as well as data regarding heating and ventilation regimes and occupancy patterns were collected.

Collected data were analyzed and interpreted in view of the buildings' thermal performance, comfort conditions, transition between various spaces within the hammam, and the dependency of indoor climate on outdoor environmental parameters (Mahdavi and Orehounig 2008). Measured acoustical and visual parameters were evaluated.

In addition to evaluation and interpretation of indoor environmental conditions, the monitored data was also used to calibrate digital performance simulation models of a number of the objects studied. Specifically, thermal and acoustical performance simulation models were generated. These calibrated models were applied in two complementary ways. First, detailed simulation runs allowed exploring possible reasons for certain trends in measured data. For example, available heating system information (e.g. heating schedule data) could be critically examined and partially falsified based on comparison of measured and simulated data. Second and more importantly, simulation runs allowed predicting the consequences of alternative options for the renovation,

restoration, reuse, and adaptation of these buildings. Thus, performance implications of the utilization of modern technologies and products (e.g. thermal insulation and acoustical absorption materials), in the culturally and historically sensitive context of traditional bath buildings, could be carefully scrutinized before such interventions would be actually carried out (Orehounig and Mahdavi 2009).

3.2. Selected buildings

3.2.1. Overview

Altogether 5 buildings in 5 different countries have been targeted for the project. These are located in Egypt, Turkey, Morocco, Syria, and Algeria. The following map (Figure 12) shows the location of the selected cities. Case study visits took place between February 2006 and May 2007, during these visits the 5 main objects have been studied, some additional objects have been briefly visited for comparison purposes. In this chapter the five main objects are described in the following. Further two objects have been considered for the acoustical survey, namely Hammam Belebjaoui and Hammam Bougouffa in Constantine, Algeria.



Figure 12 Locations of selected cities

The selected objects represent a sample over different periods and climates. The oldest object is Hammam Ammouneh in Damascus from the Ayyubid period in 13th century, followed by Hammam Saffarin in Fez from the Marinid period in 14th century. Hammam Şengül in Ankara was built in 16th century but has been significantly changed in 19th century. Hammam Suq al Ghazal was built in 1730 followed by Hammam Bab al-Bahr in Cairo in 19th century as the newest one. Average Outside temperatures vary from 11.3°C in Ankara, Turkey to 22.2°C in Cairo, Egypt. The following table summarizes the main parameters of the studied objects.

Table 1 Summarized parameters of Hammams

		Bab al Bahr	Şengül	Saffarin	Ammouneh	Suq al Ghazal
	Code	BAB	SEN	SAF	AMH	SAG
	Location	Cairo, Egypt	Ankara, Turkey	Fez, Morocco	Damascus, Syria	Constantine, Algeria
	Avg. θ_e [°C]	22.2	11.3	17.7	17.4	15.7
	Century	1900	1600	1400	1300	1800
	Floor Area [m²]	190	670	380	95	200
	Gender (male/female)	m+f	m+f	m+f	m	m+f
	Twin-bath		x	x		
Room sequence	Changing Room	x	x	x	x	x
	Cold Room	x		x		x
	Warm Room		x	x	x	
	Hot Room	x	x	x	x	x
Water system	Hot water plunge pool	x				
	Wash basins	x	x		x	
	Bucket system			x		x
Heating system	Hypocaust		x	x		x
	Under floor duct system				x	
	Hot water pool	x				

3.2.2. Hammam Bab al-Bahr, Cairo, Egypt

3.2.2.1. General

The first designated object is Hammam Bab al-Bahr in Cairo, Egypt. It was built probably in the Ottoman period during 19th century. The hammam is located in a busy shopping street near the northern border of the old city in Cairo (Mikats 2007). Most of the original spaces are still in use, although modifications have been taken place. Hammam Bab al-Bahr operates almost 24 hours a day. It is alternatively used by women from 9:00 to 17:00, and by men in the evening starting from 19:00 till 7:00 in the morning. The time in between is usually used for cleaning.



Figure 13 Entrance of Hammam Bab al-Bahr (picture by A. Mahdavi)



Figure 14 Interior view of hot room in Hammam Bab al-Bahr (picture by A. Mahdavi)

3.2.2.2. Spatial organization

Hammam Bab al-Bahr is located below street level and is accessed through few steps, which lead to a bent corridor, before reaching the **changing room** called the "maslakh". The "maslakh" shows an almost rectangular floor plan and is covered by a flat wooden roof with a central hexagonal prism shaped dome (called Shukhshikha). The space is divided into the central area and two raised platforms which are used for relaxing after the bath, eating, smoking, and changing. Two additional side rooms function as a more private place for changing cloths.

An enclosed corridor connects the maslakh with the **cold room** (Bayt awwal) and the toilette facilities. The "Bayt awwal" is unheated but due to the close proximity to the heated area temperatures are also moderate in winter times, this is why it is sometimes used as winter changing room. It is covered by a dome with the typical openings.

The heated area of the hammam, i.e., the **hot room** or "Bayt al-Harara" consists of a central room and six side rooms. The octagonal central room is covered by a flat roof, originally it was equipped with a domed roof. In the center of the room an octagonal platform is located, which is used for scrubbing. Two vaulted iwans function as room extension in north and west, 3 additional side rooms are equipped with washing facilities and showers. From the main room a few steps lead to the vaulted "Maghtas",

where the actual heat source, a hot water pool is situated (HAMMAM 2006g, HAMMAM 2006b).

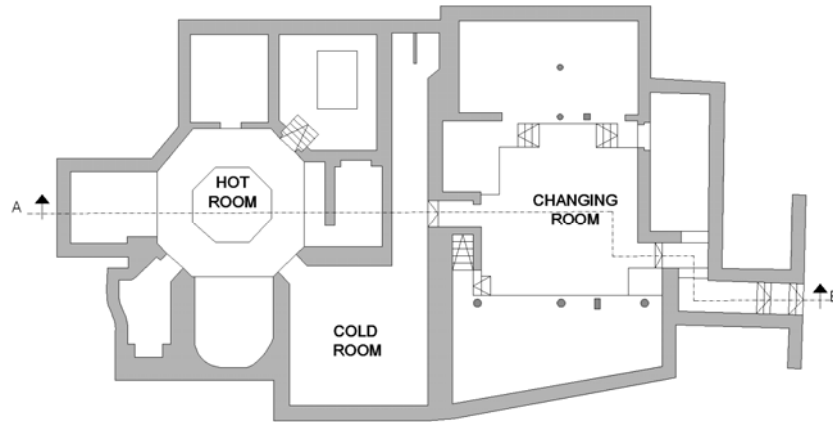


Figure 15 Floor plan of Hammam Bab al-Bahr

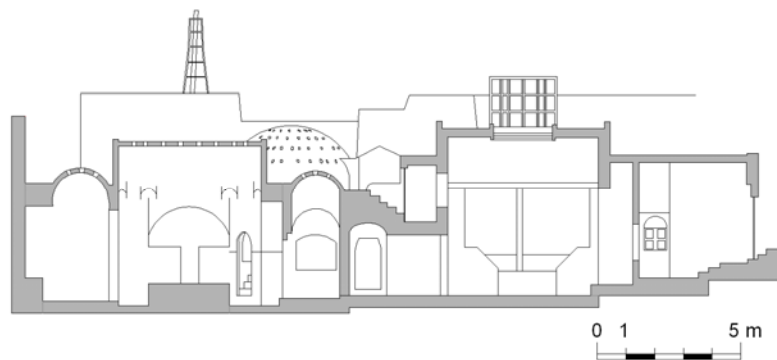


Figure 16 Section of Hammam Bab al-Bahr

3.2.2.3. Technical details

Material

Walls and domes are made of brick with lime mortar, covered by a plaster finish. The surfaces of the wet spaces are made of either stone or ceramic tiles. The entrance area shows also wooden constructions, such as the wooden ceiling with lime mortar. Floors are mainly covered by marble or sandstone slabs.

Heating and energy consumption

Hammam Bab al-Bahr doesn't have a hypocaust system. Rather, it is heated by the hot plunge pool "Maghtas". The original waste-fired boiler had been replaced by a gas-oil fired boiler which provides the hammam with hot water. An additional butane-gas fired boiler has been installed,

apparently for additional water heating during winter time. For space heating and cooking in the changing room paraffin is used. Table 2 summarizes the annual delivered energy in form of Gas and Paraffin for heating and electricity for lights and other appliances. The water is stored in a hot water storage tank. Two separate pipe systems are in use, the first one supplies the plunge pool with hot water, the secondary pipe supplies water to the fountain, hot taps, and showers. The annual water consumption for filling the hot pool, providing water to the fountains, taps and showers is estimated to be about $4420 \text{ m}^3 \cdot \text{a}^{-1}$ (HAMMAM 2006g).

Table 2 Breakdown of the total annual delivered energy consumption for Hammam Bab al-Bahr (HAMMAM 2006g, 51)

Form of Delivered Energy	Annual Delivered Energy Consumption (kWh/a)
Gas-Oil	540 867
Paraffin	33 742
Electricity	4 528
Total	579 137

3.2.3. Hammam Şengül, Ankara, Turkey

3.2.3.1. General

The "Şengül Hamami" is one of the three historic hammams in Ankara which is still in use. It is located in "İstiklal mahallesi" district and shows typical characteristics of ottoman architecture. Şengül was built in 16th century and restored in 19th century. It is a double hammam with separate parts for men and women. Working hours for women are from 06:00 to 19:00 and for men from 05:00 to 22:00.



Figure 17 Outside view of Hammam Şengül (picture by A. Mahdavi)



Figure 18 Interior view of hot room in Hammam Şengül (HAMMAM 2006f)

3.2.3.2. Spatial organization

The entrance of the men's section is at the center of the façade and opens onto a public square. The women's entrance is located on a side street with a blind façade.

In case of the men's section, the **changing room** (Soyunmalik) is entered directly, whereas in the women's section a transition space protects the privacy of undressing from the public street. The "Soyunmalik" in both sections is two-storied and shows an almost rectangular floor plan with high windows and a wooden roof structure. The women's section contains a central table for socializing, and a wall fountain, the men's section a central fountain. The surrounding area is divided into small private chambers for changing cloths.

The **warm room** is called "Iliklik", this space is, compared to the first room rather small. It functions as a transition space between the undressing area and the hot area and gives access to toilette facilities and storage spaces. The warm room in the women's section is currently used as additional bathing space whereas in the men's section it is used for washing towels and as a rest space.

The **hot room** is called "Sicaklik". It contains a central room and two iwans in the women section and three iwans in the men section. All rooms are covered by domes, the central room is equipped with a marble slab used for scrubbing. The iwans are furnished with washing basins receiving both hot and cold water. The central room gives access to sauna spaces which originally functioned as steam rooms called "Sicaklik halvether" (HAMMAM 2006f, HAMMAM 2006a).

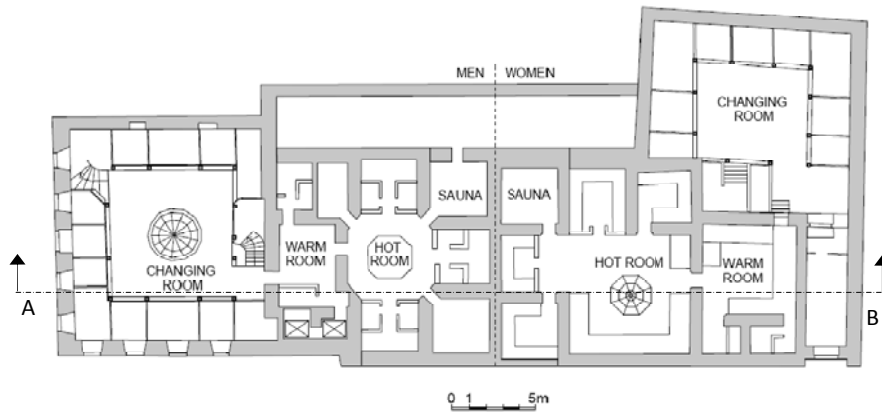


Figure 19 Floor plan of Hammam Şengül

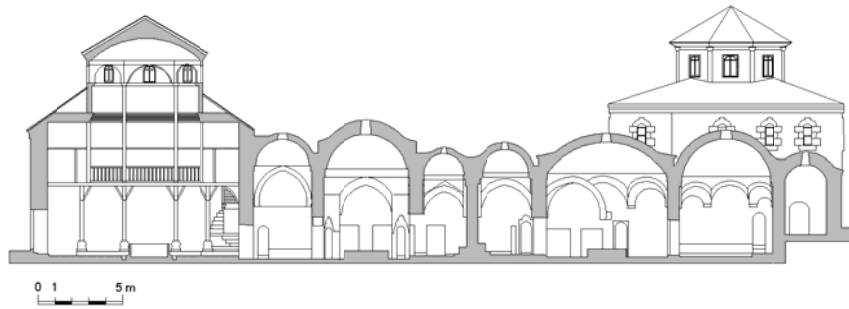


Figure 20 Section of Hammam Şengül

3.2.3.3. Technical details

Material

Walls are made using a local stone (rubble stone). The façade has new stone wall facing. Partition walls are made of marble. Domes are made of brick. The original roof covering of the bathing spaces was later replaced by concrete. The changing room is covered by a wooden roof structure and ceramic roof tiles.

Heating system

The furnace is located along the hot rooms, it is based on a coal-fired boiler system which provides heating for the hot water and supplies the hypocaust underneath the hot room with hot steam. The street side of the hammam is equipped with multiple chimneys which can be opened and closed by a control system. In the changing rooms extra space heating is provided by coal stoves. The following table (Table 3) summarizes the annual primary energy consumption for the hammam. The annual water consumption is estimated to be $21\,788\text{ m}^3\cdot\text{a}^{-1}$ (HAMMAM 2006f).

Table 3 Breakdown of the total annual delivered energy consumption for Hammam Şengül (HAMMAM 2006f, 70)

Form of delivered energy	Annual delivered energy consumption (kWh/a)
Coal for water heating	625 625
Coal for space heating by the hypocaust	208 542
Coal for extra winter space heating	171 667
LPG for catering	3 019
Electricity	22 302
Total	1 031 155

3.2.4. Hammam Saffarin, Fez, Morocco

3.2.4.1. General

Hammam Saffarin is situated in the historic district Quaraouiyine in the medina of Fez. It is located at the Saffarin square which is famous for coppersmith workshops. The double bath consists of a women section, which dates back to the Marinid period, most likely built in the 14th century, and the men section, which was originally a lime kiln and later converted to a bath (HAMMAM 2006e). Women opening hours are from 7:00 till 20:00 o'clock and men opening hours from 7:00 till 24:00 o'clock. The clientele who uses the hammam is mostly from the neighborhood.



Figure 21 Outside view of Hammam Saffarin



Figure 22 Inside dome in changing room in Hammam Saffarin

3.2.4.2. Spatial organization

The Saffarin hammam contains a historical women section and relatively new men section. The entrance opens up onto a public square and is used by both women and men.

Women section

A bent corridor leads to the original **changing room** (Mashlah or El Ghelsa) of the women section. It has a square floor plan with four columns

supporting round arches, which carry the grand octagonal central dome plus four additional similar but smaller domes placed in the corners (HAMMAM 2007c). Adjacent rooms function as place for prayers and as storage room. The changing area of the mashlah is equipped with benches and lockers. Furthermore a cold water fountain can be found against the wall to the hot area. Natural light is provided through several openings in the dome area. The floor is covered by squared ceramic tiles whereas more decorative painted tiles cover parts of the walls and the fountain.

From the changing area leads a as small transition room to the El Wasti or warm room and further to the **cold room** (El Berrani). Originally the cold room could be entered directly from a small corridor, but this entrance was closed since the toilette facilities have been located there. The Berrani shows a rectangular floor plan covered by a barrel vault, the walls are halfway covered by tiles.

The **warm room** (wasti) of Hammam Saffarin is divided by an arch into two areas, both covered by barrel vaults. The main space is surrounded by each two niches.

The **hot room**, called dakhli can be accessed through a centered opening. It is rectangular and covered by a barrel vault which is intersected by an additional orthogonal vault. The dakhli displays 3 additional niches and a hot water basin which is used by the customers for filling their buckets.

Men section

The changing room of the men section is divided by a timber partition wall to separate the reception area from the changing area. The floor is paved with rectangular tiles. From the changing room one proceeds to the cold room known as "Barrani", that is the first bathing chamber.

The next room, the warm room "wasti", differs from the women section as it has just a main room and no side chambers.

The hot room "dakhli" is covered by a dome with glass covered openings. A small niche accommodates the hot water basin.

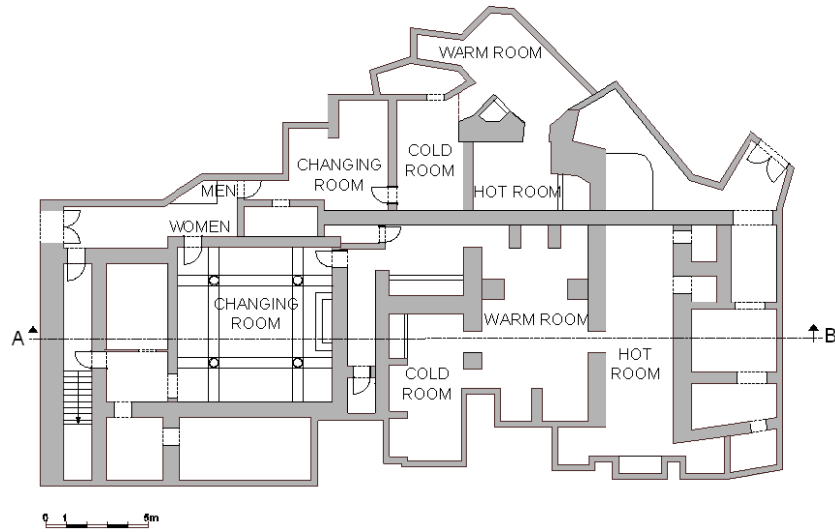


Figure 23 Floor plan of Hammam Saffarin

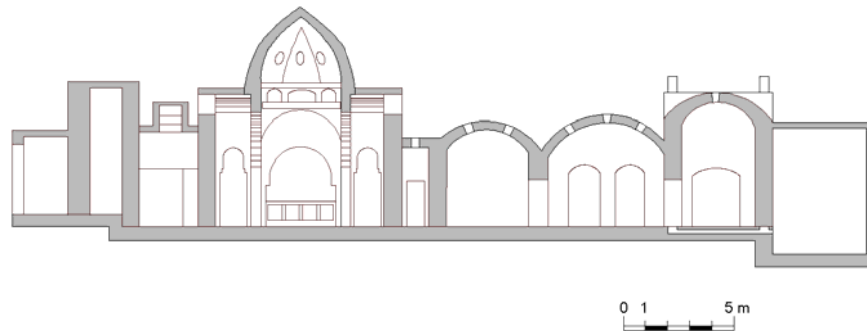


Figure 24 Section of Hammam Saffarin

3.2.4.3. Technical details

Material

Walls are made of either stone or common brick with lime mortar. As the surface finish a lime-based plaster is used. Vaults and domes are made out of brick. Floors are covered by ceramic tiles in the men section and white marble in the women section.

Heating system

The furnace is located next to the hot rooms and uses wood and wood shavings collected from the carpenters for heating the water and supplying hot smoke for the hypocaust system below the hot room. The hot smoke exhausts from the 4 chimneys located in the corners of the hot room. The annual water consumption is estimated with $12\,319\text{ m}^3\cdot\text{a}^{-1}$ (HAMMAM 2007c). The following table (Table 4) summarizes annual energy consumption of the building.

Table 4 Breakdown of the total annual delivered energy consumption for Hammam Saffarin (HAMMAM 2007c, 91)

Form of delivered energy	Annual delivered energy consumption (kWh/a)
Waste wood for water heating	986 016
Waste wood for space heating by hypocaust	134 457
Electricity	5 215
Total	1 125 688

3.2.5. Hammam Ammouneh, Damascus, Syria

3.2.5.1. General

Hammam Ammouneh was built in the Ayyubid period (1193-1260) and is located in the "al Uqayba quartier" close to the northern gate of the old city. Hammam Ammouneh was used only by male-customers till the Restoration in 2007. Opening hours were from 8:00 till 24:00.



Figure 25 Hammam Ammouneh outside view



Figure 26 Changing Room of Hammam Ammouneh

3.2.5.2. Spatial organization

The entrance to Hammam Ammouneh is placed in the corner of the building and leads a few steps under street level.

After a small corridor a second door gives access to the **changing room** (mashlah or Barrani). The mashlah shows a rectangular floor plan enclosed by 4 iwans. The central area is covered by a dome. Within the iwans the floor level is a few steps higher than the central area and covered by carpets. Along the walls benches are located which are used for undressing. An octagonal basin is located in the center of the room. Several windows in walls and the dome provide the mashlah with daylight.

A straight corridor (originally referred to as **cold room**) connects the mashlah with the bathing spaces. It shows two separate areas in north and south, one is used for toilette facilities and the other was originally used for hair removal. The entrance to latter space has changed from the corridor to the warm room. The corridor area is covered by a dome which is pierced with openings for daylight. Two metal doors separate the mashlah from the corridor and the bathing spaces.

The following room (the **warm room**) is called the wastani. It consists of a central square plan with a long iwan, and is covered by a dome. The central area is equipped with a cold water marble basin located on the northern corner. An additional room, which is nowadays accessed through the hot room was originally part of the warm room.

The **hot room** (called harrara or Jouani) consists of a main central squared area, which is covered by a dome and several additional compartments. The west side of the harrara provides access to an additional room. Small stone basins providing hot and cold water are located in almost all spaces (HAMMAM 2007b, HAMMAM 2006d).

The Hammam was restored July 2007 until February 2008, the above description correlates with the situation before restoration, since all measurements were conducted before July 2007.

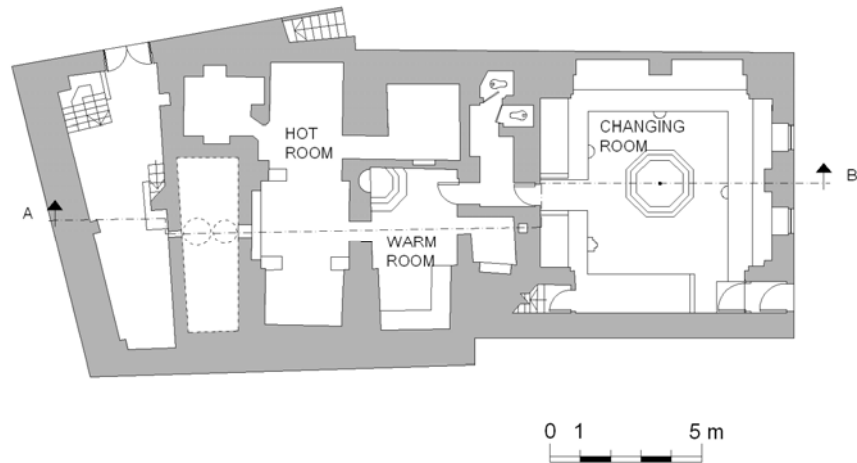


Figure 27 Floor plan of Hammam Ammouneh

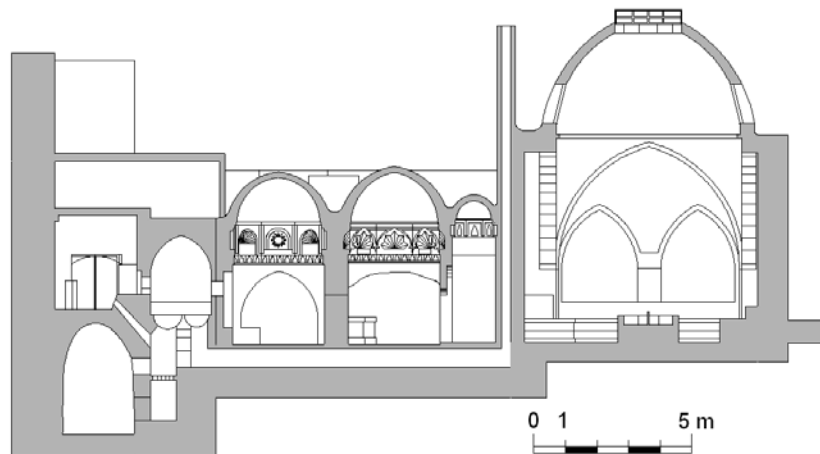


Figure 28 Section of Hammam Ammouneh

3.2.5.3. Technical details

Material

Walls are constructed out of local stone. The façade is partly covered by white and black oil painting in a diagonal striped pattern. Domes and vaults are made of brick. Floors are covered by yellow and black stone tiles. The same pattern can be found at arches in the changing room. Over the original lime based covering of the roof, a cement based surface finish was applied which caused major damage.

Heating system

Hammam Ammouneh still used the traditional heating system during the local survey in the year 2007. Waste wood was used for water and space heating (HAMMAM 2007b). Space heating was provided by under floor ducts, where the smoke from the furnace passes along a duct under the

floor of the hot room and rises up in a chimney in the wall. The duct system is spread out into the side chambers. The following table summarizes the annual energy consumption of the building. The total annual hot water supply was $3074 \text{ m}^3 \cdot \text{a}^{-1}$ (HAMMAM 2007b).

Table 5 Breakdown of the total annual delivered energy consumption for Hammam Ammouneh (HAMMAM 2007b, 79)

Form of delivered energy	Annual delivered energy consumption (kWh/a)
Waste wood for water heating	258 954
Waste wood for space heating by duct system	100 704
Electricity	13 157
Propane for Cooking	10703
Total	383 518

3.2.6. Hammam Suq al-Ghazal, Constantine, Algeria

3.2.6.1. General

Hammam "Suq al Ghazal" was built in the ottoman period (most likely in 1800). It is located in the medina of Constantine in the "Suq el Tadjar" neighborhood (HAMMAM 2006c). It is used by women and men alternately; daily opening times are from 8:30 to 12:30 for women and from 13:00 to 18:00 for men. It was estimated that from Saturday to Wednesday approximately 13 people and on Thursday and Friday about 40 people use the hammam.



Figure 29 Entrance of hammam Suq al-Ghazal



Figure 30 connection changing room and cold room

3.2.6.2. Spatial organization

The façade of the Hammam Suq al-Ghazal shows two doors, one for entering the hammam and one for entering the furnace area. Between the doorway and the changing room a small transition space is located, which is called Skiffa. This space is a common feature in Algerian

hammams. It is meant to reduce air draughts and provide more privacy for the changing room.

The **changing room** (mashlah) shows a squared double story floor plan. The roof construction is carried by orange painted wooden columns in the first floor, which are prolonged as stone arches in the second floor. The mashlah is covered by an octagonal dome, which is nowadays hidden under a pitched roof. The ground floor is surrounded by raised platforms.

The **cold room** shows a rectangular floor plan (see Figure 31), covered by a barrel vault, which was originally equipped with the typical round openings. These have been blocked and replaced by two squared openings for daylight. The cold room is equipped with a cold water basin.

From the cold room you enter a 2m² **transition space** which is called SAS. There are doors on both sides, to the cold room and also to the hot room which reduces heat loss from the heated area. The SAS is equipped with stone benches on two sides.

The **hot room** is the main bathing space. Its almost rectangular floor plan is covered by three barrel vaults, which are supported from four central columns (see Figure 32). The central area is equipped with a raised platform, which is used for scrubbing. Next to the furnace wall a hot water basin is located, from which customers get hot water in their buckets. On the opposite side two open bathing chambers are located for private bathing.



Figure 31 Internal view cold room



Figure 32 Internal view hot room

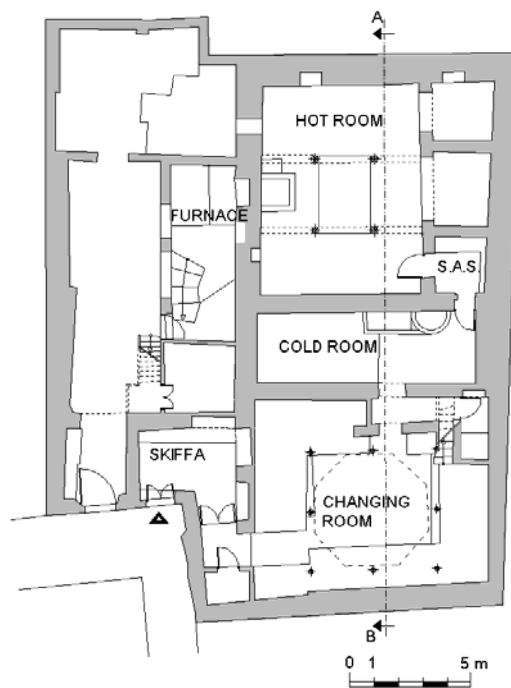


Figure 33 Floor plan of Hammam Suq al Ghazal

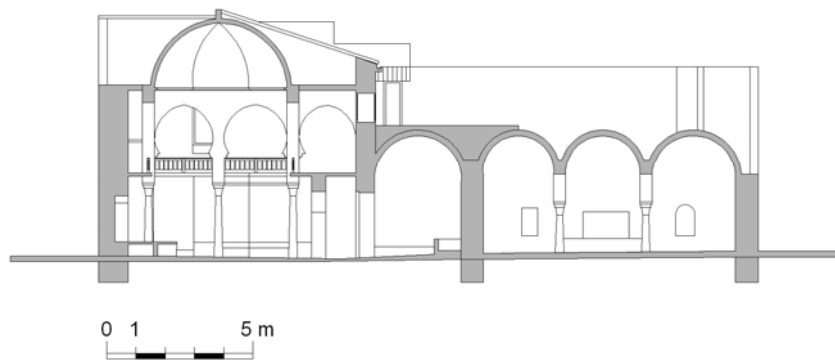


Figure 34 Section of Hammam Suq al Ghazal

3.2.6.3. Technical details

Material

Foundations of the building are in stone. Masonry is made of brick hold together with lime mortar. The original dome is hidden beneath a pitched roof covered with bent tiles (HAMMAM 2007a). Floors in the undressing room and in the hot room are out of marble. The raised platforms in the changing room and floors in cold room are covered with ceramic tiles.

Heating system

The furnace is located next to the hot room. The original fuel – recycled material – has been replaced by gas. The hammam has retained the original hypocaust system, where smoke travels beneath the hot room and exhausts through chimneys in the partition walls. The annual energy demand of the building is summarized in the following table (Table 6). According to calculations (HAMMAM 2007a) the thermal efficiency of the hot water system (space heating and water heating) lies by 31%. This indicates that the actual heat delivered to the space is much smaller than the calculated values in this table. The annual total water consumption was estimated with $884 \text{ m}^3 \cdot \text{a}^{-1}$. The typical water use was estimated to be 4 to 6 buckets per person (HAMMAM 2007a).

Table 6 Breakdown of the total annual delivered energy consumption for Hammam Suq al Ghazal (HAMMAM 2007a, 66)

Form of delivered energy	Annual delivered energy consumption (kWh.a ⁻¹)
Mains propane gas for water heating	41 756
Mains propane gas for space heating by hypocaust	132 226
Electricity	1 104
Total	175 086

3.3. Measurements

3.3.1. Overview

Toward an improved technical understanding of building performance features of traditional architecture, high-resolution empirical performance measurements are needed. Therefore a matrix of outdoor and indoor environmental parameters to be monitored is used, which mainly relate to the thermal visual and acoustical performance of the objects studied. Long time measurements of outdoor parameters (dry bulb temperature, relative humidity, global horizontal radiation, wind speed, wind direction) and indoor parameters (temperature, relative humidity, and illuminance) were conducted over a period of one year (for each building). Furthermore, acoustical and illuminance spot-measurements were performed in various spaces of the selected buildings.

3.3.2. Thermal parameters

3.3.2.1. External parameters

A weather station was installed in proximity of each hammam to monitor outdoor air temperature and relative humidity, global horizontal irradiance, wind speed, and wind direction. Two different types of weather stations were utilized. For the buildings in Cairo, Ankara, Fez, and Constantine the Onset product HOBO-Weather Station along with the Software products Boxcar-pro and Hoboware were used (Onset Company 2009). In case of the outdoor parameters in Damascus we chose the weather station DKSTAT 1 together with the Software Infralog (Driesen and Kern Company 2009). The following table summarizes the measurement schedule.

Table 7 Overview of the external weather data collection period for the five buildings

year	2006			2007				2008	
month	4	7	10	1	4	7	10	1	4
BAB									
SEN									
SAF									
AMH									
SAG									

Cairo

To allow for the undisturbed operation of the weather station, it was not directly installed on the roof of the hammam. Rather it was mounted on the roof a close-by building some 300 meters away (see Figure 35). The measurements started March 2006 and were completed in April 2007.



Figure 35 weather station in Cairo

Ankara

The weather station was mounted on the roof a close-by office building some 500 meters away (see Figure 36). The measurements started July 2006 and were completed in July 2007.



Figure 36 weather station in Ankara

Fez

The weather station was mounted on the roof a close-by Medressa some 150 meters away (see Figure 37). The measurements started November 2006 and were completed in December 2007.



Figure 37 weather station in Fez

Damascus

The weather station was mounted on the roof of a close-by complex (historical documentation center) some 400 meters away (see Figure 38). The reporting period started February 2007 and ended in October 2007.



Figure 38 weather station in Damascus

Constantine

In case of the Constantine case study, the weather station was installed in January 2008 on the roof of a close-by complex (Medressa) located some 200 meters from the hammam (see Figure 39). During the period May 2007 and January 2008 outside parameters (temperature, relative humidity and illuminance levels) were measured with an internal data logger mounted below the roof of the studied object. The reporting period ended in June 2008.



Figure 39 weather station in Constantine (picture by Samira Debache)

3.3.2.2. Internal parameters

Indoor climate parameters were measured in various rooms of the hammams over a period of one year. Each building was equipped with seven to twelve data loggers which measured every 5 to 10 minutes the air temperature, relative humidity, and illuminance levels. For each case study one person from the local research team was trained in downloading data and maintenance of the sensors. The downloaded measurements were sent on a regular basis to the Vienna University of Technology. The hammams in Cairo, Ankara, Fez and Constantine were equipped with Hobo U12-012 data loggers (Onset Company 2009). In case of the Syrian hammam internal parameters were measured with Humlog 10THC data loggers together with the software Smart Graph (E+E Elektronik Ges.m.b.H 2009). The following table shows a summary of the schedules for monitoring internal data.

Table 8 Overview of the internal hygro-thermal data collection period for the five buildings

year	2006			2007				2008	
month	4	7	10	1	4	7	10	1	4
BAB									
SEN									
SAF									
AMH									
SAG									

Cairo

Seven data loggers were installed in various rooms of the Hammam Bab al-Bahr. Data was logged in 5 minutes time steps from March 2006 until April 2007. The following figure (Figure 40) shows a floor plan with corresponding data logger locations.

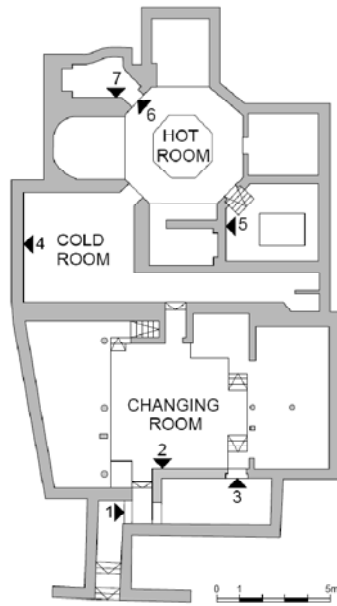


Figure 40 Sensor locations in Hammam Bab al-Bahr

Ankara

Twelve indoor data loggers were placed in different locations in the hammam, namely 6 loggers in the women's section and 6 loggers in the men's section. The exact data logger locations can be found on the following floor plan (Figure 41).

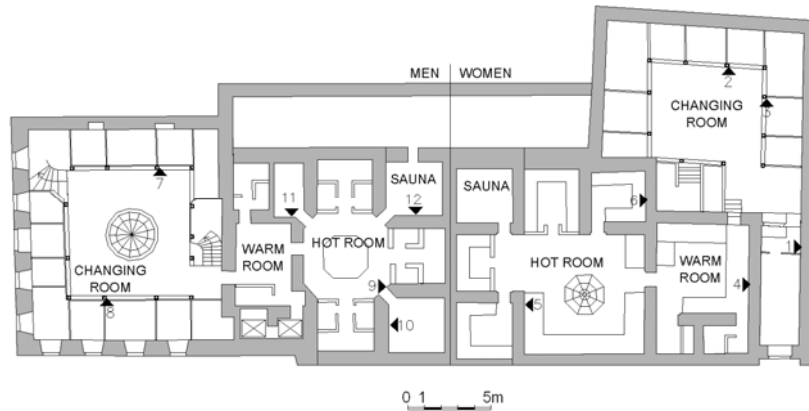


Figure 41 Sensor locations in Hammam Şengül

Fez

Ten indoor data loggers were placed in different locations in the hammam, namely 5 loggers in the women's section, 4 loggers in the men's section and 1 logger in the entrance area. The following floor plan (Figure 42) shows the sensor locations.

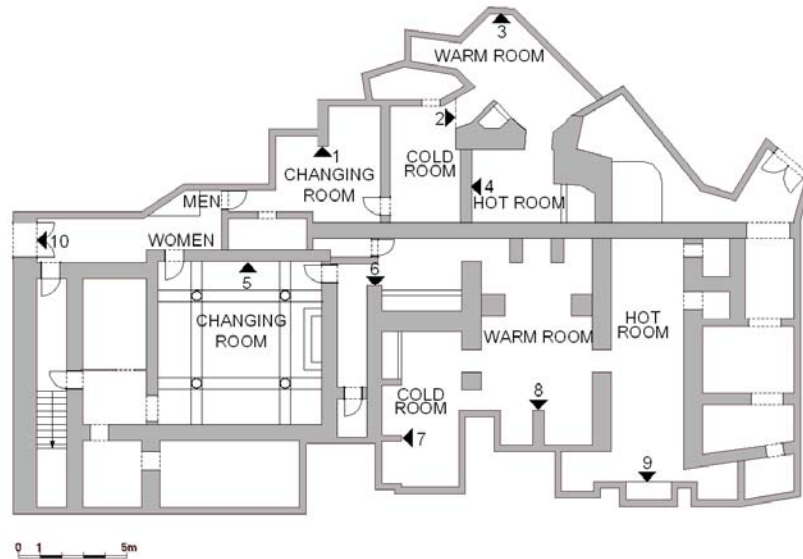


Figure 42 Sensor locations in Hammam Saffarin

Damascus

Eleven indoor data loggers were placed in different locations in the hammam, namely 3 loggers in the entrance area and 8 in warm and hot room area. The following floor plan (Figure 43) shows the sensor locations during the measuring period.

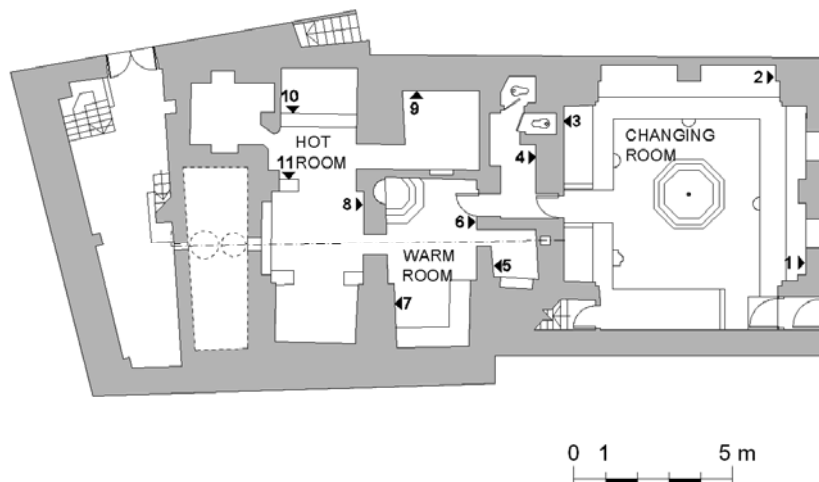


Figure 43 Sensor locations in Hammam Ammouneh

Constantine

Eight indoor data loggers were placed in different locations in the hammam, namely 1 logger on the exit to the roof of the hammam, 3 loggers in the entrance area, 1 in the cold room, 1 in the S.A.S. and 2 in the hot room. Figure 44 shows the sensor locations on a floor plan.

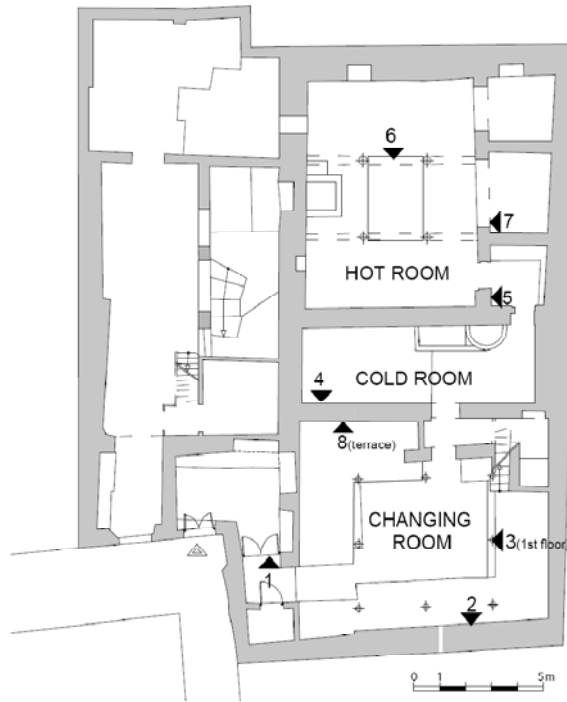


Figure 44 Sensor locations of Hammam Suq al-Ghazal

3.3.3. Acoustical parameters

During the case study visits acoustical measurements were performed in 3 countries, namely Morocco, Syria and Algeria. In case of the first two hammams ambient sound levels were measured in a couple of spaces. During these measurements, the respective spaces were in use. Note that the latter measurements were conducted on a short-term basis. Thus, they provide a snapshot of the prevailing ambient sound levels and are not representative in strict statistical terms. In Algeria, frequency-dependent reverberation times were measured. Reverberation time measurements were conducted in empty (non-occupied) conditions. As measurement equipment a sound level meter (RION NA-29 E) was used in Morocco and Syria, and for the reverberation time a hand-held analyzer (RION 28) was used (Rion 2009). The following table (Table 9) shows an overview of the performed acoustical measurements.

Table 9 Overview of the performed acoustical measurements

Building	Space	Code	V [m ³]	Measurement (Reverberation time)	Measurement (Ambient sound level)	Simulation (Reverberation time)
Hammam Suq al-Ghazal (Constantine, Algeria), 18 th century	Hot Room	SAG	280	Yes	No	Yes
Hammam Belebjaoui (Constantine, Algeria), 18 th century	Hot Room	BEL	145	Yes	No	Yes
Hammam Bougouffa (Constantine, Algeria), 18 th century	Hot Room	BOU	185	Yes	No	Yes
Hammam Ammouneh, (Damascus, Syria), 13 th century	Changing Room	ACH	260	No	Yes	No
	Warm Room	AWR	115			
	Hot Room	AHR	150			
Hammam Saffarin (Fez, Morocco), 14 th century	Changing Room	SCH	360	No	Yes	No
	Cold Room	SCR	100			
	Warm Room	SWR	180			
	Hot Room	SHR	230			

3.3.4. Visual parameters

In course of the local visits, spot measurements of indoor illuminance levels in hammams were performed. In all five hammams horizontal illuminance measurements were conducted considering both daylight and electrical light. In case of the hammams in Constantine and Ankara in addition to indoor illuminance levels, daylight factors were measured. For all light measurements illuminance meters "T-10" were used (Konica Minolta 2009).

3.4. Data Analysis

3.4.1. Overview

This chapter summarizes the main terms and variables, which are used towards compressing and representing the results of data analysis in the present work.

3.4.2. Thermal analysis

3.4.2.1. Mean monthly values

Hourly temperature and humidity values were calculated based on the measured data for each month and visualized in time-series plots.

3.4.2.2. Relative temperature

Relative temperature was calculated as follows:

$$\Delta\theta_{rel} = \frac{\theta_i - \theta_e}{\theta_e} \cdot 100 [\%] \quad \text{Eq. 1}$$

3.4.2.3. Temperature range

Temperature range over opening hours was calculated for the main spaces of the hammams.

3.4.2.4. Transition between spaces

To explore the thermal transition in the course of progression from one space of the hammam to another, Figures show the mean monthly indoor temperatures (for four different months) in changing room, cold room and/or warm room, and hot room.

3.4.2.5. Thermal comfort

In order to explore thermal comfort conditions in changing rooms of the hammams, data was plotted on psychometric charts, which allow for the concurrent representations of values of temperature and humidity in a room.

In contrast to Fangers comfort zones theory (Fanger 1970) it has been suggested that people adjust to prevailing seasonal outdoor conditions. Thus, the neutrality Temperature (Szokolay 2004) is dependent on the mean temperature of the month and is calculated as follows:

$$T_n = 17.6 + 0.31 \cdot T_{o,av} \quad \text{Eq. 2}$$

Based on the neutrality temperature, the comfort index Standardized effective temperature SET has been established, which also takes occupants' clothing (clo) and metabolic rate (met) into account. Furthermore, SET combines the effects of temperature and humidity. The

neutrality temperature is equal to SET at a relative humidity level of 50%. For higher relative humidity values the SET is lower and for lower relative humidity values SET is accordingly higher.

3.4.2.6. Cumulative temperatures

Cumulative indoor temperatures during opening hours were calculated for the spaces changing room, cold room, warm room, and hot room. Likewise, the prevailing outdoor conditions in the course of the applicable measurement periods were expressed in terms of cumulative temperatures.

3.4.3. Acoustical analysis

Measured ambient sound levels and reverberation times were evaluated. Specifically, measured reverberation times were compared with pertinent target values. Toward this end, desirable ranges for the selected objects (space function, space size) were needed. This is, however, not trivial, as the use patterns of the spaces are, in this case, not clearly stated. On the one hand, speech intelligibility would be desirable, given the social (communication) function of such spaces. On the other hand, a certain impression of reverberant field in these spaces is naturally expected (given the volume and surface properties) and probably appreciated. Moreover, people sometimes sing in traditional hammams and use occasionally background music in modern baths during (wellness) training sessions. Given these considerations and upon consultation of pertinent literature (see, for example, Fasold and Veres 2003), target values were assumed for the selected object as per Table 10.

Table 10 Assumed appropriate (target) reverberation times (in seconds) for the selected spaces

	SAG	BEL	BOU
Target	1.1	1.0	1.0

3.4.4. Visual analysis

Spot measurements of the visual environment were processed in terms of horizontal illuminance levels and daylight factors in a number of rooms of some of the selected hammams.

3.5. Simulations

3.5.1. Overview

In addition to evaluation and interpretation of indoor environmental conditions, the monitored data was also used to calibrate digital performance simulation models of a number of the objects studied. Two different kinds of simulations were performed. Specifically, thermal performance simulation models were generated for three buildings (Bab al-Bahr in Cairo, Şengül in Ankara, and Suq al-Ghazal in Constantine). Likewise, acoustical performance simulation models were generated for three baths (Suq al-Ghazal, Bougouffa, and Belebджаoui in Constantine, Algeria) (Orehounig and Mahdavi 2009).

These calibrated models were applied in two complementary ways.

- First, detailed simulation runs allowed exploring possible reasons for certain trends in measured data. For example, available heating system information (e.g. heating schedule data) could be critically examined and partially falsified based on comparison of measured and simulated data.
- Second and more importantly, simulation runs allowed for the prediction the consequences of alternative options for the renovation, restoration, reuse, and adaptation of these buildings. Thus, performance implications of the utilization of modern technologies and products (e.g. thermal insulation and acoustical absorption materials), in the culturally and historically sensitive context of traditional bath buildings, could be carefully scrutinized before such interventions would be actually carried out.

3.5.2. Thermal simulations

3.5.2.1. The method

Thermal simulation models were generated for three hammam- buildings namely Bab al-Bahr in Cairo, Şengül in Ankara, and Suq al-Ghazal in Constantine. The process for the generation and application of calibrated simulation models for the selected hammams is illustrated in Figure 46. An initial simulation model was generated based on collected geometry, construction, and operation data. Obtaining construction information as well as data pertaining to occupancy and ventilation patterns in hammam was rather difficult. Initial simulation assumptions were based on in-situ observations. The corresponding data were, however, successively refined with the aid of local research partners. To run the simulations, weather

files were generated based on data obtained from the locally installed weather stations. The initial simulation results (e.g. indoor air temperature values) could be then compared to the measurements, leading to a calibrated version of the simulation model. Using such a calibrated model, alternative scenarios for the thermal improvement of the building can be assessed and evaluated (Mahdavi et al. 2007).

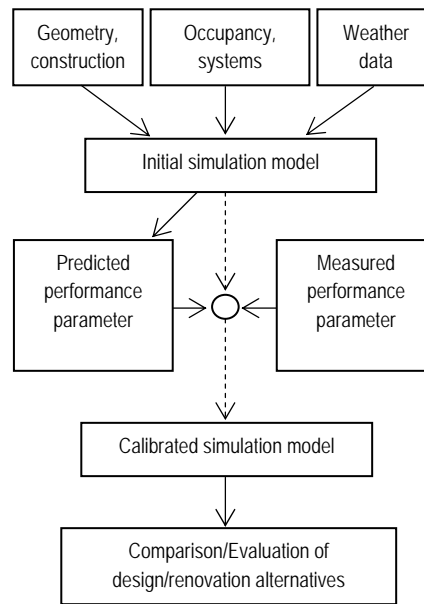


Figure 45 Illustrative depiction of the process of simulation model generation, calibration, and application (Mahdavi et al. 2007)

3.5.2.2. Simulation tool

For thermal simulations the software A-Tas from EDSL was used (EDSL 2009). This software tool simulates dynamically the thermal performance of buildings and there systems. The general approach is to achieve the thermal state of the building through a series of hourly snapshots. "This approach allows the influences of the numerous thermal processes occurring in the building, their timing, location and interaction, to be properly accounted for." (EDSL 2007, 3) The example of a geometry model constructed in A-Tas is shown in Figure 46.

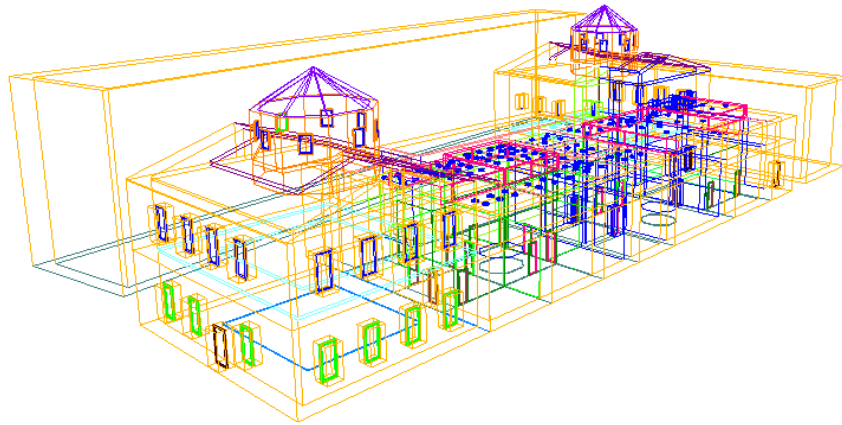


Figure 46 Example of a geometry model (Hammam Şengül) in Tas

3.5.2.3. Cairo model

A simulation model of the Cairo hammam was generated using the building's geometry. Thermally, the hammam was modeled in terms of ten distinct zones (see Table 11 for area and volume of the zones). Material assumptions are based on information from local research partners and observations at the site (see Table 12 for construction information). Furthermore, collected external data was used to generate an hourly weather file.

Table 11 Modeled Zones

	Zone	m ²	m ³
1	Changing Room	83.1	447.2
2	Corridor	9.6	36.9
3	Cold Room	24.8	95.3
4	Hot Room	31.5	153.2
5	HR-Pool	12.7	52.3
6	HR-Bathroom	6.5	25.1
7	HR-Shower 1	4.7	18.3
8	HR-Shower 2	8.3	32.1
9	HR-Washroom 1	7.3	28.2
10	HR-Washroom 2	7.4	28.5

Table 12 Simulation assumption regarding construction data (U-value, mass, g-value)

	Construction	Material	U-value [W.m ⁻² .K ⁻¹]	m [kg.m ⁻²]	g-Value [-]
1	Roof CH	Wooden ceiling with 30 cm lime mortar above	1.76	315	-
	Roof HR	Brick, rubble stones with lime mortar	1.76	315	-
2	Walls	Brick, rubble stones with lime mortar	1.1	525	-
3	Floor CH	Marble and Limestone slabs	1.6	317	-
	Floor HR	Marble and Limestone slabs	1.6	317	-
4	Glazing		5.8	10	0.4

Internal gains

Model input assumptions regarding heating energy, internal gains (occupants, lighting, etc), ventilation, and their respective schedules were based on a rough survey conducted by the local research partners and additional information collected during the site visit (see Table 13) (HAMMAM 2006g).

Table 13 Simulation assumption regarding internal gains (people, lights), air change rate

Zone	Air change rate [h ⁻¹]	Internal gains [W.m ⁻²]
CH	0.6 – 1	8.4
CR	0.3 – 0.5	9.4
HR	0.1	12.7

Heating

There exists no dedicated space heating system in the Cairo's hammam. Rather, the space is heated because the pool in hot room is regularly filled with hot water. Thus, it was estimated that the effective heating energy released in the space was based on pool volume and water supply temperature (as obtained via a spot measurement in the course of the site visit).

To exemplify the possibilities of model calibration, the assumptions pertaining to heating power is a good case in point. The information provided to the research team at the site suggested that the pool water was changed twice a day. However, long-term indoor temperature measurements in hot room in general and in the pool area in particular imply that the pool water is actually changed only once every day, namely late afternoon. This information, together with the measured indoor air

temperatures provided the basis for the calculation of heat transfer rate from the pool water to room air.

A pool filling was estimated with 4 m³, additional water use for pool top ups, fountains, taps and showers was estimated with 2.4 m³ per day. Hot water supply was measured as 62°C, furthermore initial pool temperatures are measured as 52°C. It was suggested that 83% of water used in the hammam is hot water (HAMMAM 2006g). Taking these values into consideration the heating power to the space could be calculated. In changing room additional space heating was provided due to a stove used for cooking tea. Cold room is just heated via the heating of the hot room. Associated heating power assumptions are provided in Figure 47.

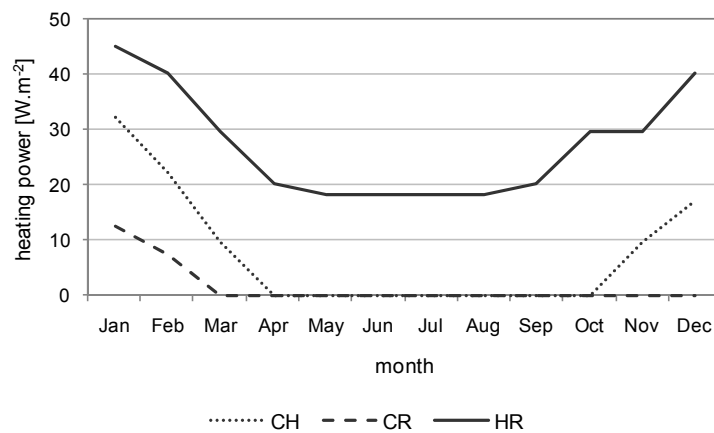


Figure 47 Space heating assumptions (W.m⁻²) for BAB

3.5.2.4. Ankara model

A model of the Ankara hammam was generated, with 17 distinctive zones, namely 7 zones in the women part and 9 in the men part. The rest of the hammam spaces were represented in terms of a zone called "Rest" (see Table 14 for area and volume of the zones). Material assumptions are based on information from local research partners and observations at the site (see Table 15 for construction information).

Table 14 Modeled Zones of SEN

	Zone	m ²	m ³
1	Entrance Women	16.3	87.9
2	CH Women	177.7	1090.4
3	WR Women	29.1	206.9
4	Toilettes Women	8.8	53.0
5	HR-middle Women	80.2	534.5
6	HR-Sauna Women	9.2	55.8
7	HR-Side-room Women	10.2	61.9
8	CH Men	222.3	1310.6
9	WR Men	17.0	119.6
10	Toilettes Men	11.1	67.2
11	WR-Side-room Men	7.1	42.7
12	HR-middle Men	59.6	378.7
13	HR-Bathroom 1 Men	12.1	73.1
14	HR-Bathroom 2 Men	6.0	36.0
15	HR-Sauna Men	10.4	63.2
16	HR-Pool Men	14.6	88.6
17	Rest	45.6	275.8

Table 15 Simulation assumption regarding construction data (U-value, mass, g-value)

	Construction	Material	U-value [W.m ⁻² .K ⁻¹]	m [kg.m ⁻²]	g-Value [-]
1	Roof CH	Timber, roof tiles	0.6	128	
2	Roof HR	reinforced concrete	1.8	1100	
3	Walls	Rubble stone	0.7	1620	
4	Floor CH	Marble on compressed earth	1.3	2370	
5	Floor HR	Marble on Stone	0.8	3670	
6	Glazing		5.6		0.69

Internal gains

Based on information of the local case study team it was estimated that 35 men and women use the hammam during the week and around 60 at the weekend. Sensible gains due to lights and equipment were determined based on measurements (HAMMAM 2006f). Ventilation rates and internal gains were simplified as follows (see Table 16):

Table 16 Summarized air change rates and internal gains

Zone	Air change rate [h^{-1}]	Internal gains [W.m^{-2}]
CH	0.2 – 0.5	0 – 3.5
WR	0.1 – 0.3	0 – 4.5
HR	0.1 – 0.3	0 – 6.4

Heating assumptions

As already mentioned in Section 3.2.3, Hammam Şengül uses a combined system for water and space heating. The boiler uses coal for water heating, the exhausted flue gases provide additional space heating via the hypocaust system.

Heating through hot water

The total annual water consumption was estimated to be 21 788 m³. This leads to a daily water consumption from 60 000 l for both women and men. It was estimated that 20 000 l were used in the hot room and 10 000 l in the warm room. The typical hot water supply was measured as 45 °C, cold water inlet was estimated as 25 °C in summer and 10 °C in the winter months. 4 different outflow temperatures of the water from the space for the whole year were estimated due to the relation of outdoor to prevailing indoor temperatures.

Hypocaust system

Floor temperatures were measured during the case study visit in Ankara July 2006. It was suggested that the typical floor temperature in the hot room was around 38 °C (HAMMAM 2006f). Very low surface temperatures were measured in warm room, which leads to the assumption that the hypocaust of the warm room was blocked in summer months. Based on measured internal monthly temperatures the radiation from the hypocaust system to the space could be calculated for each month.

Furthermore additional space heating is provided in the changing room in winter months. This could be calculated as a function of prevailing outdoor conditions.

Associated heating power assumptions are provided in Figure 48.

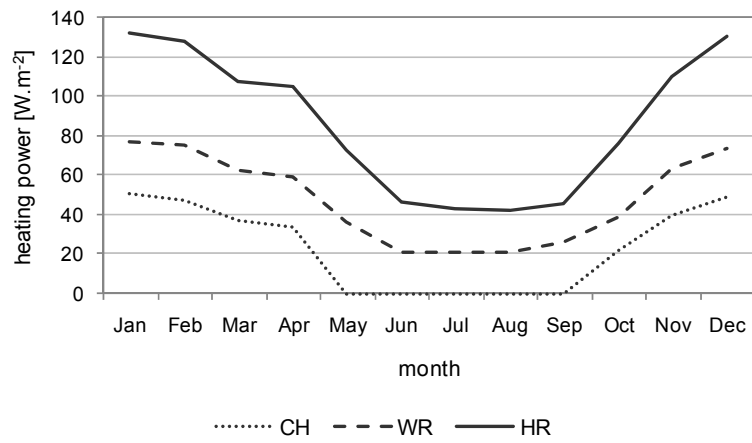


Figure 48 Space heating assumptions ($W.m^{-2}$) for SEN

3.5.2.5. Constantine model

A model of the Constantine hammam was generated, with 6 distinctive zones. In the following table (Table 17) information about zone name, area and volumes are summarized. Based on information of the local case study team, it was assumed that masonry was made of limestone and brick. Assumptions regarding construction are summarized in Table 18.

Table 17 Modeled Zones

	Zone	m ²	m ³
1	Changing Room	125.86	397.87
2	Changing room Transition	3.46	9.31
3	Cold Room	29.97	104.68
4	SAS	5.24	19.66
5	Hot Room	73.45	260.21
6	Furnace	108.49	168.11

Table 18 Simulation assumption regarding construction data (U-value, mass, g-value)

	Construction	Material	U-value [W.m ⁻² .K ⁻¹]	m [kg.m ⁻²]	g-Value [-]
1	Roof CH	limestone mortar, brick, wood and tiles	0.38	582	
2	Roof HR	Limestone mortar, brick and cement mortar	2.18	409	
3	Walls CH	Limestone with mortar	1.0	1800	
4	Walls HR	Limestone with mortar	0.8	2400	
5	Floor CH	Tiles, limestone and soil	0.7	1560	
6	Floor HR	Marble, limestone and soil	0.7	2490	
7	Glazing	Single glazing	5.6		0.4

Internal gains

It was suggested that 13 people per day use the hammam from Saturday to Wednesday and 40 people on Thursday and Friday.

Internal gains due to lighting were based on assumptions during the site visit (HAMMAM 2007a). Ventilation rates are summarized in Table 19.

Table 19 Assumptions regarding air change rate and internal gains

Zone	Air change rate [h ⁻¹]	Internal gains [W.m ⁻²]
CH	0.1 – 0.5	0 – 4.6
CR	0.1 – 0.5	0 – 1.4
HR	0.1	0 – 8.4

Heating assumptions

Based on an invoice for water supply for a trimester period, an annual water consumption of $669 \text{ m}^3.\text{a}^{-1}$ was extrapolated (HAMMAM 2007a). Water meter readings were taken by the local case study team which indicated a daily consumption of $3.36 \text{ m}^3.\text{d}^{-1}$, (1226 m^3 per year). Typical water use was between 4 and 6 buckets per person. It was estimated that 13 people during the week and 40 people on Thursday and Friday use the hammam, implying a water consumption of $756 \text{ m}^3.\text{a}^{-1}$ (bucket volume from 0.02 m^3). These three estimations imply to a total water consumption of $884 \text{ m}^3.\text{a}^{-1}$.

Furthermore, it was suggest that the typical ratio of hot and cold water buckets varies between 1:3 and 2:4 (i.e. 30% of hot water use). The measured average hot water supply was 70°C . Cold water inlet temperature was measured at 28°C . Taken this into account, an average temperature of 41°C of all water used within the hot space could be calculated.

Based on the assumption that 884 m^3 of water are used within a year it could be estimated that approximately 2400 liters per day were used in the hammam. Since the cold room is for the time being not used as a washing space, it was estimated that all the water was used within the hot room which would lead to a $33 \text{ l.m}^{-2}.\text{d}^{-1}$.

It was suggested that the water cools down approximately 10 K before it leaves the room. This would imply a heating power of roughly 16 W.m^{-2} .

The total space heating output of the hypocaust system was calculated as 40968 kWh.a^{-1} (HAMMAM 2007a). In order to estimate the monthly heating load by the hypocaust the relationship to the prevailing average outside temperature was used. The following figure (Figure 49) shows the calculated results. Note that for the months from July to December, the average monthly temperature of a dedicated Meteonorm file was used.

For comparison purpose, the space heating demand was also derived by the numerical simulation model using the measured values of indoor temperatures. The results are shown in the following figure (Figure 49). The actual assumptions used for the simulation model is summarized in figure 50.

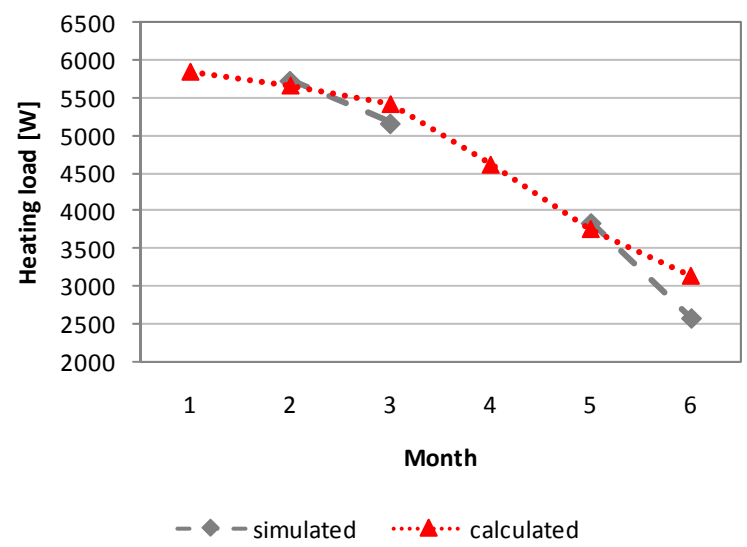


Figure 49 Heating load of hammam SAG calculated based on energy use data and simulated based on measured indoor temperature values

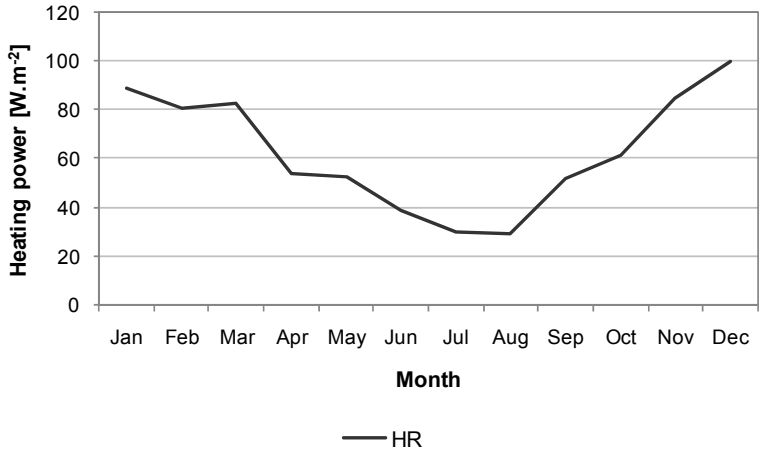


Figure 50 Heating power assumptions for the simulation model (SAG)

3.5.2.6. Parametric studies

After calibration of the simulation model parametric studies were carried out. First, improvement options of the building envelope were tested. Secondly, the influence of the high thermal mass on the overheating tendency of the changing room during summer months and the influence on the heating loads during winter time were explored.

Simulation-based comparison of alternative improvement options

Three different scenarios were selected to illustrate the utility of the calibrated simulation models toward comparison of thermal improvement possibilities of the buildings (in this case, BAB, SEN, and SAG). The first scenario (S1) represents the existing conditions. The second scenario (S2) involves the improvement of the thermal insulation of the roof construction. The third scenario (S3) involves, in addition to the thermal improvement in S2, the use of double-glazing (instead of the existing single-glazing) for windows (CH) and roof apertures (CR, WR, and HR) of the buildings. The respective U-value and g-value assumptions (for roof and glazing) in these scenarios are summarized in Table 20 (Orehounig and Mahdavi 2009).

Table 20 U-value and g-value assumptions regarding the pertinent building components for thermal simulation scenarios S1 to S3

		U-value [$\text{W}\cdot\text{m}^{-2}\cdot\text{K}^{-1}$]		g-value
		Roof	Glazing	Glazing
BAB	S1	1.80	5.80	0.54
	S2	0.28	5.80	0.54
	S3	0.28	1.36	0.41
SEN	S1	1.21	5.60	0.69
	S2	0.19	5.60	0.69
	S3	0.19	1.36	0.40
SAG	S1	1.39	5.60	0.40
	S2	0.20	5.60	0.40
	S3	0.20	1.36	0.41

Simulation-based inquiry into the thermal mass effect

Plans for new bath buildings deviate – mostly due to cost and space saving considerations – from the highly massive construction styles of traditional hammams. It was thus of interest to consider the implications of a rather low-mass construction style for the thermal performance (heating loads, overheating tendency). To explore this difference, simulations were used

to compare the performance of the existing buildings with virtual counterparts that would resemble them in all aspects other than the high thermal mass. Thereby two sets of simulation runs were performed, one to compute overheating tendency (in CH of the hammams) during the summer period, and one to obtain annual heating loads for all spaces. The respective simulation assumptions regarding air change rates, internal gains, and heating set points are summarized in Tables 21 (overheating simulation) and 22 (heating load simulation). Note that the surface density of wall and roof elements in the existing buildings (high thermal mass scenario) range from 315 to 2400 kg.m⁻². However, the assumed surface density for the low thermal mass scenario was approximately 180 kg.m⁻².

Table 21 Assumptions pertaining to air change rates (ACH in h⁻¹), internal gains (W.m⁻²), and heating set point (°C) for the study of thermal mass impact on overheating in hammams (CH)

	Opening hours			Closing hours		
	CH	CR/WR	HR	CH	CR/WR	HR
ACH	0.5	0.5	0.5	1	0.3	0.3
Internal gains	10	10	10	0	0	0
Heating set point	-	30	35	-	20	25

Table 22 Assumptions pertaining to air change rates (ACH in h⁻¹), internal gains (W.m⁻²), and heating set point (°C) for the study of thermal mass impact on the hammams' heating loads

	Opening hours			Closing hours		
	CH	CR/WR	HR	CH	CR/WR	HR
ACH	0.5	0.5	0.5	0.3	0.3	0.3
Internal gains	10	10	10	0	0	0
Set point for heating	25	30	35	15	20	25

Overheating tendency results are shown in terms of Mean Overheating (OH_m as per Eq. 3) of the indoor air in CH.

$$OH_m = \sum_{i=1}^n \frac{\theta_i - \theta_r}{n} \quad \text{Eq. 3}$$

In the above equation, θ_i denotes indoor air room temperature (°C) at hour i , θ_r the reference indoor air temperature for overheating (°C), and n the total number of considered hours over the summer period (opening hours). Note that the term $\theta_i - \theta_r$ (in Eq. 3) is considered only for those hours when $\theta_i > \theta_r$. In the illustrative example, the reference overheating temperature (θ_r) was assumed to be 27 °C.

3.5.3. Acoustic simulation

For some of the already mentioned objects, the reverberation time and ambient sound levels could be measured. Subsequently, these spaces were modeled with the aid of a computational tool for room acoustics simulation. From measurement results, a general impression of the acoustical performance of these spaces can be expected to emerge. Specifically, the acoustical features of these spaces were examined in the light of the kind of activities they are meant to accommodate. Moreover, the comparison of measurement and simulation results allows the evaluation of the reliability of acoustical simulation tools (as applied to such spaces) in view of their effectiveness toward design support (Mahdavi et al. 2008b). Acoustical simulations were performed for 3 objects, namely Hammam Suq al-Ghazal and two additional hammams (Hammam Belebdjaoui and Hammam Bougouffa) in Constantine, Algeria.

3.5.3.1. Simulation tool

Reverberation times were simulated for three buildings (Hammams Suq al Ghazal, Belebdjaoui, and Bougouffa). Simulations were performed using a commercially available room acoustical simulation and auralization tool (Christensen 2005). This tool provides different computational means for either simplified or detailed room acoustic simulations. For the purposes of the present research, the tool's detailed computational approach was employed, whereby responses from point sources are calculated using a hybrid calculation method: While the early reflections are computed using a combination of image source model and ray-tracing, the late reflections are calculated using a special ray-tracing process that generates secondary sources. These radiate energy locally from the surfaces of the walls. Further details on the algorithms applied in the simulation tool may be found in Christensen 2005.

The input data assumptions concerning the absorption coefficient data for surface finishes were based on various sources of information available (architectural documentation, plan documentation, literature, simulation tool's database). Note that one important purpose of the simulation studies was to explore the magnitude of deviations that can be expected when simulation runs based on information available to the designers (or their expert consultants) are to predict (post-construction) measured values. Reliable information on the discrepancies between acoustical simulation and measurement results is frequently lacking. Therefore, it is often difficult to judge the dependability of simulation at the design stage. Thus, in the present case, material properties for simulation input were defined independent of (and unaffected by) the measurement results.

To compute the reverberation times, virtual loudspeakers were placed in the model in the same location as the real sound source in the course of measurements. Likewise, the location of virtual microphone positions in the model matched those of the real microphone during the measurements (Mahdavi et al. 2008a).

3.5.3.2. Simulation models

As already mentioned acoustical simulation models were generated for three Hammams namely Suq al Ghazal (SAG), Bougouffa (BOU), and Belebjaoui (BEL). Figure 51 shows the corresponding used models. Table 23 shows assumptions regarding surface percentage and the scattering factor of the materials used for the simulation model. The input data assumptions concerning the absorption coefficient data for surface finishes were based on various sources of information available (literature, simulation tool's database) and are summarized in Table 24.

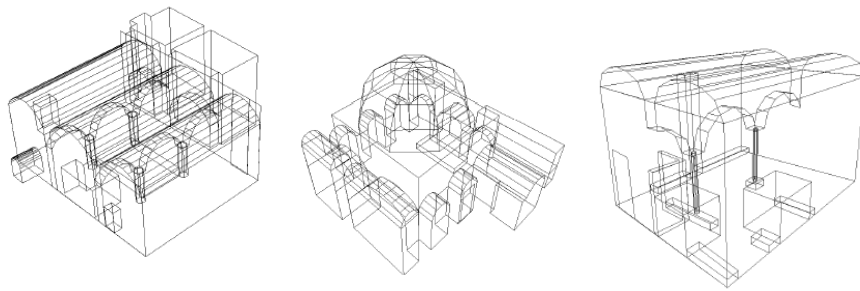


Figure 51 Odeon-model of SAG, BEL, and BOU (Kainrath 2008)

Table 23 Model input assumptions regarding surface percentage (%), area (m²), and scattering factor (Scat) of materials used in SAG, BEL, and BOU (Kainrath 2008)

Hamмам	Building Element	Nr.	Scat	m ²	%
SAG	Floor	3	0.1	75	18.7
	Benches	2	0.05	20	5.0
	Water	1	0.5	2	0.5
	Doors	5	0.05	3	0.7
	Windows	6	0.05	1	0.2
	Ceiling, Wall, Columns, Doms	4	0.05/0.4	300	74.8
BEL	Floor, Benches	2	0.1	60	20.9
	Water	1	0.5	5	1.7
	Doors	5	0.05	2	0.7
	Ceiling, Wall, Columns, Doms	4	0.05/0.4	220	76.7
BOU	Floor, Benches	2	0.1	50	22.5
	Water	1	0.5	3	1.5
	Doors	5	0.05	2	1.0
	Ceiling, Wall, Columns, Doms	4	0.05/0.4	160	75.0

Table 24 used materials and there respecting sound absorption coefficients (Kainrath 2008)

NR.	Material	Frequency [Hz]							
		63	125	250	500	1000	2000	4000	8000
1	Water in Pool	0.01	0.01	0.01	0.01	0.02	0.02	0.03	0.03
2	Tiles	0.01	0.01	0.01	0.01	0.02	0.02	0.02	0.02
3	Stone	0.02	0.02	0.02	0.02	0.02	0.02	0.02	0.02
4	Plaster	0.02	0.03	0.03	0.03	0.04	0.05	0.05	0.05
5	Doors	0.14	0.14	0.10	0.06	0.08	0.01	0.01	0.01
6	Glazing	0.35	0.35	0.25	0.18	0.12	0.07	0.04	0.04

3.5.3.3. Improvement scenarios

To improve the acoustical situation in the hot room, scenarios were developed for the Hammam Bougouffa. This involves three different conditions (see Table 25). The first condition represents the status quo. The second condition involves the treatment of parts of the wall surface with a humidity-resistant acoustic plaster. The third condition involves the treatment of the same wall surface area with an alternative (broad-band) acoustical absorber. The respective absorption coefficient values are shown in Table 25 (Mahdavi et al. 2008b).

Table 25 used materials and there respecting sound absorption coefficients

Simulation condition	Building material	Frequency [Hz]						
		125	250	500	1000	2000	4000	
C1	Status quo	0.03	0.03	0.03	0.04	0.05	0.05	
C2	Acoustic plaster	0.15	0.19	0.29	0.46	0.58	0.7	
C3	Broad-band acoustical absorber	0.64	0.87	0.84	0.62	0.47	0.5	

4. Results

4.1. Overview

This chapter summarizes the main results. It is divided into hygro-thermal indoor conditions, acoustical, and visual measurement results, and the simulation results. Further details of the results can be found in the appendix.

4.2. Hygro-thermal Indoor Conditions

The first part of the results section deals with hygro-thermal indoor conditions in the selected buildings. Thereby, results are structured in terms of hourly indoor values for reference days for selected months. Secondly, a selection of the relative temperature values for all hammam-spaces is given. The third part shows the indoor air temperature ranges within the observation period during opening hours. Finally, the thermal comfort conditions in the hammams' changing rooms are summarized.

4.2.1. Cairo

4.2.1.1. Hourly values for reference days

The following figures (Figure 52 to Figure 55) show the hourly temperature values for reference days over the whole measurement period from March 2006 to February 2007 for changing room (CH) (Figure 52), cold room (CR) (Figure 53), hot room (HRa) (Figure 54), and pool room (HRb) (Figure 55). Figure 56 shows, in addition, the external temperature measured during the same period. The sensor locations are marked on the corresponding floor plans.

Changing Room

During summer months, from June to September, as well as in May and October, temperature in the changing room follow slightly the shape of the outside temperature. In colder months, temperatures are higher from 20:00 to 6:00. This might be due to the fact that men often stay overnight and space heating is provided at that time by a stove (see Figure 52).

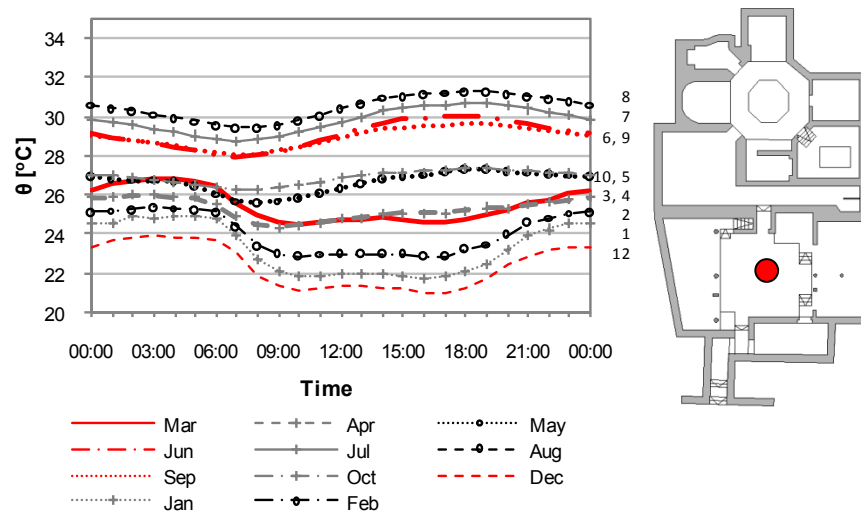


Figure 52 Indoor air temperature [°C] in CH of BAB for the observation period March 2006 to February 2007

Cold Room

As shown in Figure 53, temperatures in the cold room slightly rise from 10:00 to 16:00. In the colder months the increase was a little larger, which implies that the door to the hot room was kept more open. A part of the increase during summer time could also be caused by the higher outdoor temperatures.

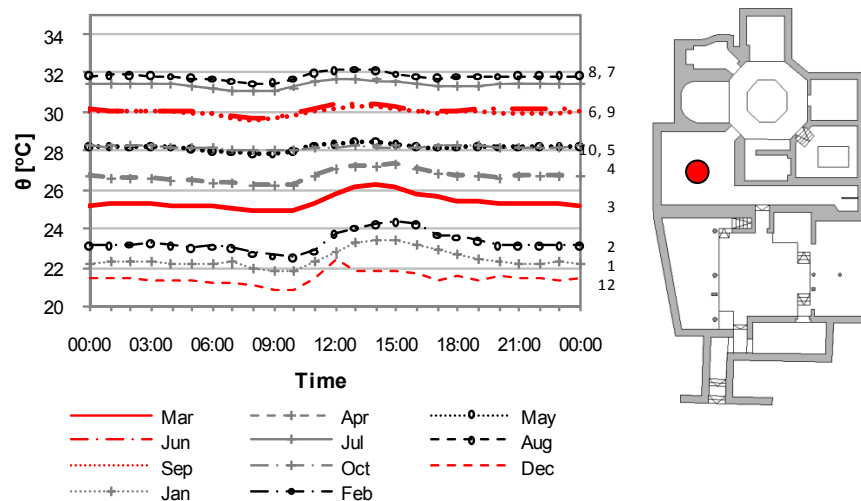


Figure 53 Indoor air temperature [°C] in CR of BAB for the observation period March 2006 to February 2007

Hot Room

As mentioned before, the hot area is mainly heated by filling the hot pool (maghtas). The information provided to the research team at the site suggested that the pool water was changed twice a day. However, our long-term indoor temperature measurements in the hot area in general and in the pool area in particular imply that the pool water is actually

changed only once every day, namely late afternoon (see, as an indicative sign, the 3K rise of indoor temperature shown in Figures 55).

The central space of the hot room shows a quite stable temperature distribution during operation time. Temperatures lay 50% of the time over 33°C. During summer months, temperatures are about 3K higher than the rest of the time (see Figure 54).

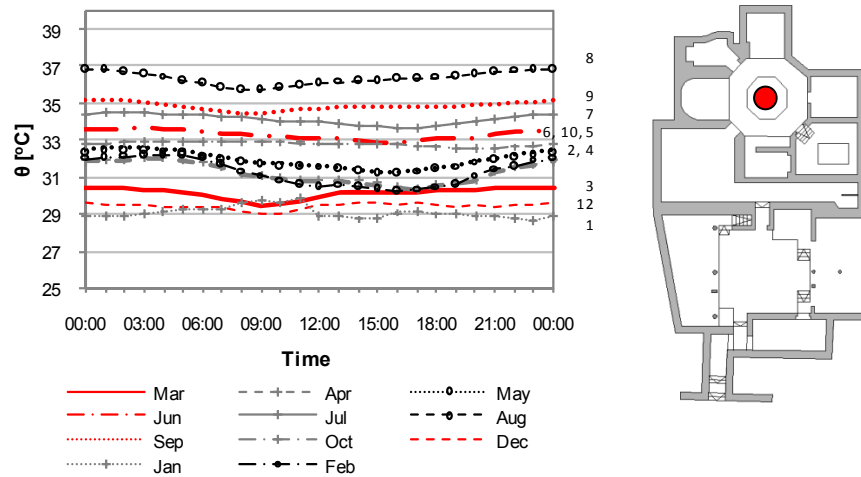


Figure 54 Indoor air temperature [°C] in HRa of BAB for the observation period March 2006 to February 2007

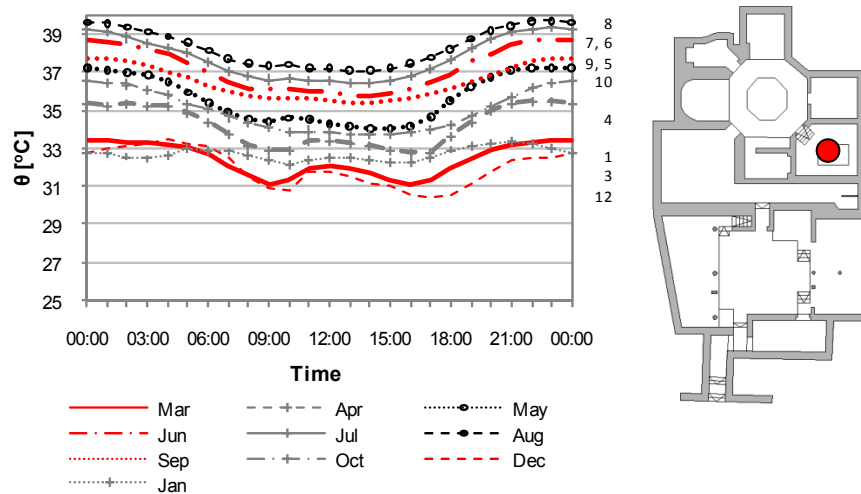


Figure 55 Indoor air temperature [°C] in HRb of BAB for the observation period March 2006 to February 2007

Outside

The following figure (Figure 56) shows the external temperature measured during the observation period.

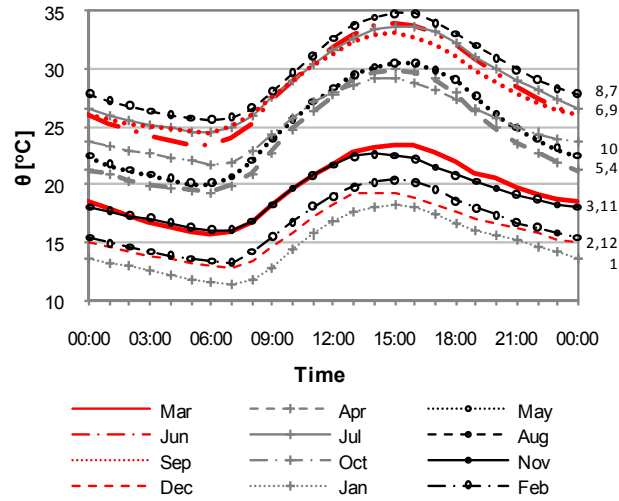


Figure 56 Outside air temperature [$^{\circ}\text{C}$] of BAB for the observation period March 2006 to February 2007

To allow for a convenient comparison of the hygro-thermal conditions in different spaces of the hammam during the same time period, the following figures (Figures 57 to 62) show the hourly temperature and relative humidity values (for the reference months July 2006, October 2006, and January 2007) for the entrance area (EN), the changing room (CH), the cold room (CR) the main hot room (HRa), and the Pool room (HRb). Note that these figures include also the respective average outside temperature (EX). Further results from May 2006 to March 2007 are given in the appendix (Section 8.2.1).

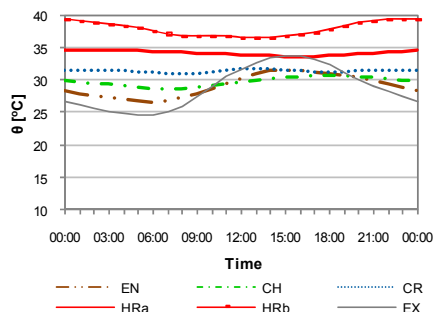


Figure 57 Temperature θ_{i+e} [$^{\circ}\text{C}$] Cairo July 2006

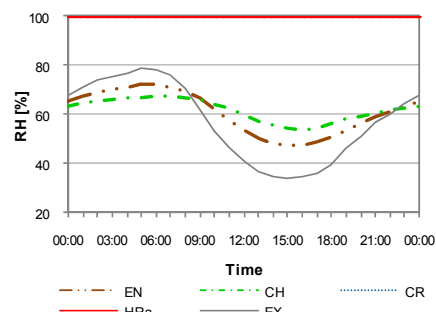


Figure 58 Relative Humidity RH [%] Cairo July 2006

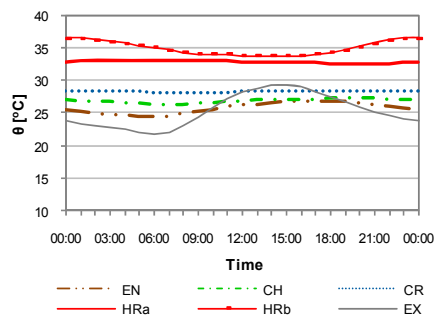


Figure 59 Temperature θ_{it} [°C] Cairo October 2006

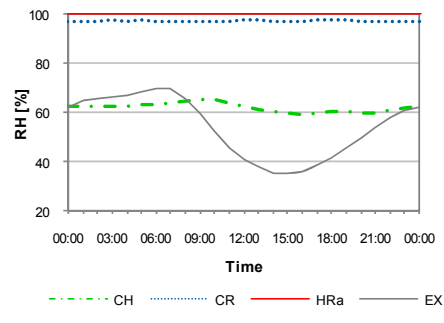


Figure 60 Relative Humidity RH [%] Cairo October 2006

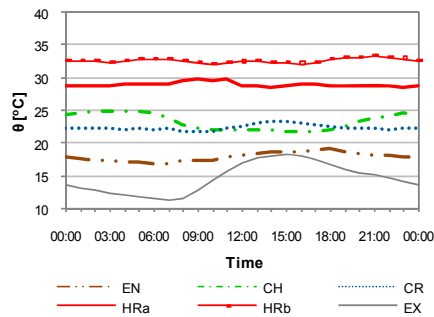


Figure 61 Temperature θ_{it} [°C] Cairo January 2007

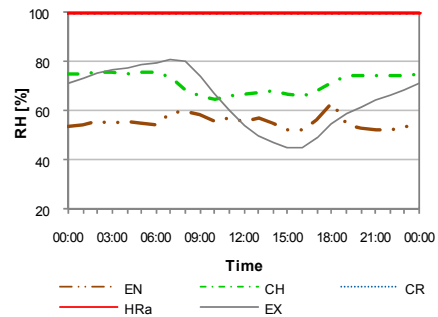


Figure 62 Relative Humidity RH [%] Cairo January 2007

4.2.1.2. Relative Temperature

The following figures (Figure 63 and 64) show relative temperatures (see Eq.1) for the months July and January for various spaces in the hammam. They visualize the connection between measured indoor and outdoor temperatures.

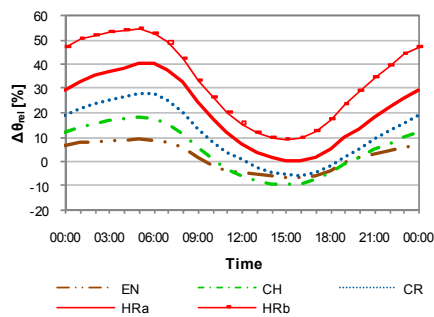


Figure 63 Relative Temperature [%] in July 2006

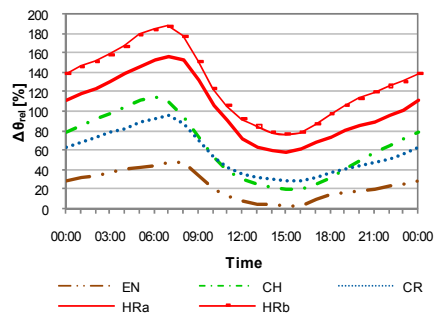


Figure 64 Relative Temperature [%] in January 2007

4.2.1.3. Temperature distribution

The distribution of the prevailing temperature ranges during the opening hours over the observation period March 2006 to February 2007 were calculated for the changing room, the cold room, the hot room, and the pool room (see Figures 65 to 68). Figure 69 shows the corresponding outdoor air temperature distribution.

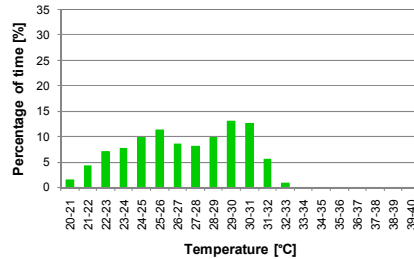


Figure 65 Temperature distribution in changing room of BAB during opening hours

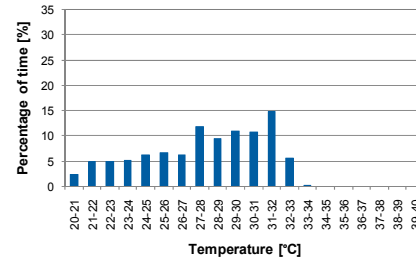


Figure 66 Temperature distribution in cold room of BAB during opening hours

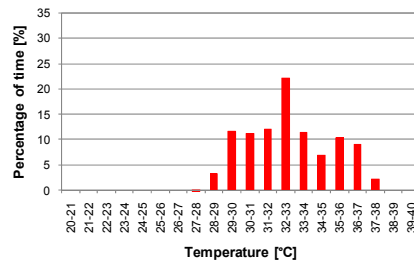


Figure 67 Temperature distribution in main hot room of BAB during opening hours

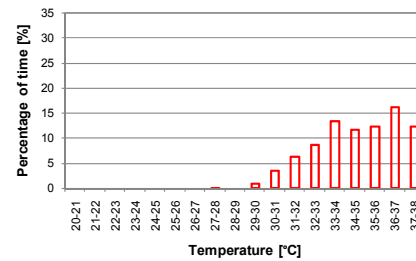


Figure 68 Temperature distribution in pool room of BAB during opening hours

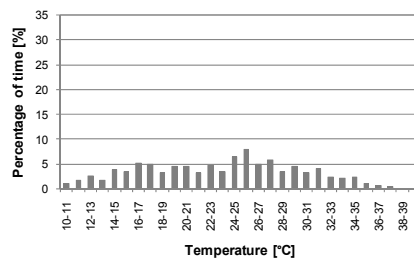


Figure 69 Temperature distribution of External temperature

4.2.1.4. Thermal Comfort conditions

Changing Room

Figure 70 shows the results of hourly hygro-thermal measurements in the changing room of the hammam (for reference days in January, April, July and October) in a psychometric chart. Note that the figure includes also the SET lines (see section 3.4.2.5) for the relevant months.

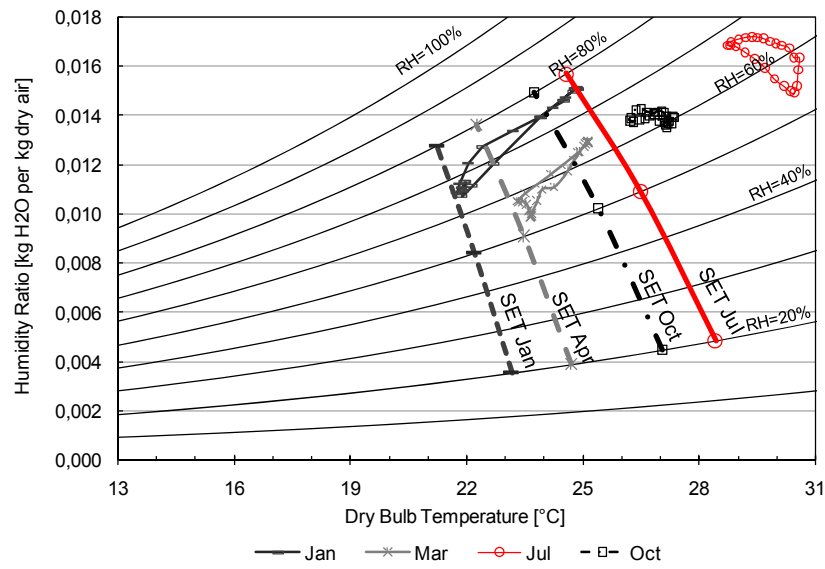


Figure 70 Depiction of indoor climate conditions in the changing room in BAB for July and October 2006, January and April 2007, compared to Standardized Effective Temperature SET for each month

4.2.2. Ankara

4.2.2.1. Hourly values for reference days

The following figures (Figure 71 to 75) show the hourly temperature values for reference days over the whole measurement period from July 2006 till June 2007 for changing room (CH), warm room (WR), and hot room (HR) of the women section as well as the changing room and hot room of the men section. Figure 76 shows, in addition, the external temperature measured during the same period. The sensor locations are marked on the corresponding floor plans.

Changing Room

The changing rooms of the Turkish hammam are not heated during summer months. Pattern of indoor air temperatures are similar to the prevailing outside temperature. In the colder months from November to April changing rooms seem to be heated, due to the steeper rise of temperature during daytime. Temperatures in mens' changing room are more stable and do not drop as much as those in the women section, which could be due to the fact that men opening hours are longer in the evening.

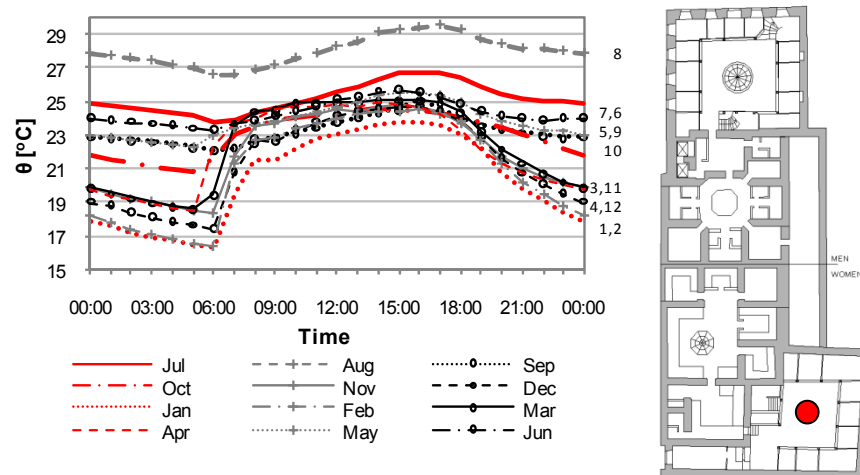


Figure 71 Indoor air temperature [°C] in CH of women section in SEN for the observation period July 2006 to June 2007

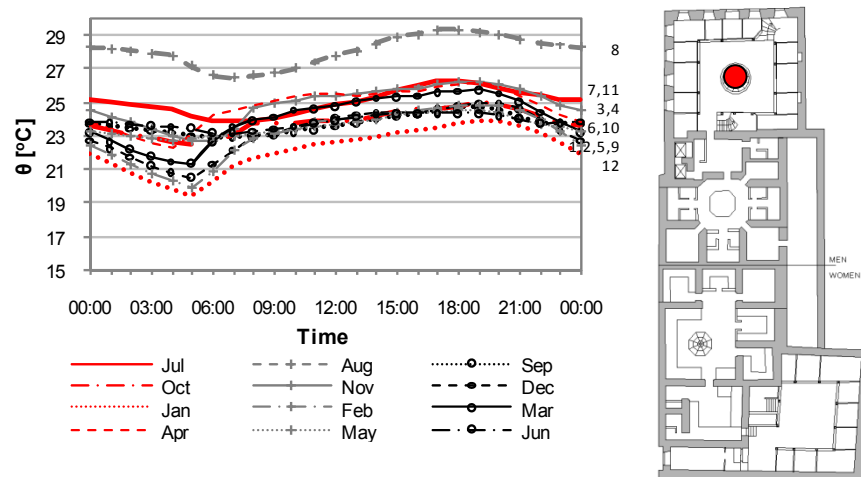


Figure 72 Indoor air temperature [°C] in CH of men section in SEN for the observation period July 2006 to June 2007

Warm Room

Temperatures of womens' warm room are fairly stable during summer months and do not drop in the night as much as in winter. Temperatures vary between 24°C in January and 31°C in August.

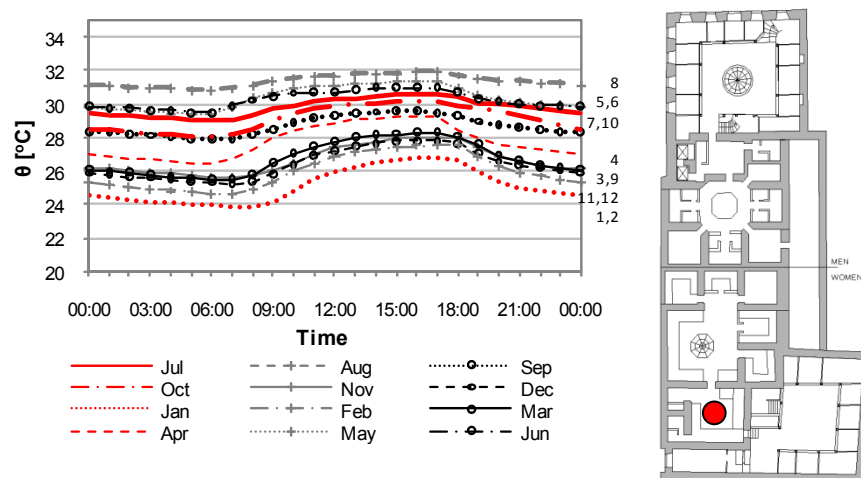


Figure 73 Indoor air temperature [°C] in WR of women section in SEN for the observation period July 2006 to June 2007

Hot Room

Temperatures of womens and mens hot rooms are very stable during the day. In summer months temperatures are about 37°C and 34°C in winter.

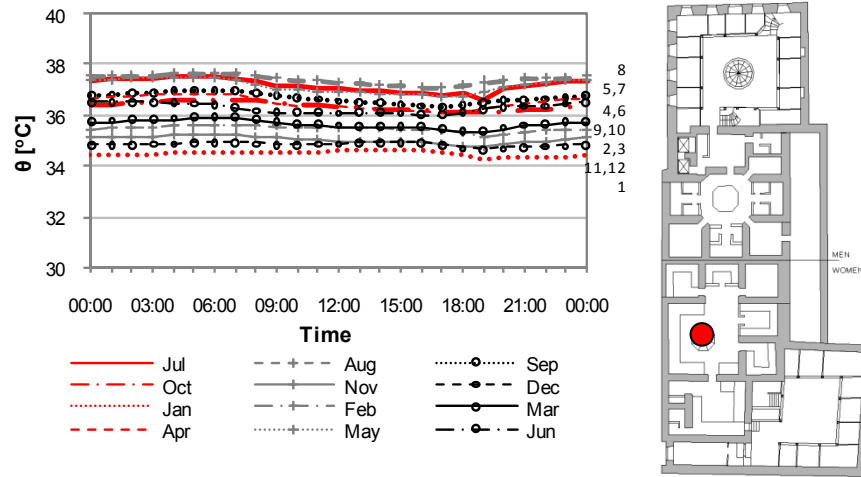


Figure 74 Indoor air temperature [°C] in HR of women section in SEN for the observation period July 2006 to June 2007

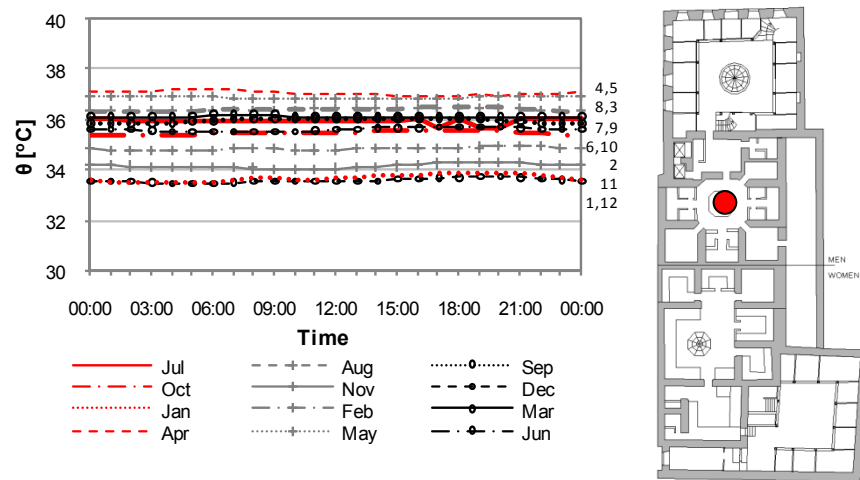


Figure 75 Indoor air temperature [°C] in HR of men section in SEN for the observation period July 2006 to June 2007

Outside

The following figure (Figure 76) shows the external temperature measured during the observation period.

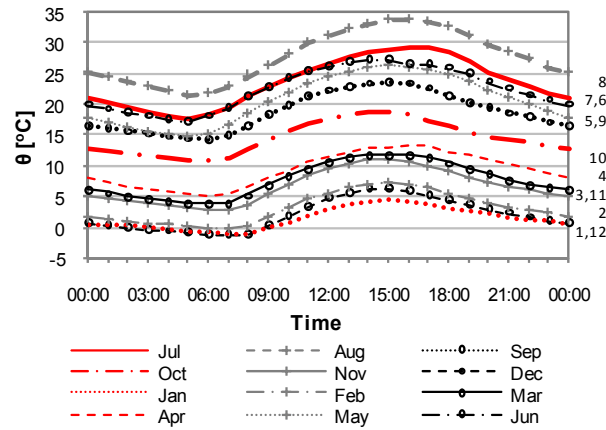


Figure 76 Outside air temperature $[\text{°C}]$ of SEN for the observation period July 2006 to June 2007

To allow for a convenient comparison of the hygro-thermal conditions in different spaces of the hammam during the same time period, the following figures (Figures 77 to 82) show the hourly temperature and relative humidity values (for the reference months August 2006, December 2006, and April 2007) for the entrance area (EN), the changing room (CH), the warm room (WR), and the hot room (HR) in the women section of the hammam Sengül. Note that these figures include also the respective average outside temperature (EX). Further results are given in the appendix (Section 8.2.2).

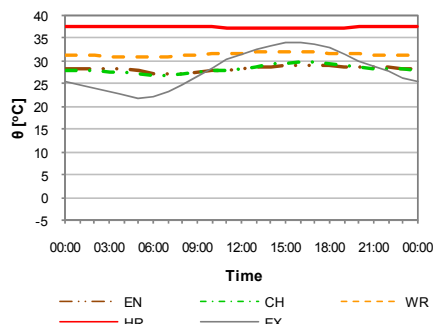


Figure 77 Temperature $\theta_{i+e} [\text{°C}]$ Ankara female-part August 2006

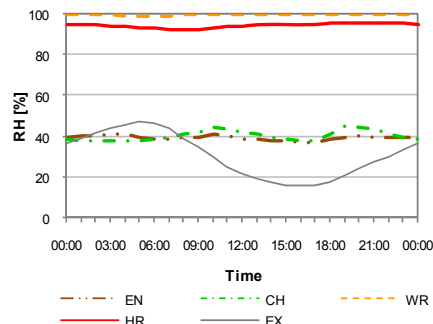


Figure 78 Relative Humidity RH [%] Ankara female-part August 2006

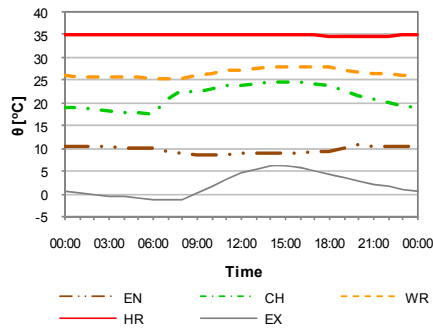


Figure 79 Temperature θ_{it} [°C] Ankara female-part December 2006

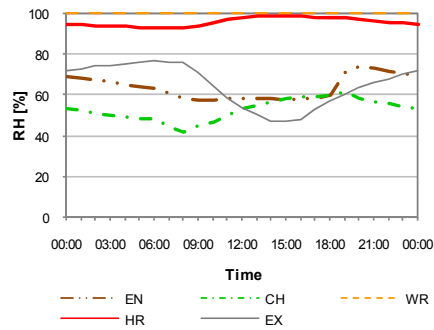


Figure 80 Relative Humidity RH [%] Ankara female-part December 2006

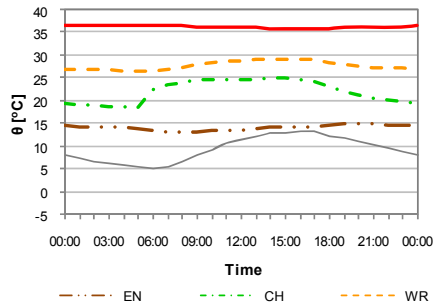


Figure 81 Temperature θ_{it} [°C] Ankara female-part April 2007

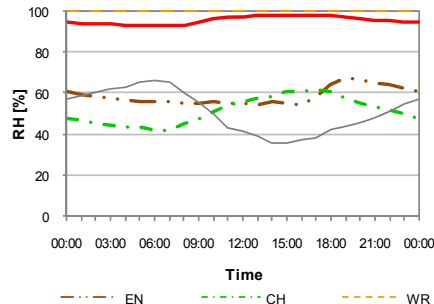


Figure 82 Relative Humidity RH [%] Ankara female-part April 2007

Following figures (Figures 83 to 88) show the hourly temperature and relative humidity values (for the reference months August 2006, December 2006, and April 2007) in changing room (CH) and hot room (HR) as well as the prevailing outdoor conditions (EX) for the men section of the hammam Şengül. Further figures can be found in the appendix (Section 8.2.2).

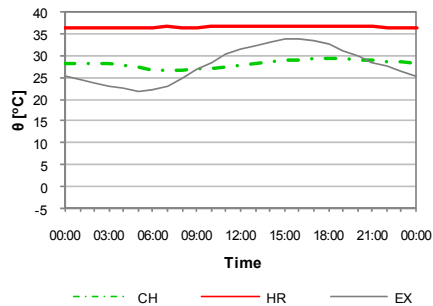


Figure 83 Temperature θ_{it} [°C] Ankara male-part August 2006

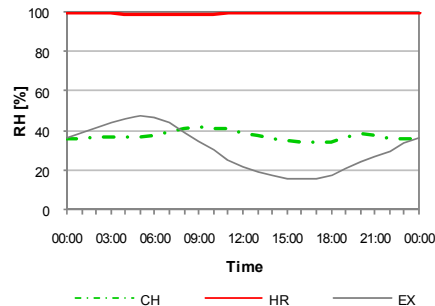


Figure 84 Relative Humidity RH [%] Ankara male-part August 2006

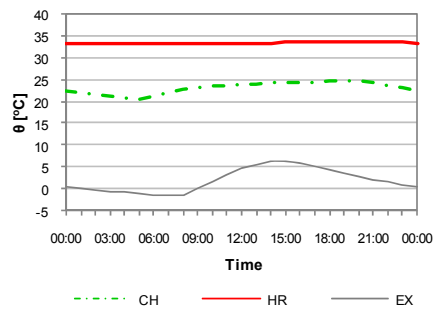


Figure 85 Temperature θ_{it} [°C] Ankara male-part December 2006

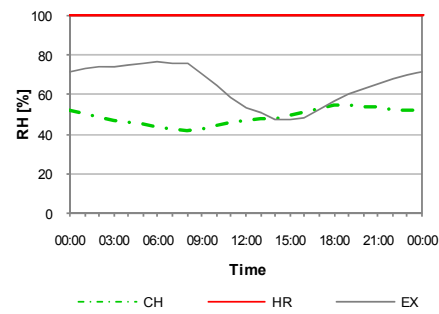


Figure 86 Relative Humidity RH [%] Ankara male-part December 2006

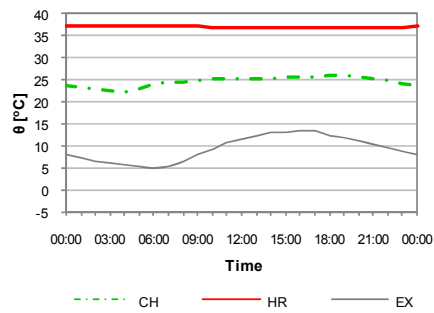


Figure 87 Temperature θ_{it} [°C] Ankara male-part April 2007

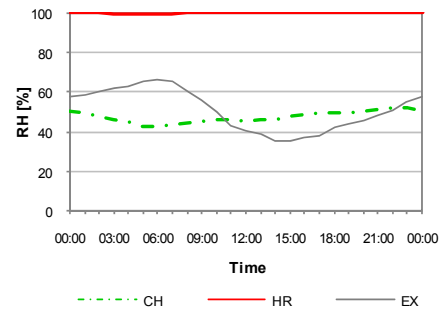


Figure 88 Relative Humidity RH [%] Ankara male-part April 2007

4.2.2.2. Relative Temperature

The following figures (Figures 89 and 90) exemplify relative temperatures for the months of August and April for various spaces in the hammam, namely entrance (ENw) changing room (CHw), warm room (WRw) and hot room (HRw) of the women section as well as changing room (CHm) and hot room (HRm) of the men section .

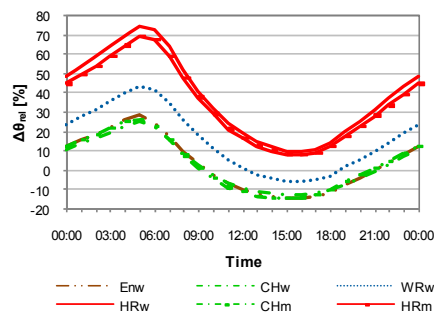


Figure 89 Relative Temperature [%] of August 2006

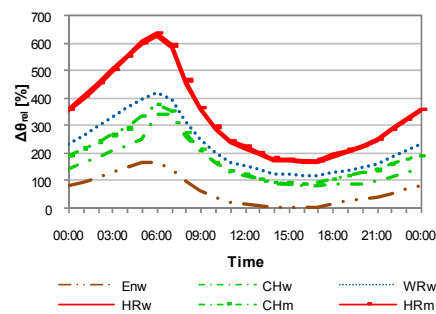


Figure 90 Relative Temperature [%] of April 2007

4.2.2.3. Temperature distribution

Temperature distribution during opening hours for the three spaces (changing room, warm room and hot room) in the women section, and for changing room and hot room in the men section are given in following figures (Figures 91 to 95). Figure 96 shows the corresponding outside temperature during the measurement period.

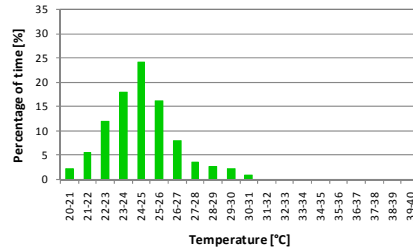


Figure 91 Temperature distribution in women changing room of SEN

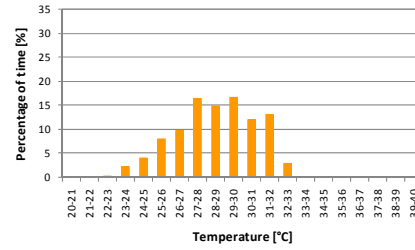


Figure 92 Temperature distribution in women warm room of SEN

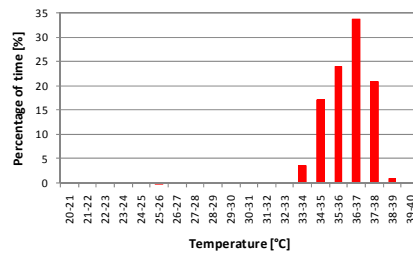


Figure 93 Temperature distribution in women hot room of SEN

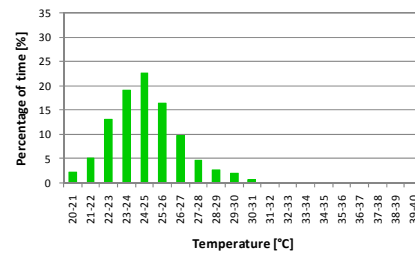


Figure 94 Temperature distribution in men changing room of SEN

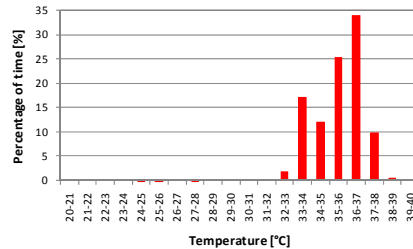


Figure 95 Temperature distribution in men hot room of SEN

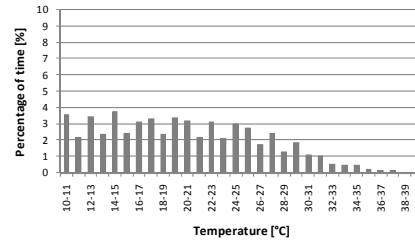


Figure 96 Temperature distribution of external temperature

4.2.2.4. Thermal Comfort conditions

Changing Room

Figure 97 shows the results of hourly hygro-thermal measurements in the changing room of the hammam (for reference days in January, April, July and October) in a psychometric chart. Note that the figure includes also the SET lines (see section 3.4.2.5) for the relevant months.

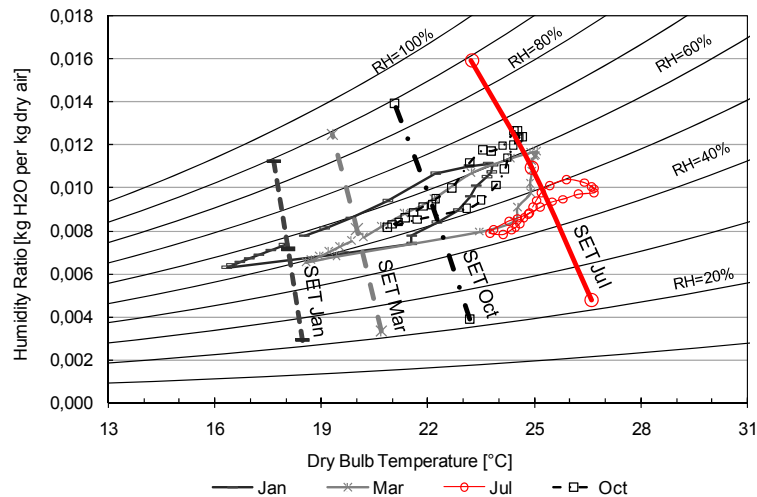


Figure 97 Depiction of the indoor climate conditions in the changing room in SEN for July and October 2006, January and March 2007, compared to Standardized Effective Temperature SET for each month

4.2.3. Fez

4.2.3.1. Hourly values for reference days

The following figures (Figure 98 to 105) show the hourly temperature values for reference days over the whole measurement period from October 2006 till September 2007 for changing room (CH), cold room (CR) warm room (WR), and hot room (HR) of the women and men sections. Figure 106 shows, in addition, the external temperature measured during the same period. The sensor locations are marked on the corresponding floor plans.

Changing Room

Temperatures in changing rooms of Hammam Saffarin follow the prevailing outside condition. The daily swing is more recognizable in men section than in women section. This could be due to the fact that the newer men section doesn't have as much thermal mass as the older women part. Temperatures lie within 25°C and 30°C during summer months and between 13°C and 22°C in winter months.

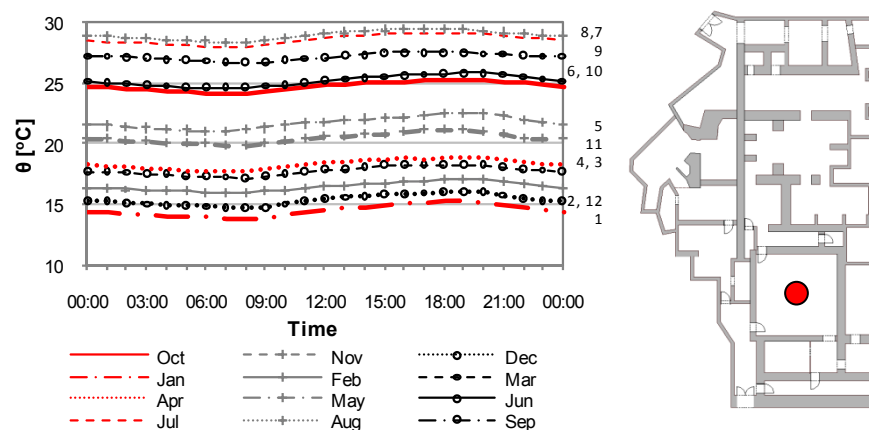


Figure 98 Indoor air temperature [°C] in CH of women section in SAF for the observation period October 2006 to September 2007

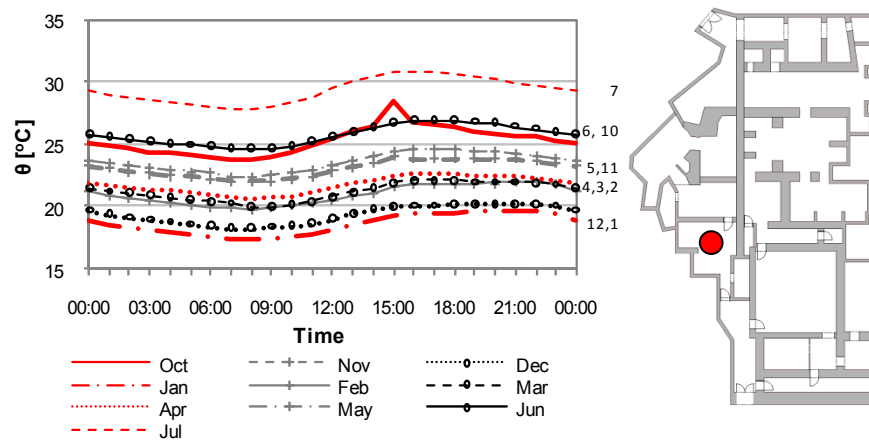


Figure 99 Indoor air temperature [°C] in CH of men section in SAF for the observation period October 2006 to September 2007

Cold Room

Temperatures in cold rooms of Hammam Saffarin vary between 27°C and 32°C. During summer time temperature curves show a more flat tendency then in winter months.

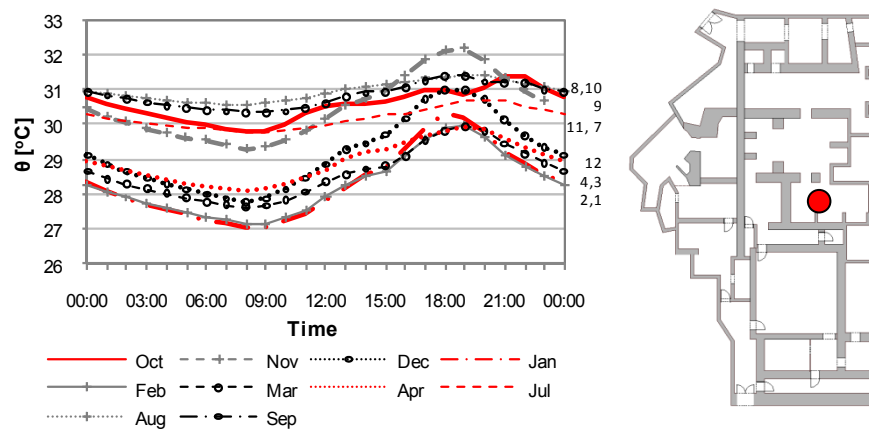


Figure 100 Indoor air temperature [°C] in CR of women section in SAF for the observation period October 2006 to September 2007

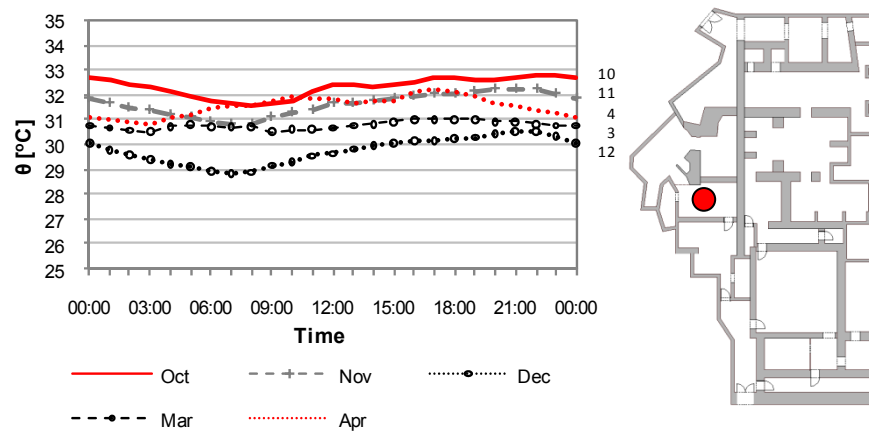


Figure 101 Indoor air temperature [°C] in CR of men section in SAF for five months during observation period

Warm Room

Temperatures in the warm room of the women section lie within 29°C and 33°C, showing similar patterns as those of the hot room. In winter months (January to March), temperatures behave slightly different. For the male section temperatures (available only for October and November) were between 32°C and 36°C.

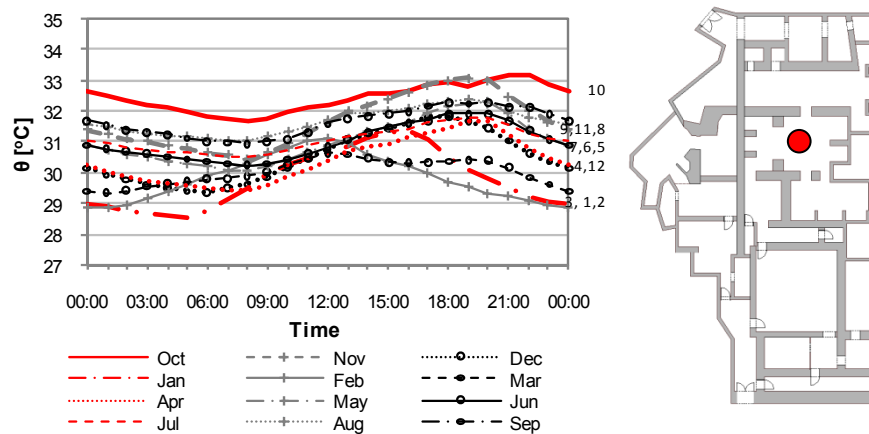


Figure 102 Indoor air temperature [°C] in WR of women section in SAF for the observation period October 2006 to September 2007

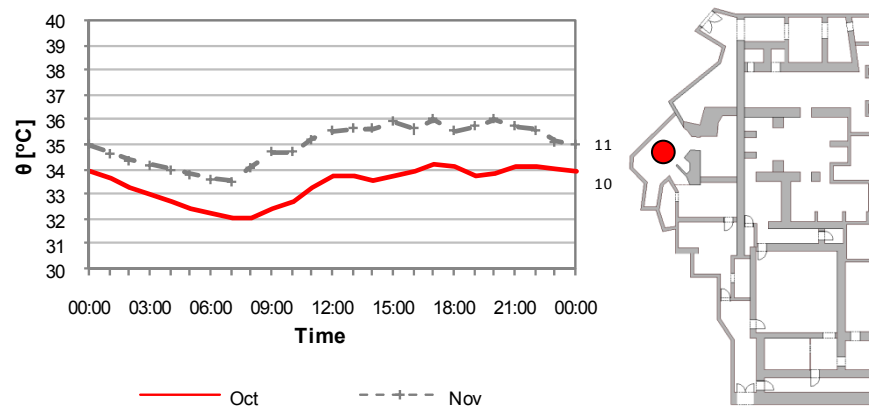


Figure 103 Indoor air temperature [°C] in WR of men section in SAF for two months during observation period

Hot Room

Hot rooms of the Hammam Saffarin are heated starting at 8:00 in the women section and 7:00 in the men section. Temperatures lie within 33°C and 35°C in the women section and 35°C and 37°C in the men section during opening hours. Due to longer opening hours in the men section temperatures are more stable than in the women section.

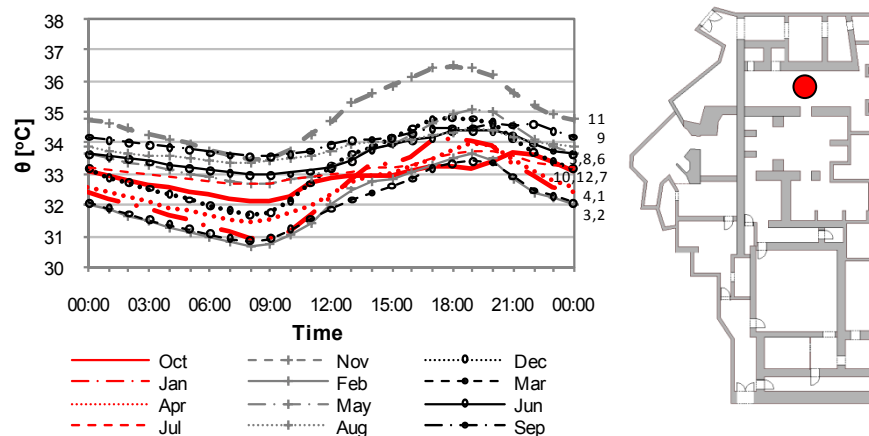


Figure 104 Indoor air temperature [°C] in HR of women section in SAF for the observation period October 2006 to September 2007

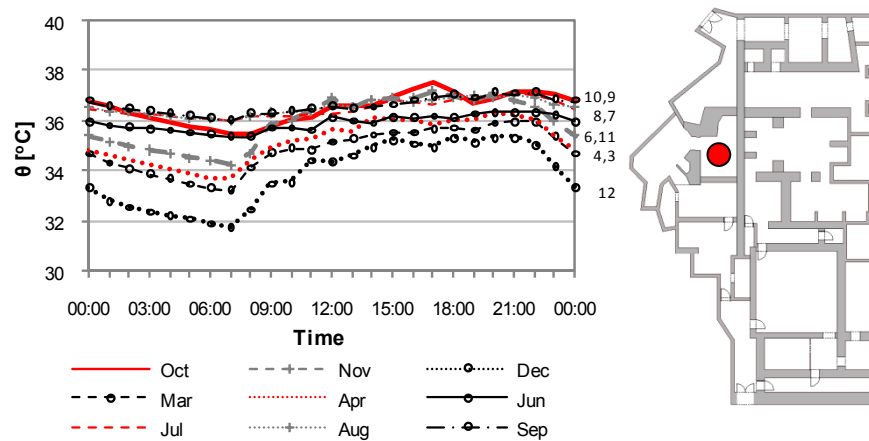


Figure 105 Indoor air temperature [°C] in HR of men section in SAF for the observation period October 2006 to September 2007

Outside

The following figure (Figure 106) shows the external temperature measured during the observation period.

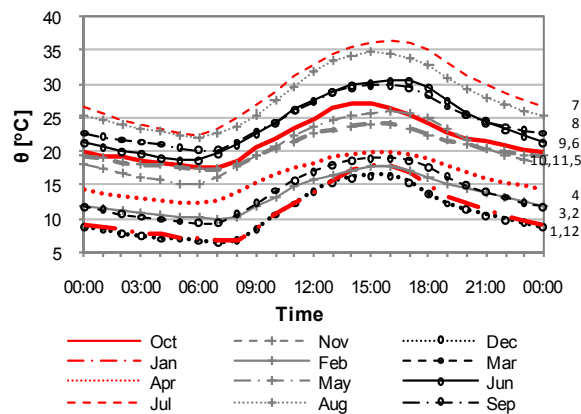


Figure 106 Outside air temperature [°C] of SAF for the observation period October 2006 to September 2007

To allow for a convenient comparison of the hygro-thermal conditions in different spaces of the hammam during the same time period, the following figures (Figures 107 to 112) show the hourly temperature and relative humidity values (for the reference months November 2006, April 2007, and July 2007) for the entrance area (EN), the changing room (CH), the warm room (WR), and the hot room (HR) in the women section of the hammam. Note that these figures include also the respective average outside temperature (EX). Further results are given in the appendix (Section 8.2.3).

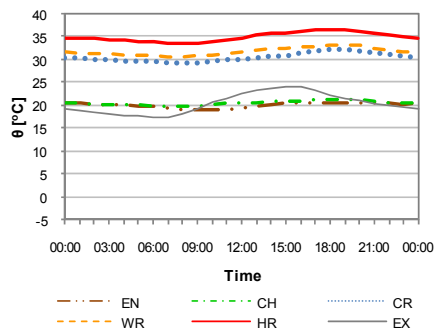


Figure 107 Temperature θ_{it_e} [°C] Fez female-part November 2006

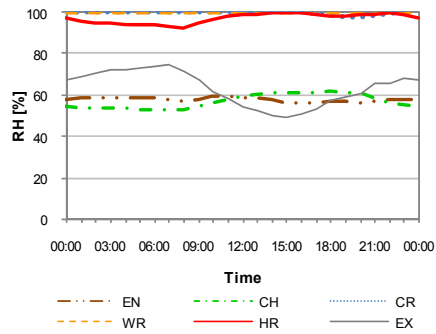


Figure 108 Relative Humidity RH [%] Fez female-part November 2006

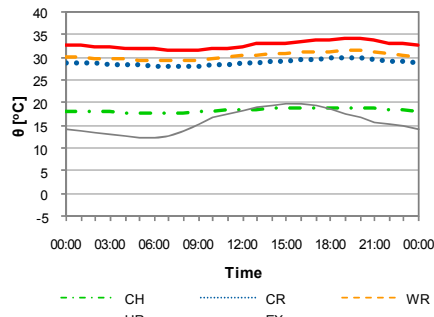


Figure 109 Temperature θ_{it_e} [°C] Fez female-part April 2007

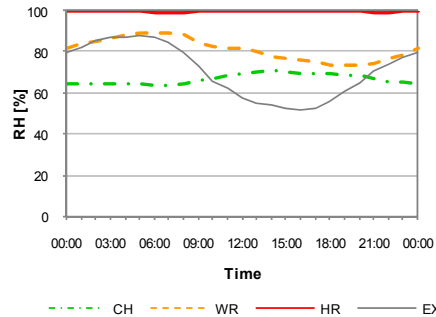


Figure 110 Relative Humidity RH [%] Fez female-part April 2007

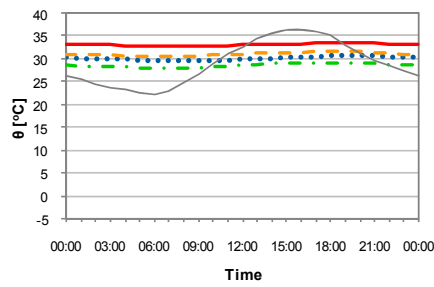


Figure 111 Temperature θ_{it_e} [°C] Fez female-part July 2007

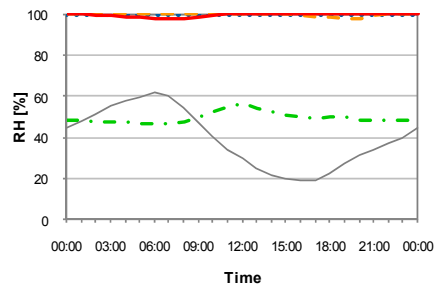


Figure 112 Relative Humidity RH [%] Fez female-part July 2007

Figures 113 to 118 display temperatures and relative humidity values for the men section. Further monthly averages for the observation period can be found in the appendix (Section 8.2.3).

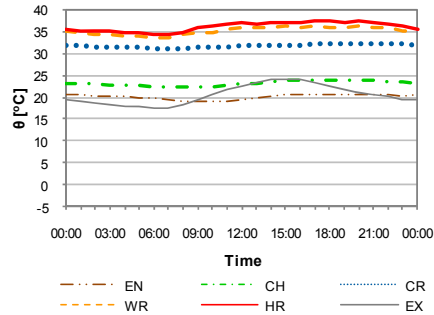


Figure 113 Temperature θ_{i+e} [°C] Fez male-part November 2006

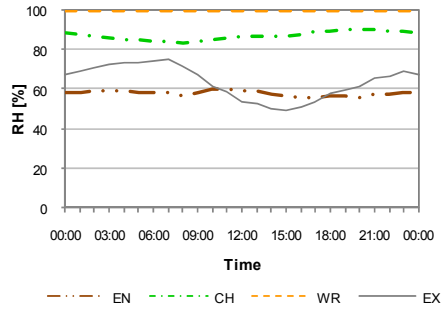


Figure 114 Relative Humidity RH [%] Fez male-part November 2006

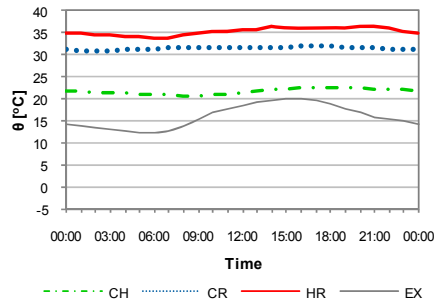


Figure 115 Temperature θ_{i+e} [°C] Fez male-part April 2007

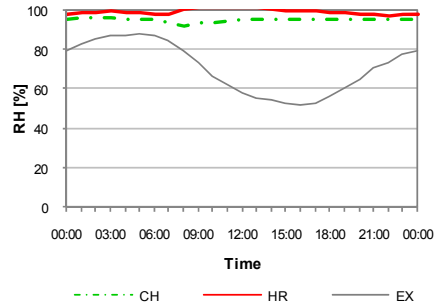


Figure 116 Relative Humidity RH [%] Fez male-part April 2007

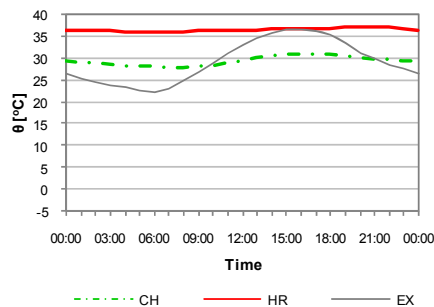


Figure 117 Temperature θ_{i+e} [°C] Fez male-part July 2007

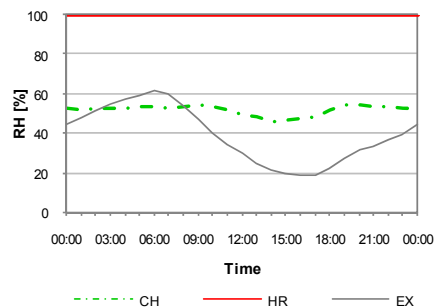


Figure 118 Relative Humidity RH [%] Fez male-part July 2007

4.2.3.2. Relative temperature

The following figures (Figures 119 and 120) show relative temperatures (see Eq.1) for the months November and April for various spaces in the hammam, namely the entrance area (EN), changing room (CHw), cold room (CRw), warm room (WRw) and hot room (HRw) of the women section and changing room (CHm), cold room (CRm), warm room (WRm) and hot room (HRm) of the men section. They visualize the connection between measured indoor and outdoor temperatures.

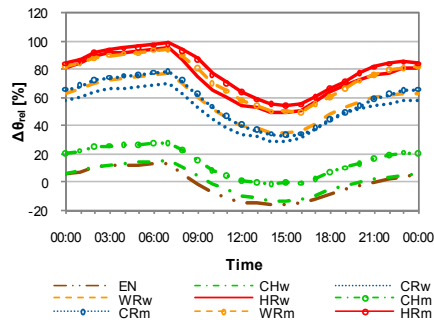


Figure 119 Relative Temperature [%] of November 2006

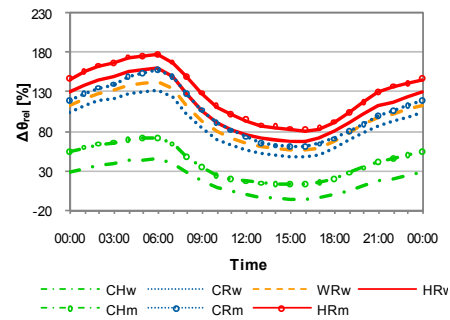


Figure 120 Relative Temperature [%] of April 2007

4.2.3.3. Temperature distribution

The distribution of the prevailing temperature ranges during the opening hours over the observation period were calculated for the changing room, the cold room, the warm room, and the hot room (see Figures 121 to 128). Figure 129 shows the corresponding outdoor air temperature distribution.

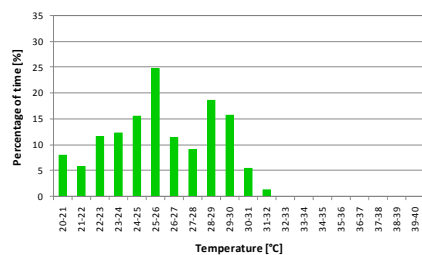


Figure 121 Temperature distribution in women changing room of SAF

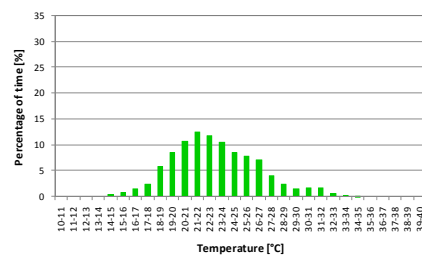


Figure 122 Temperature distribution in men changing room of SAF

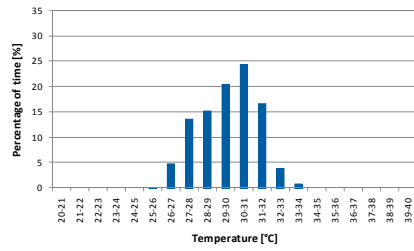


Figure 123 Temperature distribution in women cold room of SAF

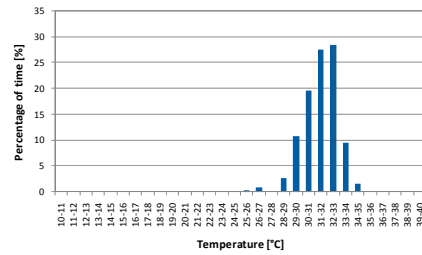


Figure 124 Temperature distribution in men cold room of SAF

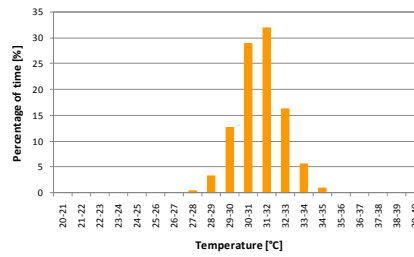


Figure 125 Temperature distribution in women warm room of SAF

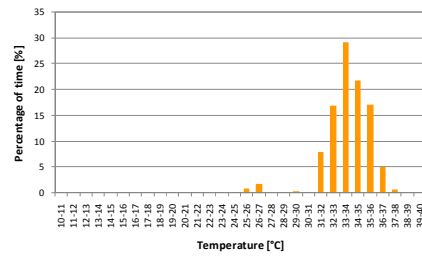


Figure 126 Temperature distribution in men warm room of SAF

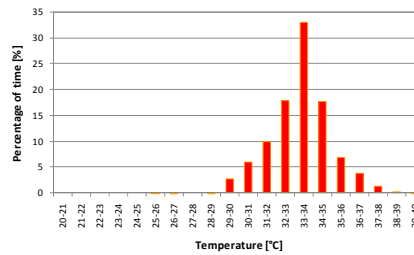


Figure 127 Temperature distribution in women hot room of SAF

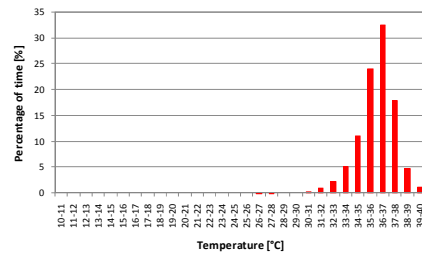


Figure 128 Temperature distribution in men hot room of SAF

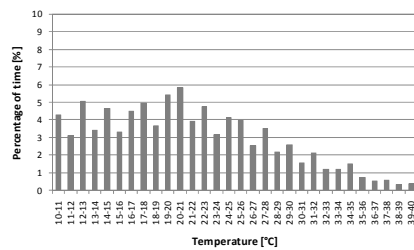


Figure 129 Temperature distribution of external temperature

4.2.3.4. Thermal Comfort conditions

Changing Room

Figure 130 shows the results of hourly hygro-thermal measurements in the changing room of the hammam (for reference days in January, April, July and October) in a psychometric chart. Note that the figure includes also the SET lines (see section 3.4.2.5) for the relevant months.

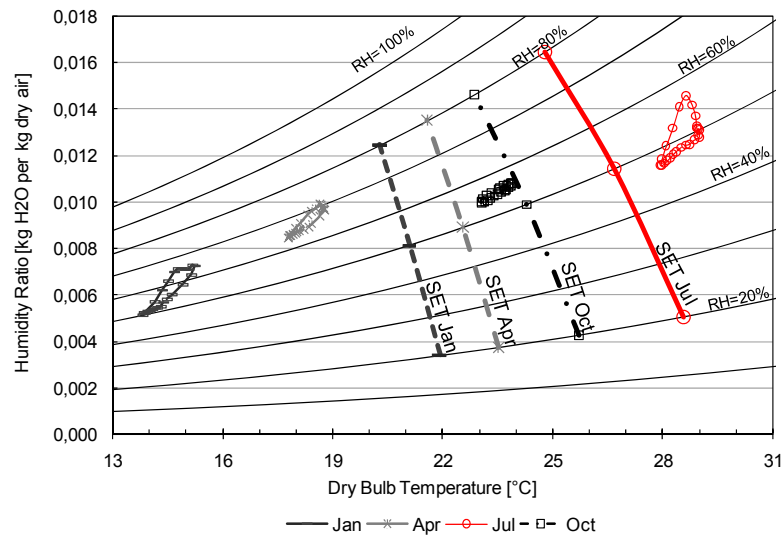


Figure 130 Depiction of the indoor climate conditions in the changing room in SAF for October 2006, January, April and July 2007, compared to Standardized Effective Temperature SET for each month

4.2.4. Damascus

4.2.4.1. Hourly values for reference days

The following figures (Figures 131 to 134) show the hourly temperature values for reference days over the measurement period from February 2007 to May 2007 for the spaces changing room, cold room, warm room, and hot room. Data collection had to be stopped after this time due to the renovation of the hammam. Figure 135 shows, in addition, the external temperature measured during the same period. The sensor locations are marked on the corresponding floor plans.

Changing Room

Changing room temperatures are very stable during the day. Temperatures drop to 15°C in February. This might be due to the absence of space heating.

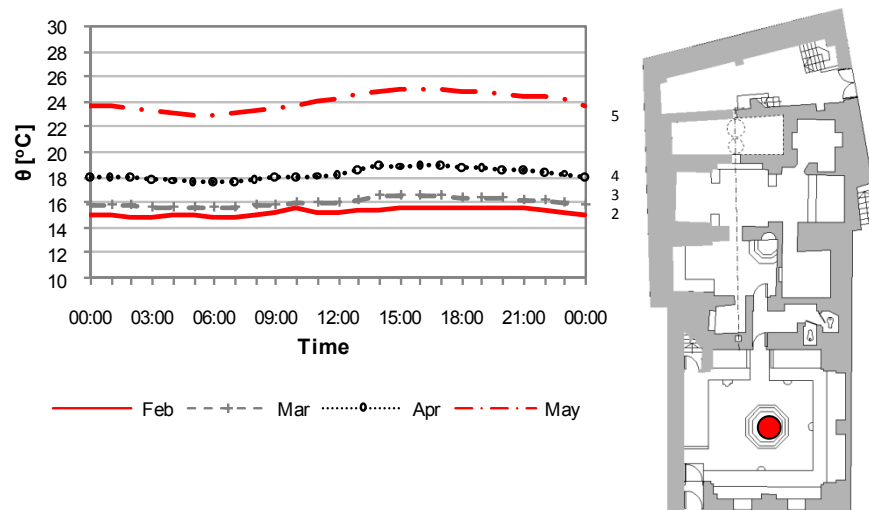


Figure 131 Indoor air temperature [°C] in CH of AMH for the observation period February 2007 to May 2007

Cold Room

The cold room of Hammam Ammouneh does not exist anymore as a designated space. Rather it houses the toilette facilities (temperatures between 25°C and 29°C).

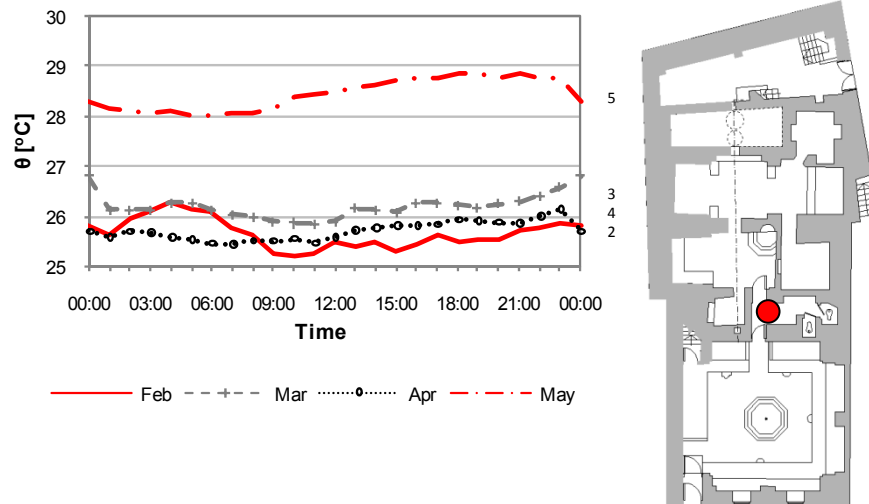


Figure 132 Indoor air temperature [°C] in CR of AMH for the observation period February 2007 to May 2007

Warm Room

The warm room has stable temperatures during the day (between 26°C in February and 30°C in May).

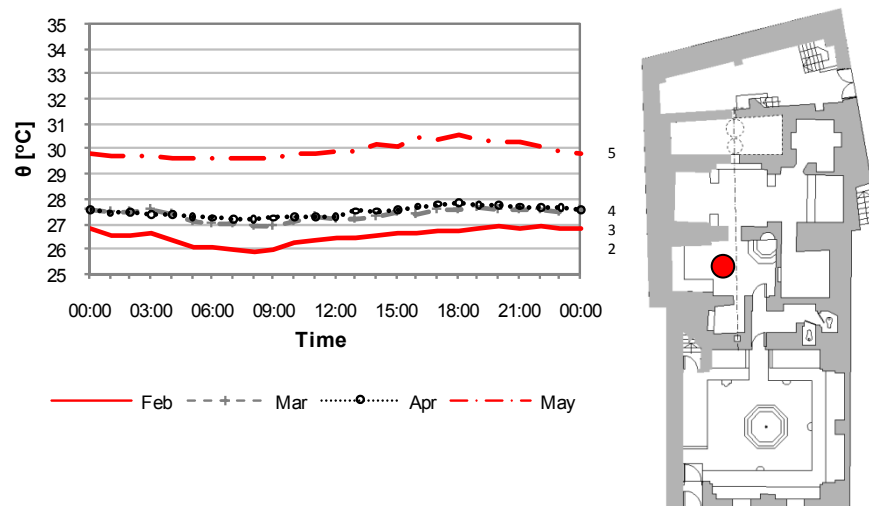


Figure 133 Indoor air temperature [°C] in WR of AMH for the observation period February 2007 to May 2007

Hot Room

Temperatures in the hot room show a slight increase during night hours (from 32°C to 33°C).

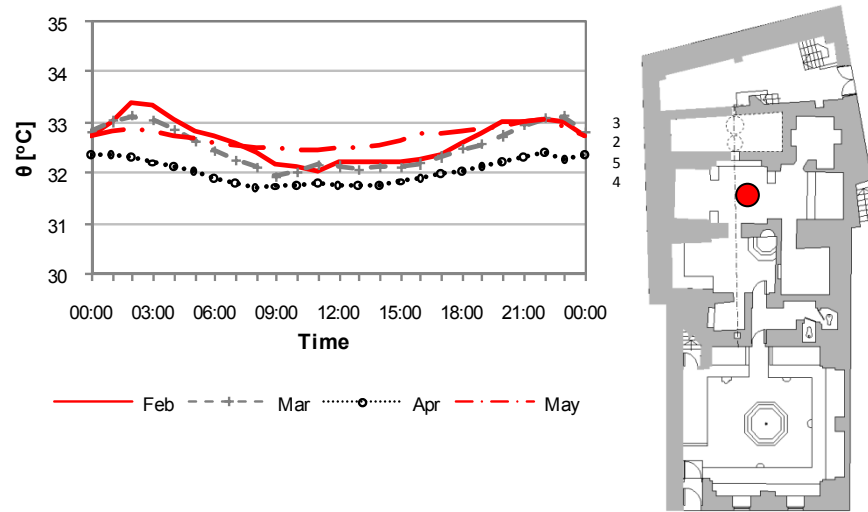


Figure 134 Indoor air temperature [°C] in HR of AMH for the observation period February 2007 to May 2007

Outside

The following figure (Figure 135) shows the external temperature measured during the observation period.

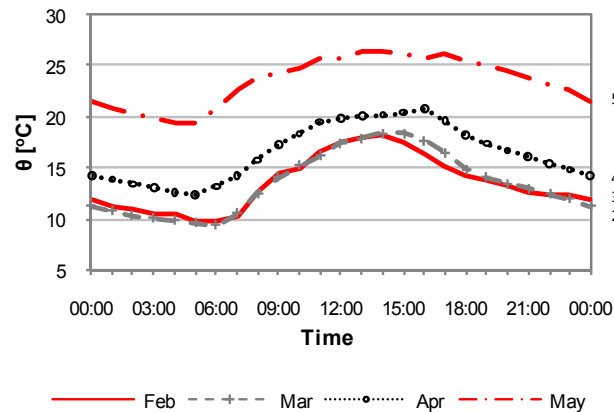


Figure 135 Outside air temperature [°C] of AMH for the observation period February 2007 to May 2007

To allow for a convenient comparison of the hygro-thermal conditions in different spaces of the hammam during the same time period (February 2007 to May 2007), the following figures (Figures 136 to 143) show the hourly temperature and relative humidity values for the changing room

(CH), the cold room (CR), the warm room (WR), and the hot room (HR). Note that these figures include also the respective average outside temperature (EX).

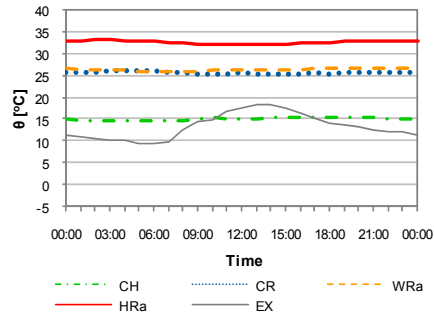


Figure 136 Temperature θ_{i+e} [°C]
Damascus February 2007

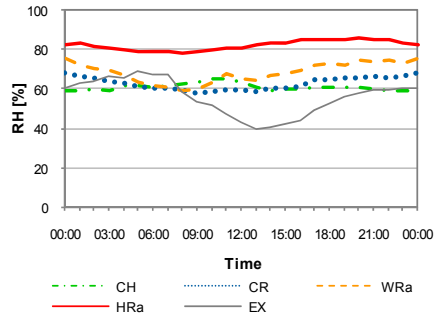


Figure 137 Relative Humidity RH [%]
Damascus February 2007

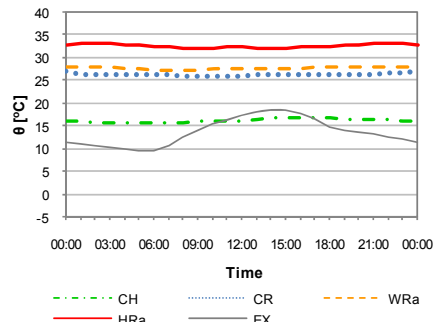


Figure 138 Temperature θ_{i+e} [°C]
Damascus March 2007

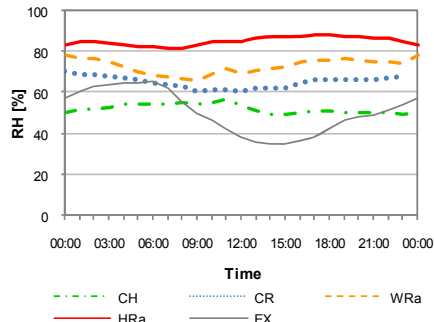


Figure 139 Relative Humidity RH [%]
Damascus March 2007

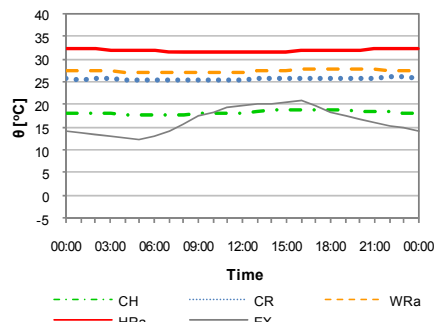


Figure 140 Temperature θ_{i+e} [°C]
Damascus April 2007

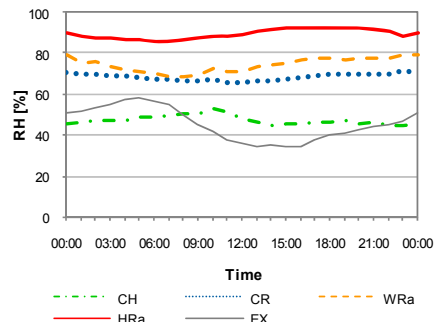


Figure 141 Relative Humidity RH [%]
Damascus April 2007

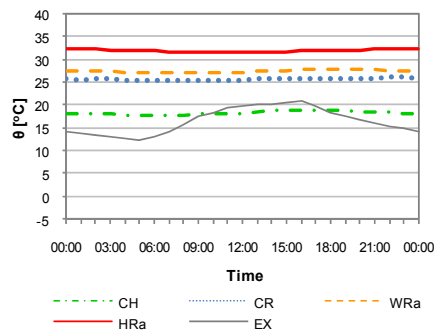


Figure 142 Temperature θ_{i+e} [°C] Damascus May 2007

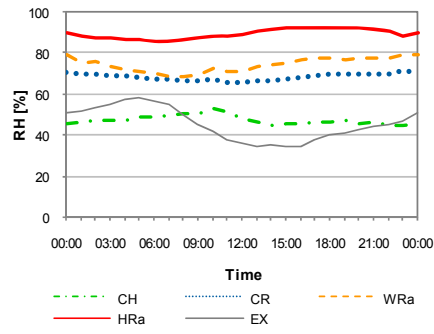


Figure 143 Relative Humidity RH [%] Damascus May 2007

4.2.4.2. Relative temperature

The following figures (Figure 144 and 145) show relative temperatures (see Eq.1) for the months February and April for various spaces in the hammam, namely the changing room (CH), cold room (CR), warm room (WR), and the hot room (HR).

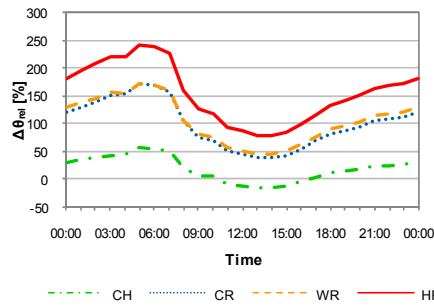


Figure 144 Relative Temperature [%] of February 2007

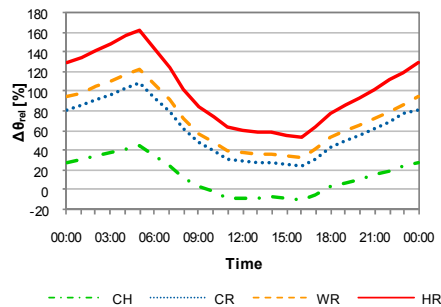


Figure 145 Relative Temperature [%] of April 2007

4.2.4.3. Temperature distribution

The distribution of the prevailing temperature ranges during the opening hours over the observation period were calculated for the four spaces changing room, cold room, warm room, and hot room (see Figures 146 to 149). Figure 150 shows the related outside temperature during the measurement period.

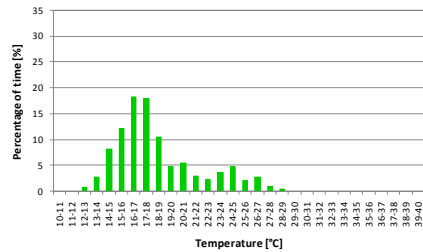


Figure 146 Temperature distribution in changing room of AMH

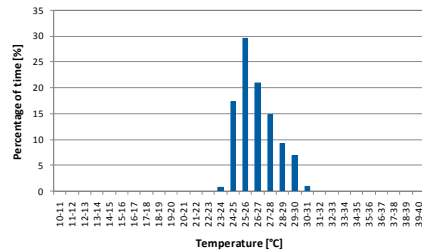


Figure 147 Temperature distribution in cold room of AMH

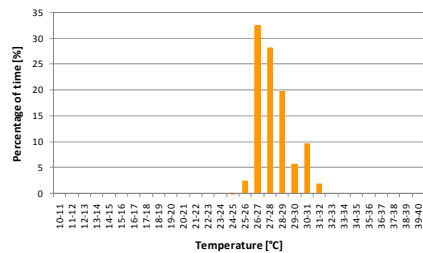


Figure 148 Temperature distribution in warm room of AMH

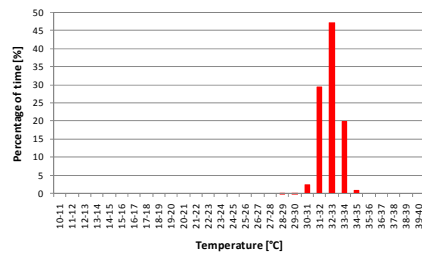


Figure 149 Temperature distribution in hot room of AMH

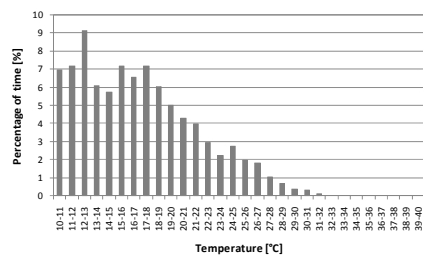


Figure 150 Temperature distribution of External Temperature

4.2.5. Constantine

4.2.5.1. Hourly values for reference days

The following figures (Figure 151 to Figure 153) show the hourly temperature values for reference days over the measurement period from July 2007 to June 2008 for changing room (CH) (Figure 151), cold room (CR) (Figure 152), and hot room (HR) (Figure 153). Figure 154 shows the prevailing outdoor temperature during this time. Note that the dedicated weather station was installed in January 2008. Previous outside conditions were monitored via a data logger mounted on the roof of the hammam. The sensor locations are marked on the corresponding floor plans.

Changing Room

Temperatures in changing room are very stable. As the changing room of Hammam Suq al Ghazal is not heated, temperatures from 14°C to 17°C occur during winter months.

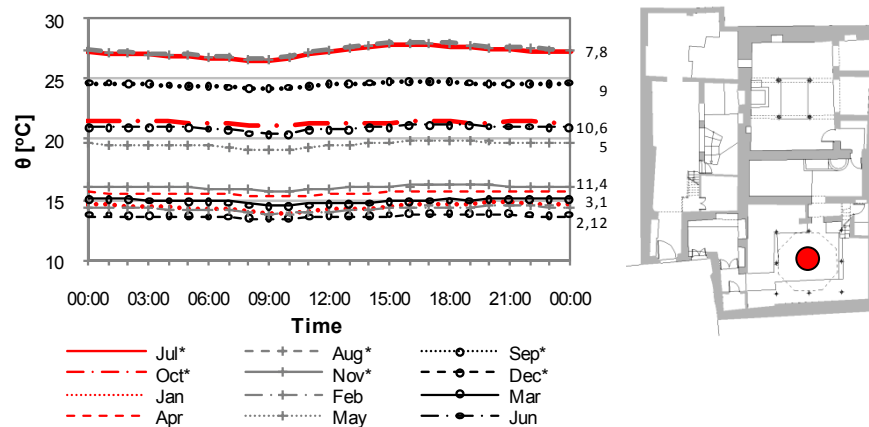


Figure 151 Indoor air temperature [°C] in CH of SAG for the observation period July 2007 to June 2008

Cold Room

Measurements for the cold room are available from January to July. The space is not heated, leading in the colder months to temperatures from 16°C to 18°C.

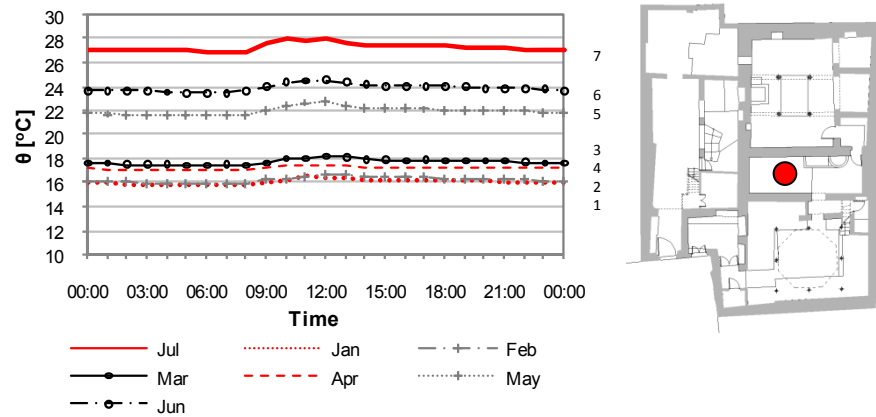


Figure 152 Indoor air temperature [°C] in CR of SAG for seven months during the observation period

Hot Room

Temperature of the hot room typically shows two peaks. One is between 6:00 and 8:00 in the morning during women opening hours. The second peak is around 17:00 to 18:00 during men opening hours. Temperatures range from 32°C to 38°C.

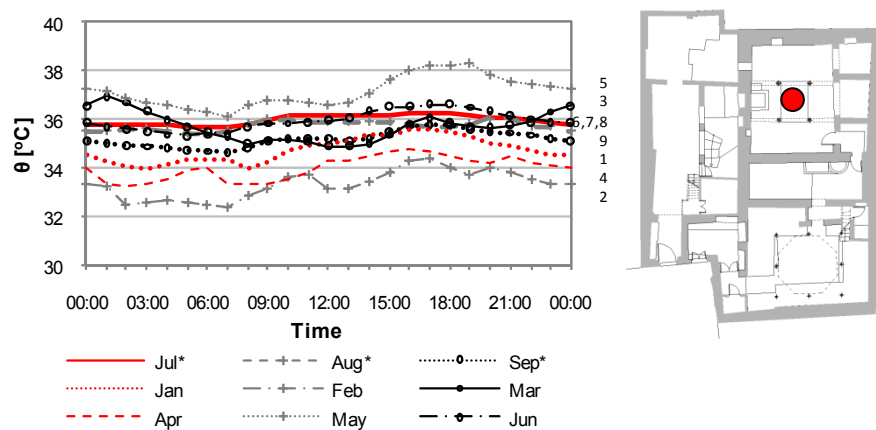


Figure 153 Indoor air temperature [°C] in HR of SAG for the observation period from July 2007 to June 2008

Outside

The following figure (Figure 154) shows the external temperature measured during the observation period.

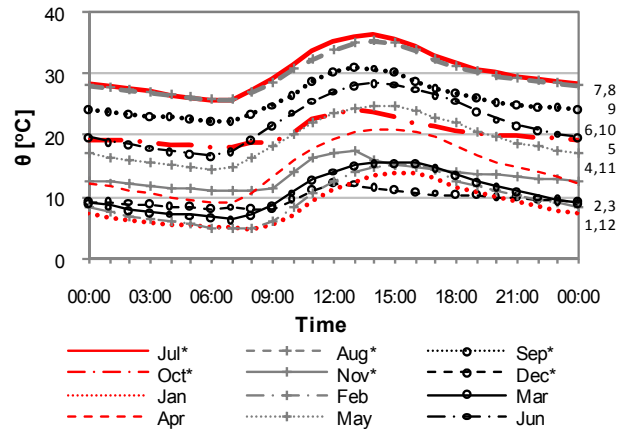


Figure 154 Outside air temperature $[\text{°C}]$ of SAG for the observation period July 2007 to June 2008

Figures show the hourly temperature and relative humidity values for the changing room (CH), the cold room (CR), and the hot room (HR) including the respective outside temperature (EX). Figures 155 to Figure 160 show exemplarily the results for the months January, April and June 2008. Further results are given in the appendix (Section 8.2.4).

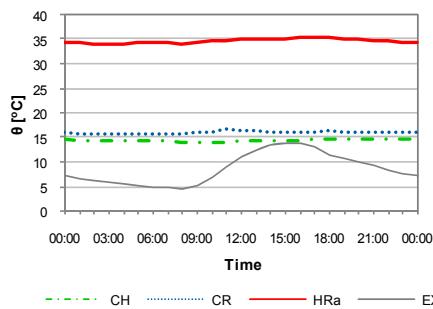


Figure 155 Temperature θ_{i+e} $[\text{°C}]$ Constantine January 2008

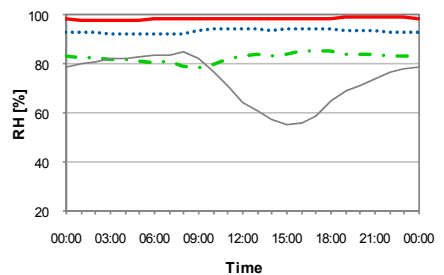


Figure 156 Relative Humidity RH [%] Constantine January 2008

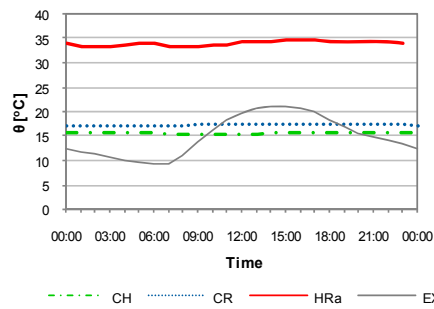


Figure 157 Temperature θ_{i+e} [°C]
Constantine April 2008

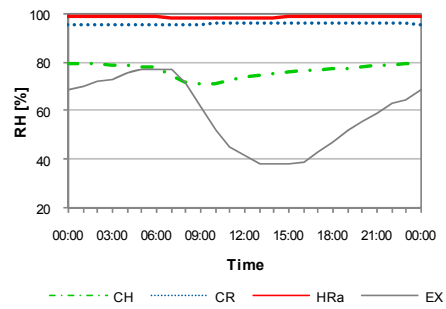


Figure 158 Relative Humidity RH [%]
Constantine April 2008

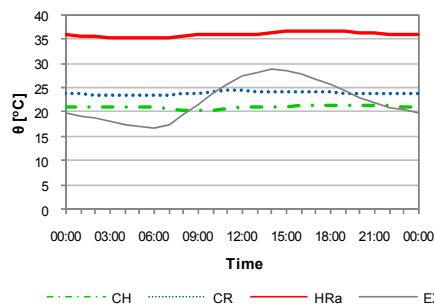


Figure 159 Temperature θ_{i+e} [°C]
Constantine June 2008

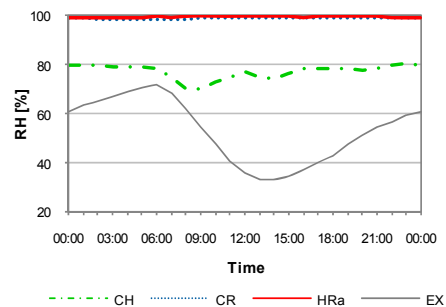


Figure 160 Relative Humidity RH [%]
Constantine June 2008

4.2.5.2. Relative temperature

The following figures (Figures 161 and 162) show relative temperatures (see Eq.1) for the months January and June for various spaces in the hammam, namely the changing room (CH), cold room (CR), and the hot room (HR).

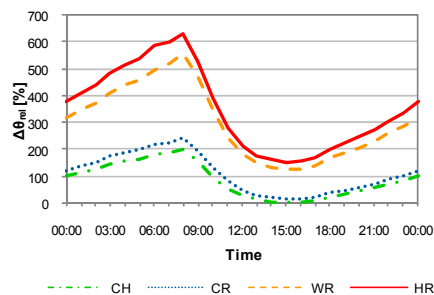


Figure 161 Relative Temperature
January 2008

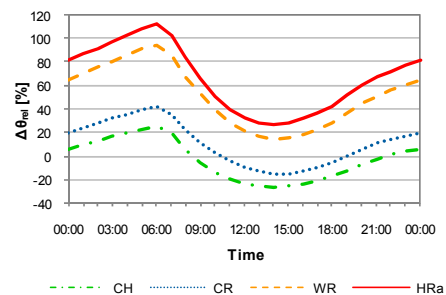


Figure 162 Relative Temperature June
2008

4.2.5.3. Temperature distribution

The distribution of the prevailing temperature ranges during the opening hours over the observation period were calculated for the spaces changing room, cold room, and hot room (see Figures 163 to 165). Figure 166 shows the related outside temperature during the measurement period.

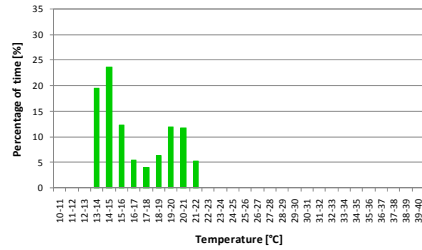


Figure 163 Temperature distribution in CH of SAG

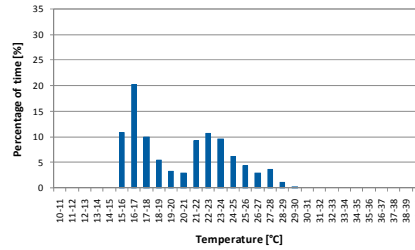


Figure 164 Temperature distribution in CR of SAG

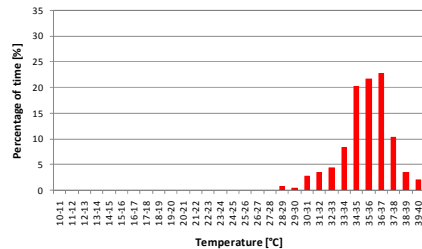


Figure 165 Temperature distribution in HR of SAG

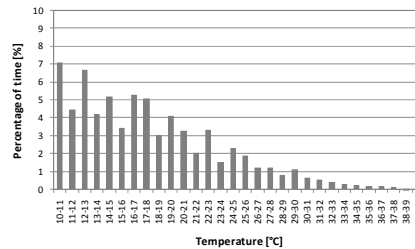


Figure 166 Temperature distribution of External Temperature of SAG

4.2.5.4. Thermal Comfort conditions

Changing Room

Figure 167 shows the results of hourly hygro-thermal measurements in the changing room of the hammam (for reference days in January, April, July and October) in a psychometric chart. Note that the figure includes also the SET lines (see section 3.4.2.5) for the relevant months.

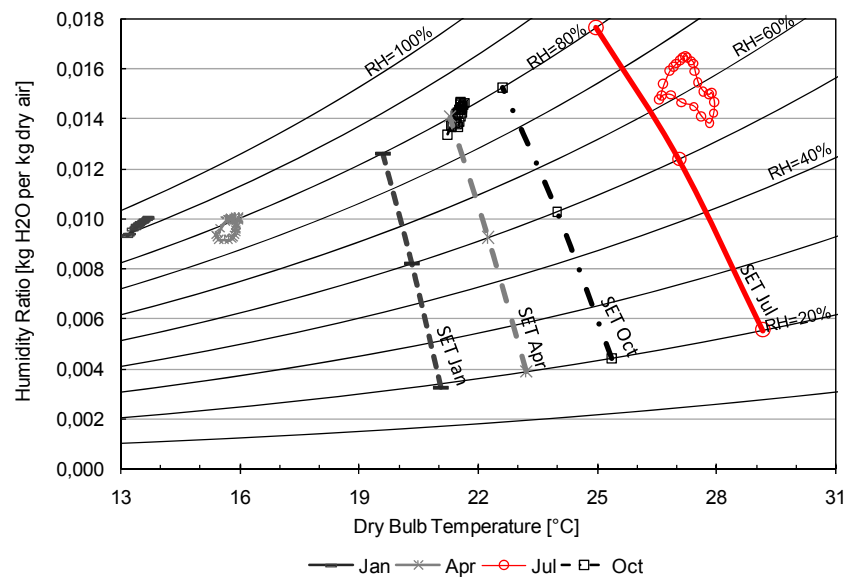


Figure 167 Depiction of the indoor climate conditions in the changing room in SAG for July and October 2007, January and April 2008, compared to Standardized Effective Temperature SET for each month

4.3. Room acoustics

Figure 168 shows the measured frequency dependent ambient sound levels of the hammams Saffarin (SAF) and Ammouneh (AMH) for the spaces changing room (SCH, ACH), cold room (SCR), warm room (SWR, AWR), and hot room (SHR, AHR). Table 26 summarizes the results of the A-weighted overall ambient sound levels.

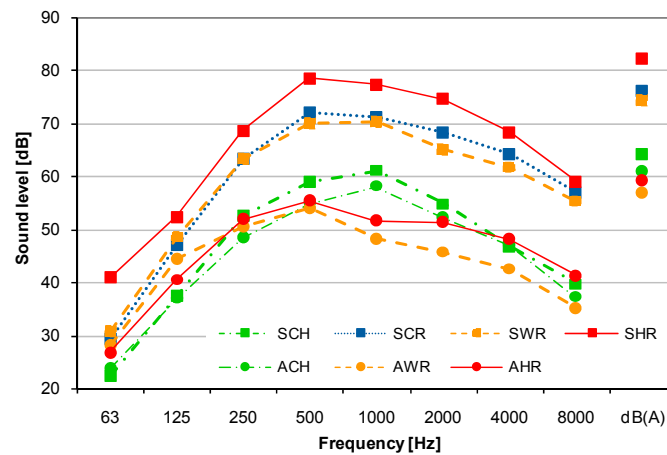


Figure 168 Frequency dependent ambient sound levels for Hammam Saffarin and Hammam Ammouneh

Table 26 A-weighted ambient sound levels (spot measurements)

	Ambient sound level [dB]			
	CH	CR	WR	HR
SAF	64	76	74	82
AMH	61	-	57	59

Figure 169 illustrates the measured reverberation times in 3 hammams in Constantine, namely Suq al Ghazal (SAG), Belebdaoui (BEL), and Bougouffa (BOU).

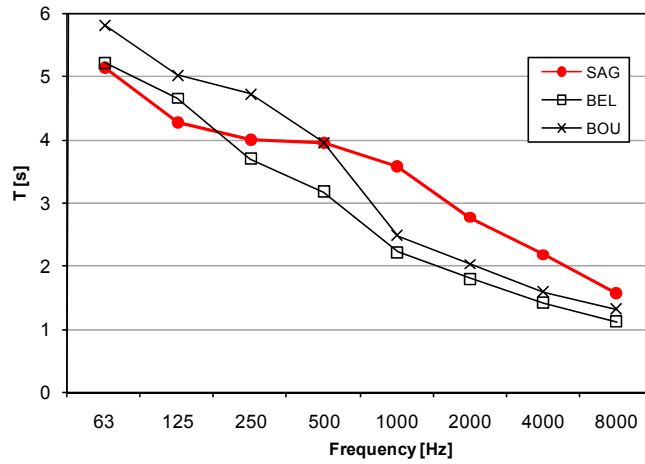


Figure 169 Measured reverberation times in SAG, BEL, BOU

Figure 170 and Table 27 show the deviation of measured reverberation time values from desirable values (%).

Table 27 deviation of measured reverberation time values from desirable values (%)

Object	Frequency [Hz]							
	63	125	250	500	1000	2000	4000	8000
SAG	367	288	264	259	225	152	98	43
BEL	422	366	270	218	122	80	42	12
BOU	481	401	371	295	148	102	58	31

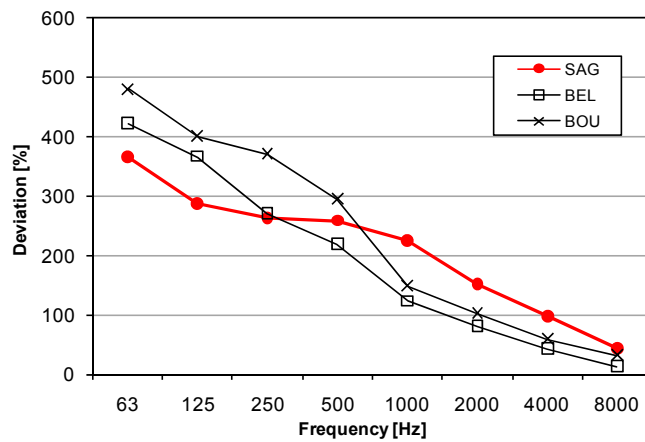


Figure 170 Deviation of measured reverberation time values from desirable values (%)

4.4. Illumination

The results of horizontal illuminance measurements (in lx, ca. 1 m above floor) in various spaces of objects BAB, SEN, SAF, AMH, and SAG are shown in Figures 171 to 175. Note that these results are of indicative character as they reflect the combined effect of daylight (at the time of the measurements) and electrical lighting (default operation mode). The results of daylight factor measurements (in %) in objects SEN and SAG are shown in Figures 172 and 176. Daylight factor denotes the measured ratio of indoor to outdoor horizontal illuminance in percentage (Mahdavi and Orehounig 2008).

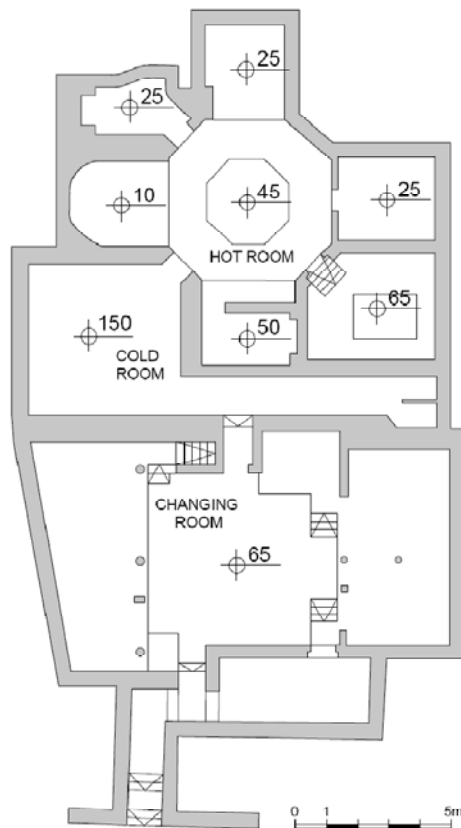


Figure 171 Results of horizontal illuminance measurements in Hammam Bab al-Bahr, March 2006 11:50 (in lx)

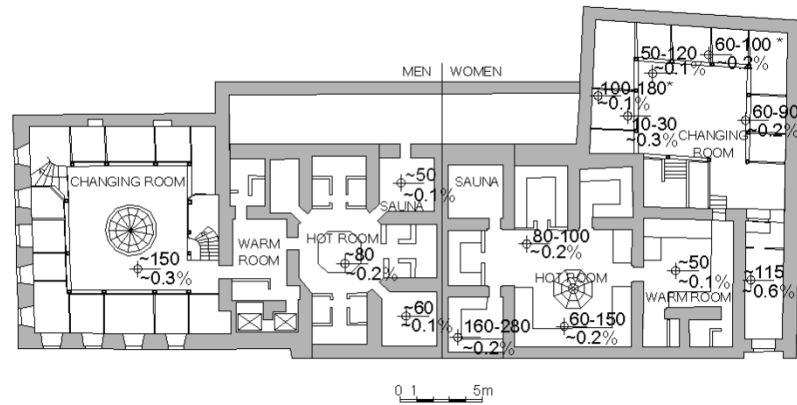


Figure 172 Results of horizontal illuminance measurements (lx) and daylight factors (%) in Hammam Şengül July 2006

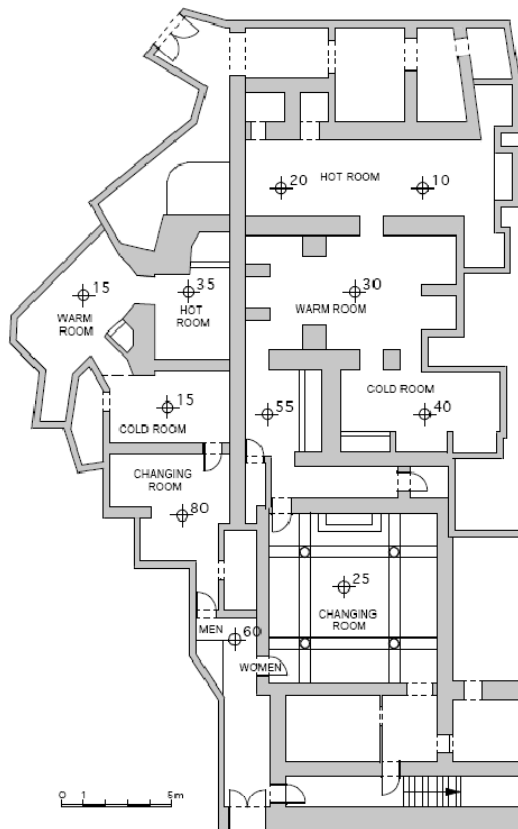


Figure 173 Results of horizontal illuminance measurements in Hammam Saffarin November 2006 9:00 (in lx)

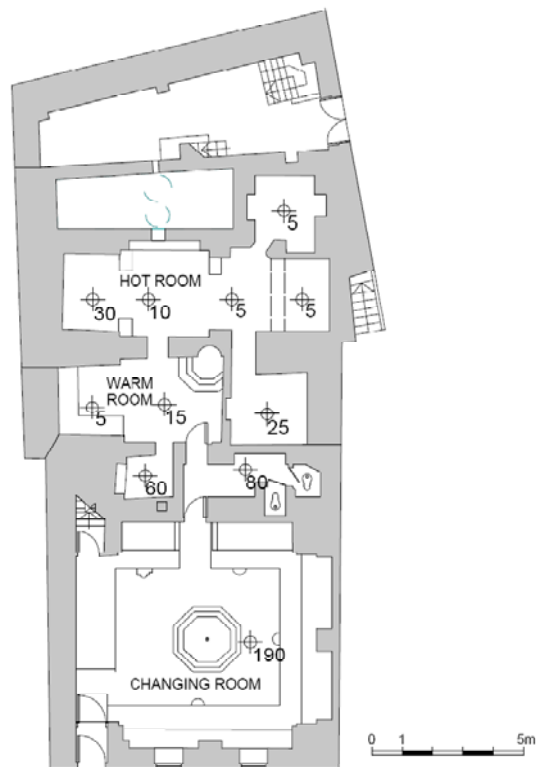


Figure 174 Results of horizontal illuminance measurements in Hammam Ammouneh February 2007 10:30 (in lx)

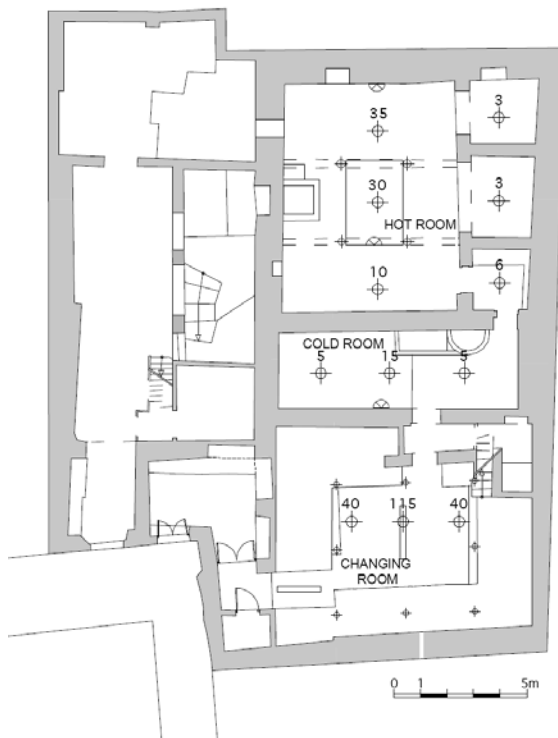


Figure 175 Results of horizontal illuminance measurements (daylight and electrical light) in Hammam Suq al Ghazal May 2007 7:30 (in lx)

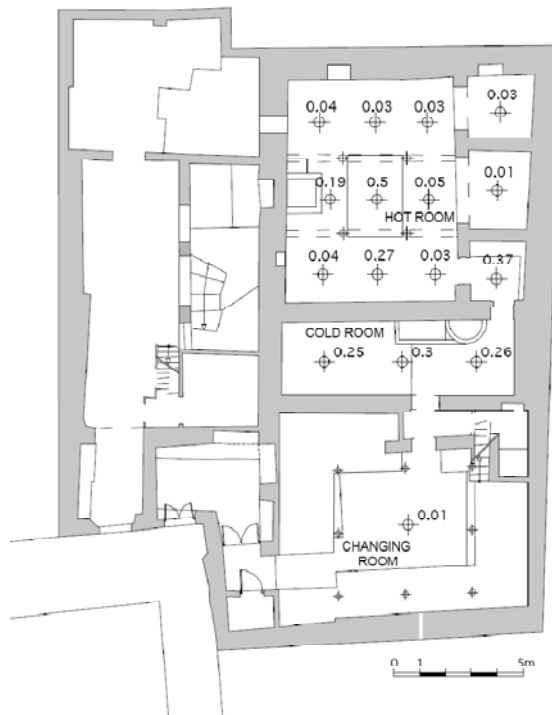


Figure 176 Results of daylight factor measurements in Hammam Suq al Ghazal May 2007 7:30 (in %)

4.5. Simulation

The first part of the simulation results section deals with reproduction of thermal and acoustical measurements in selected buildings, as described in section 3.5. Thereby, results pertain to thermal simulation models of BAB, SEN, and SAG and acoustical simulation models of SAG, BEL, and BOU. Secondly, results of parametric simulation studies are given.

4.5.1. Reproduction of measurements

4.5.1.1. Thermal Simulation model of Bab al Bahr, Cairo

Figures 178 to 193 show the comparison of measured and simulated indoor temperatures for the object Bab al Bahr (BAB). Results are given for the changing room (CH), the cold room (CR), the main hot room (HRa), and the pool room (HRb) for the months April, July, October, and January. Figure 177 gives an overview of the locations in the hammam for which simulated and measured values of temperature were compared.

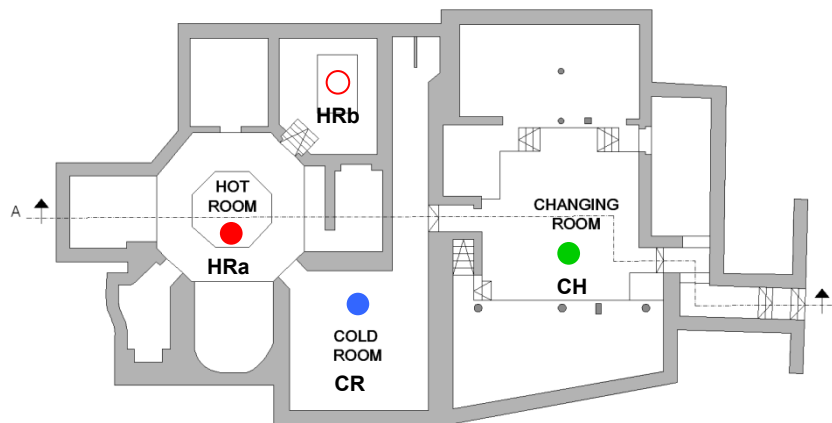


Figure 177 Summary of compared locations: CH, CR, HRa, and HRb

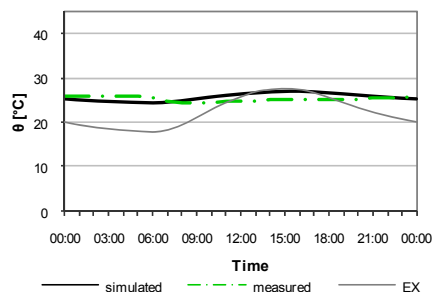


Figure 178 Simulated versus measured indoor air temperature in CH for a reference day (mean hourly values, April 2006)

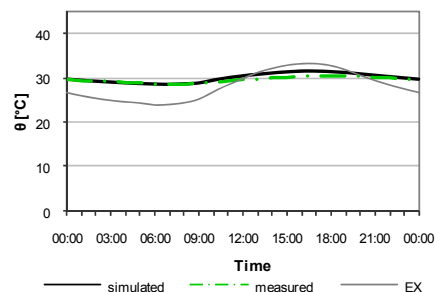


Figure 179 Simulated versus measured indoor air temperature in CH for a reference day (mean hourly values, July 2006)

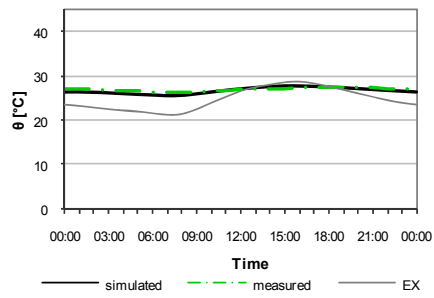


Figure 180 Simulated versus measured indoor air temperature in CH for a reference day (mean hourly values, October 2006)

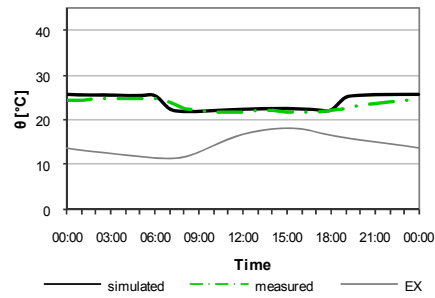


Figure 181 Simulated versus measured indoor air temperature in CH for a reference day (mean hourly values, January 2007)

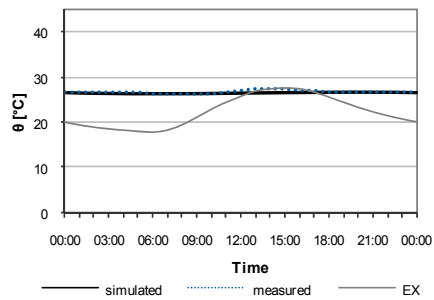


Figure 182 Simulated versus measured indoor air temperature in CR for a reference day (mean hourly values, April 2006)

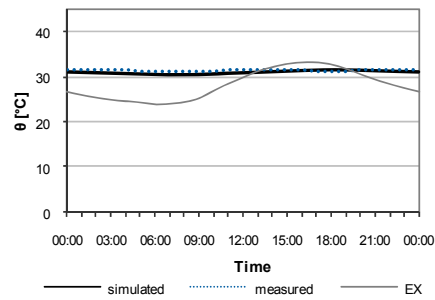


Figure 183 Simulated versus measured indoor air temperature in CR for a reference day (mean hourly values, July 2006)

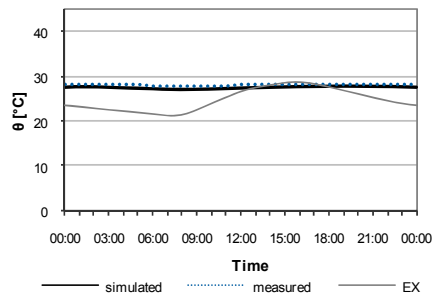


Figure 184 Simulated versus measured indoor air temperature in CR for a reference day (mean hourly values, October 2006)

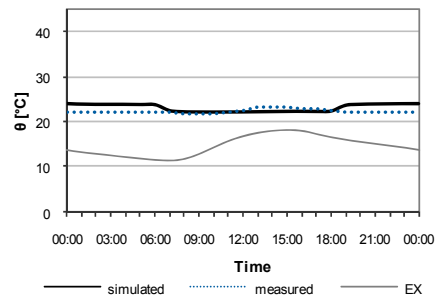


Figure 185 Simulated versus measured indoor air temperature in CR for a reference day (mean hourly values, January 2007)

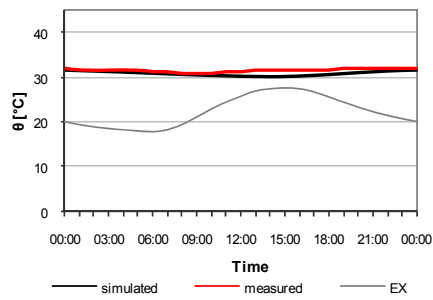


Figure 186 Simulated versus measured indoor air temperature in HRa for a reference day (mean hourly values, April 2006)

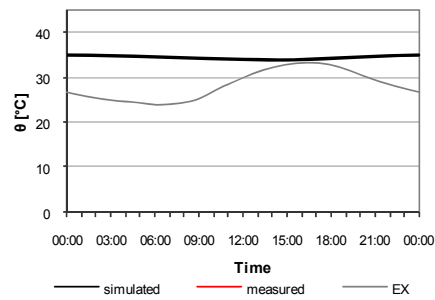


Figure 187 Simulated versus measured indoor air temperature in HRa for a reference day (mean hourly values, July 2006)

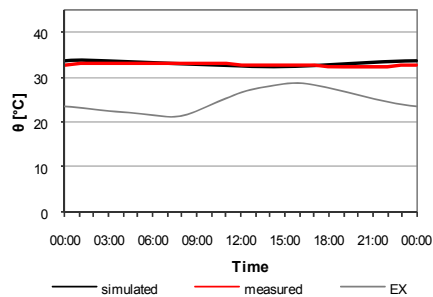


Figure 188 Simulated versus measured indoor air temperature in HRa for a reference day (mean hourly values, October 2006)

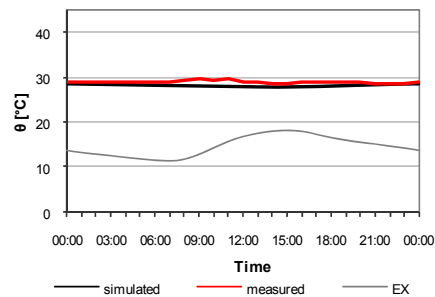


Figure 189 Simulated versus measured indoor air temperature in HRa for a reference day (mean hourly values, January 2007)

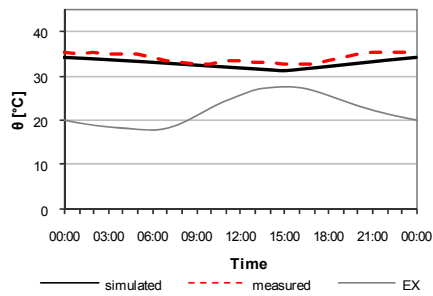


Figure 190 Simulated versus measured indoor air temperature in HRb for a reference day (mean hourly values, April 2006)

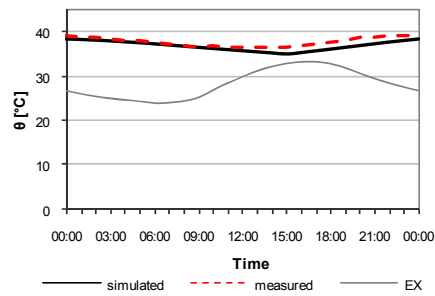


Figure 191 Simulated versus measured indoor air temperature in HRb for a reference day (mean hourly values, July 2006)

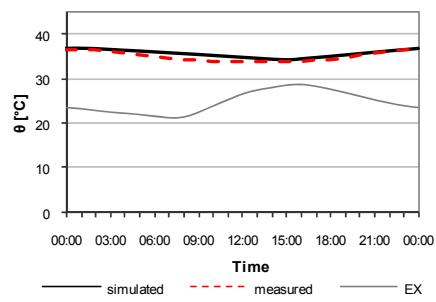


Figure 192 Simulated versus measured indoor air temperature in HRb for a reference day (mean hourly values, October 2006)

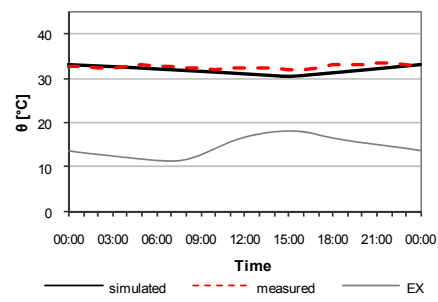


Figure 193 Simulated versus measured indoor air temperature in HRb for a reference day (mean hourly values, January 2007)

4.5.1.2. Thermal Simulation model of Şengül, Ankara

Figures 195 to 206 show the comparison of measured and simulated reverberation times for the object Şengül (SEN). Results are given for the changing room (CH), the warm room (WR), and the hot room (HR) of the women section for the months July, October, January, and April. Figure 194 gives an overview of the locations for which simulations and measurements were compared.



Figure 194 Summary of compared locations: CH, WR, and HR

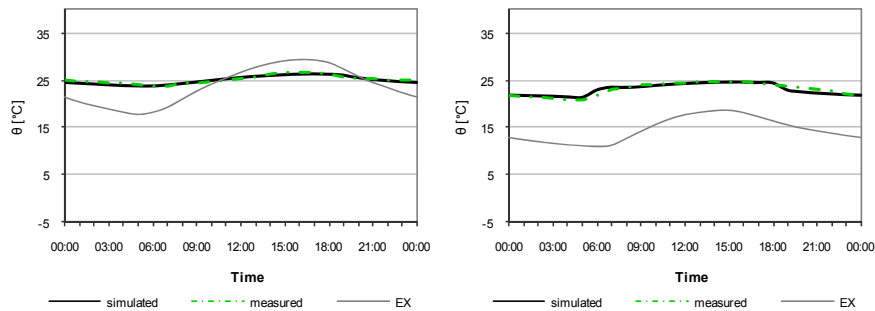


Figure 195 Simulated versus measured indoor air temperature in CH for a reference day (mean hourly values, July 2006)

Figure 196 Simulated versus measured indoor air temperature in CH for a reference day (mean hourly values, October 2006)

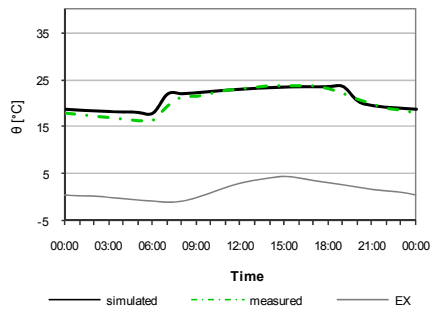


Figure 197 Simulated versus measured indoor air temperature in CH for a reference day (mean hourly values, January 2007)

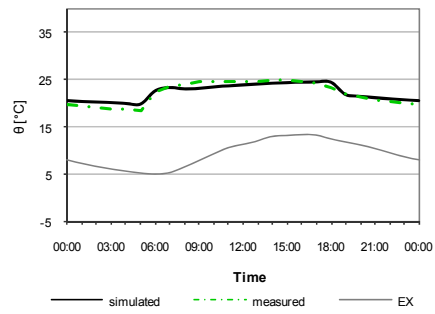


Figure 198 Simulated versus measured indoor air temperature in CH for a reference day (mean hourly values, April 2007)

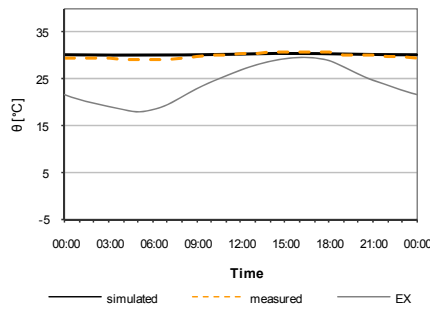


Figure 199 Simulated versus measured indoor air temperature in WR for a reference day (mean hourly values, July 2006)

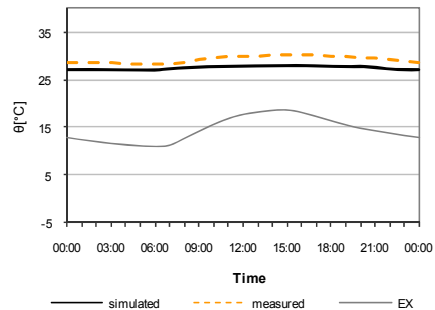


Figure 200 Simulated versus measured indoor air temperature in WR for a reference day (mean hourly values, October 2006)

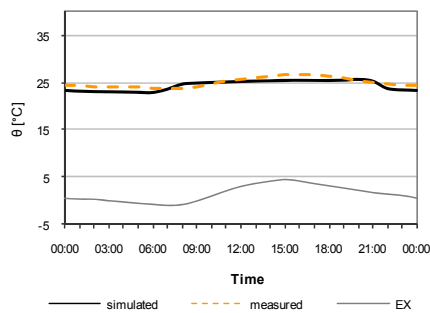


Figure 201 Simulated versus measured indoor air temperature in WR for a reference day (mean hourly values, January 2007)

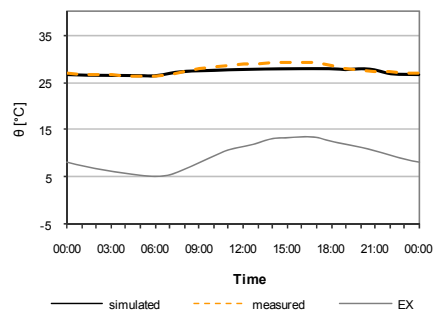


Figure 202 Simulated versus measured indoor air temperature in WR for a reference day (mean hourly values, April 2007)

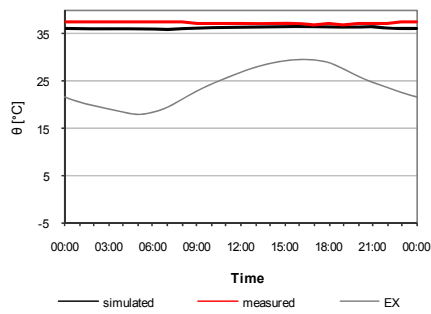


Figure 203 Simulated versus measured indoor air temperature in HR for a reference day (mean hourly values, July 2006)

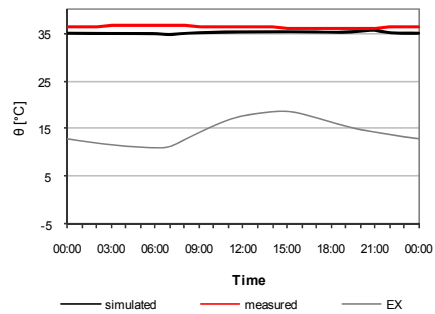


Figure 204 Simulated versus measured indoor air temperature in HR for a reference day (mean hourly values, October 2006)

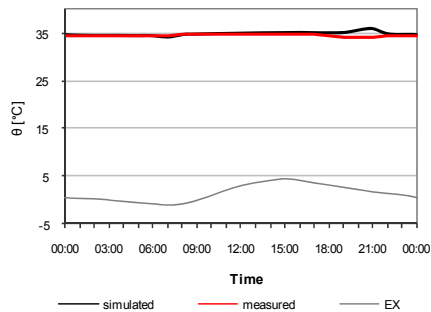


Figure 205 Simulated versus measured indoor air temperature in HR for a reference day (mean hourly values, January 2007)

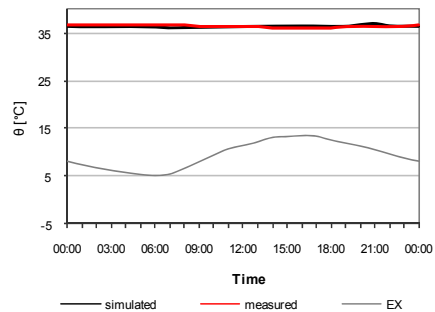


Figure 206 Simulated versus measured indoor air temperature in HR for a reference day (mean hourly values, April 2007)

4.5.1.3. Thermal Simulation model of Suq al Ghazal, Constantine

Figures 208 to 216 show the comparison of measured and simulated reverberation times for the object Suq al Ghazal (SAG). Results are given for the changing room (CH), the cold room (CR), and the hot room (HR) for the months January, March, and May. Figure 207 gives an overview of the locations for which simulations and measurements were compared.

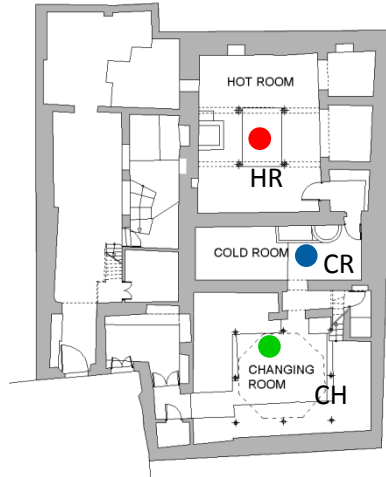


Figure 207 Summary of compared locations: CH, CR, and HR

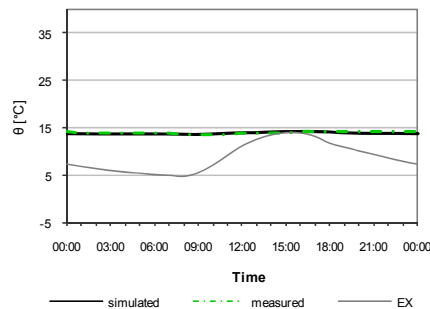


Figure 208 Simulated versus measured indoor air temperature in CH for a reference day (mean hourly values, January 2008)

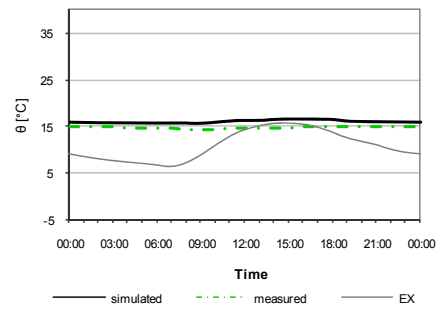


Figure 209 Simulated versus measured indoor air temperature in CH for a reference day (mean hourly values, March 2008)

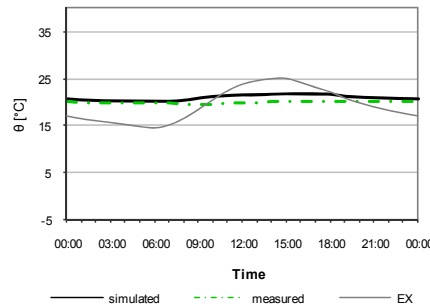


Figure 210 Simulated versus measured indoor air temperature in CH for a reference day (mean hourly values, May 2008)

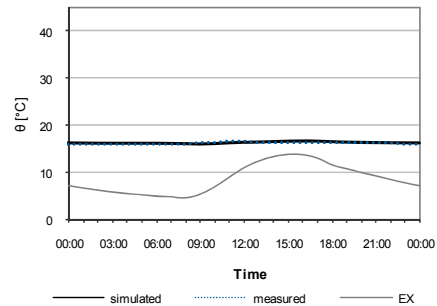


Figure 211 Simulated versus measured indoor air temperature in CR for a reference day (mean hourly values, January 2008)

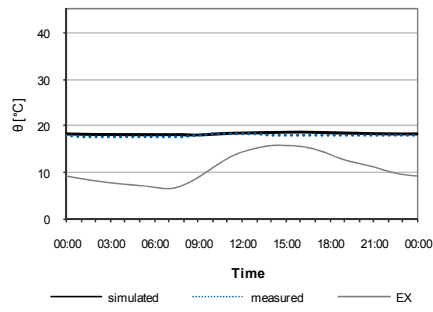


Figure 212 Simulated versus measured indoor air temperature in CR for a reference day (mean hourly values, March 2008)

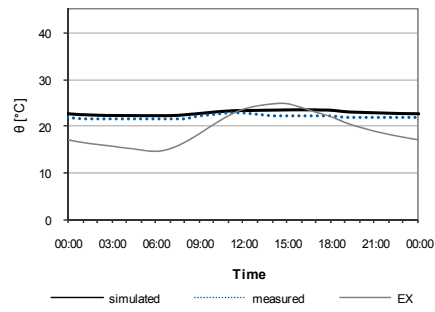


Figure 213 Simulated versus measured indoor air temperature in CR for a reference day (mean hourly values, May 2008)

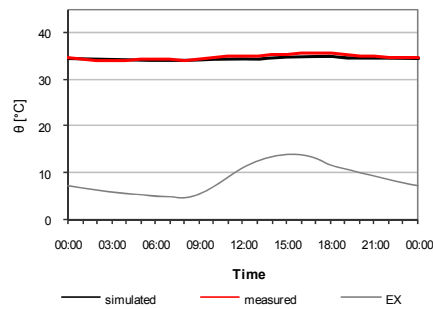


Figure 214 Simulated versus measured indoor air temperature in HR for a reference day (mean hourly values, January 2008)

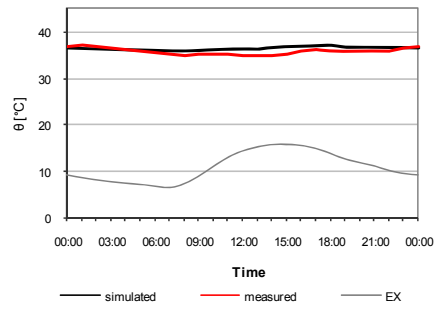


Figure 215 Simulated versus measured indoor air temperature in HR for a reference day (mean hourly values, March 2008)

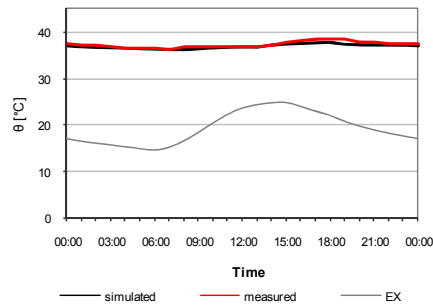


Figure 216 Simulated versus measured indoor air temperature in HR for a reference day (mean hourly values, May 2008)

4.5.1.4. Room Acoustic Simulation models

Figures 217 to 219 show the comparison of measured and simulated reverberation times for the objects Suq al Ghazal (SAG), Belebджаoui (BEL), and Bougouffa (BOU).

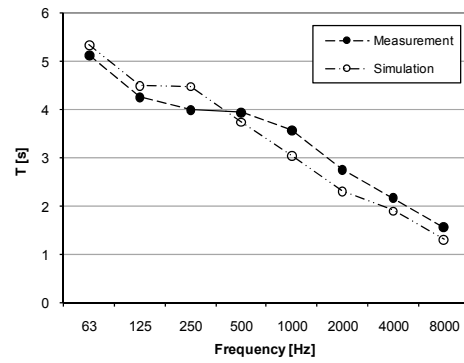


Figure 217 Simulated versus measured reverberation times in SAG

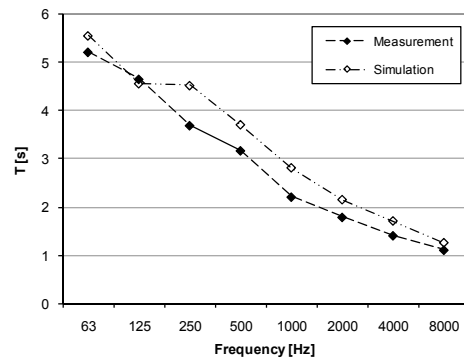


Figure 218 Simulated versus measured reverberation times in BEL

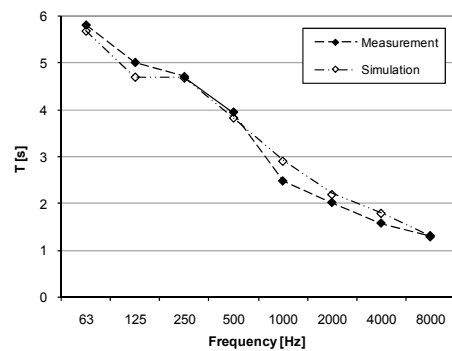


Figure 219 Simulated versus measured reverberation times in BOU

4.5.2. Parametric simulation studies

4.5.2.1. Simulation-based comparison of alternative thermal improvement options

As mentioned earlier (see section 3.5.2.6) three different scenarios were selected to illustrate the utility of the calibrated simulation models toward comparison of thermal improvement possibilities of the buildings (in this case, BAB, SEN, and SAG). The first scenario (S1) represents the existing conditions. The second scenario (S2) involves the improvement of the thermal insulation of the roof construction. The third scenario (S3) involves, in addition to the thermal improvement in S2, the use of double-glazing (instead of the existing single-glazing) for windows (CH) and roof apertures (CR, WR, and HR) of the buildings.

Table 28 summarizes simulated space heating demand for the above-mentioned scenarios. Figure 220 shows, for S3, the heating load reduction for all three buildings (in CH, CR, WR, and HR) (Orehounig and Mahdavi 2009).

Table 28 Simulated space heating demand ($\text{kWh}\cdot\text{m}^{-2}\cdot\text{a}^{-1}$) for BAB, SEN, and SAG (scenarios S1 to S3 as per Table 20)

		Space heating demand [$\text{kWh}\cdot\text{m}^{-2}\cdot\text{a}^{-1}$]			Total
		CH	CR/WR	HR	
BAB	S1	65	112	292	164
	S2	59	96	266	148
	S3	57	87	265	147
SEN	S1	237	491	640	395
	S2	217	310	416	291
	S3	206	308	410	283
SAG	S1	38	299	338	170
	S2	35	260	164	106
	S3	34	254	155	102

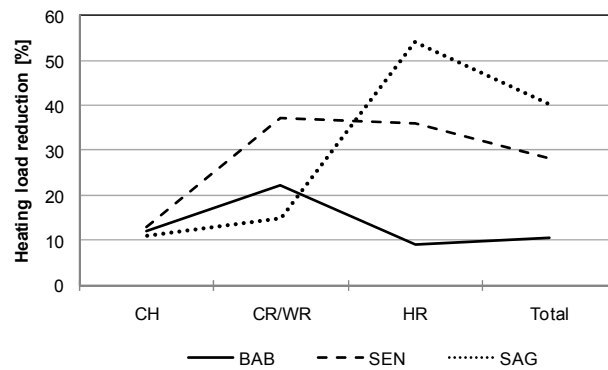


Figure 220 Heating load reduction for all 3 buildings for Scenario 3

4.5.2.2. Simulation-based inquiry into the thermal mass effect

In order to explore the effect of the large building mass on the energy performance of (thermal conditions in) the hammams, simulation studies were applied to compare conditions in an existing hammam with a virtual low-mass hammam of the same size and configuration. Two sets of simulation runs were performed, one to compute overheating tendency (in CH of the hammams) during the summer period, and one to obtain annual heating loads for all spaces. Overheating tendency results are shown in Figure 221 in terms of Mean Overheating (OH_m as per Eq. 3) of the indoor air in CH. Simulation results for annual heating loads ($kWh \cdot m^{-2} \cdot a^{-1}$) are shown in Figure 222.

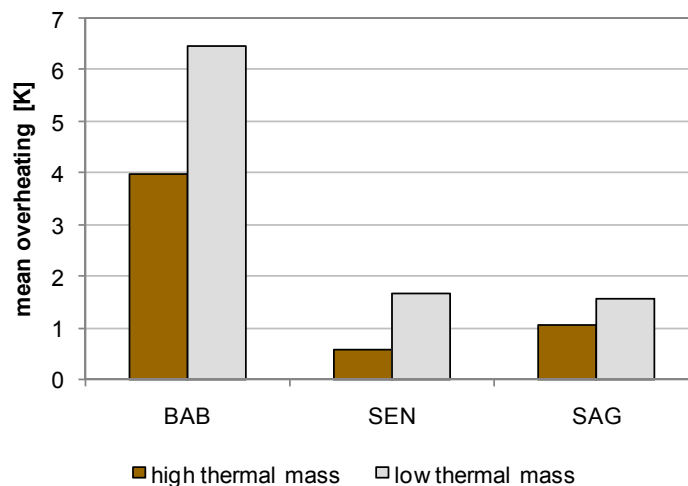


Figure 221 Mean overheating (in K) for the existing (high thermal mass) and alternative (low thermal mass) scenarios

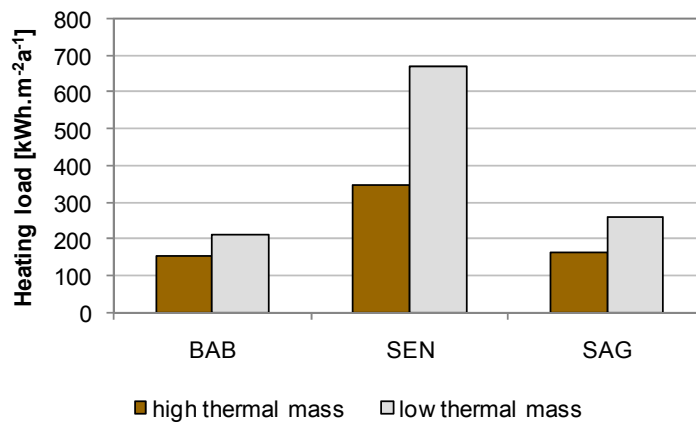


Figure 222 Heating loads (in kWh.m⁻².a⁻¹) for the existing (high thermal mass) and alternative (low thermal mass) scenarios

4.5.2.3. Acoustical improvement possibilities

Table 29 and Figure 223 show the comparison of simulated reverberation times in hot room of object BOU for three different conditions (see Table 25). The first condition represents the status quo. The second condition involves the treatment of parts of the wall surface with a humidity-resistant acoustic plaster. The third condition involves the treatment of the same wall surface area with an alternative (broad-band) acoustical absorber.

Table 29 Reverberation time of simulated improvement scenarios of BOU

BOU	63	125	250	500	1000	2000	4000	8000
Measurement	5.81	5.01	4.71	3.95	2.48	2.02	1.58	1.31
Simulation C1	5.68	4.70	4.68	3.83	2.91	2.20	1.80	1.30
2. Condition C2	3.85	3.14	2.81	2.05	1.42	1.1	0.89	0.73
3. Condition C3	1.26	1.47	1.04	1.08	1.23	1.2	1.06	0.89

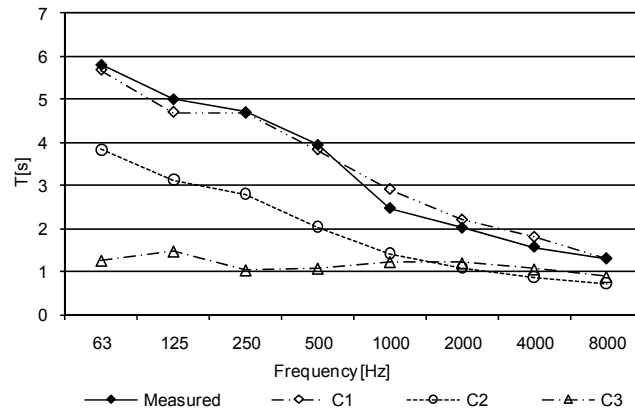


Figure 223 Reverberation time of simulated scenarios for BOU including measured values

5. Discussion

5.1. Overview

This chapter provides a summary discussion of the dissertation's main results. It is divided into sections dealing with: i) thermal quality of the buildings, ii) the visual performance, iii) the acoustical observations, and iv) the simulation studies.

5.2. Thermal quality

5.2.1. General

Figures 224 to 228 provide an overview of the thermal conditions in the selected objects based on a monitoring period of approximately one year. It shows the cumulative temperatures during opening hours for objects BAB, SEN, SAF, AMH and SAG. Indoor parameters are given for changing room (CH), cold room (CR), warm room (WR), and hot room (HR).

As these figures suggest, indoor temperatures in hot room and warm room do not vary as much as those in changing room. Hot rooms in all observed hammams provide a fairly stable and appropriate temperature range throughout the year, whereby temperatures lie 50% of the time within the range of 33°C to 40°C. Changing rooms and – to a lesser degree – cold rooms, however, display at times temperature ranges that would not be thermally appropriate for lightly clothed users. Specifically, cold rooms of the objects BAB, AMH and SAG are not heated. Likewise, the changing room is heated only in SEN and – minimally – in BAB (Mahdavi and Orehounig 2009).

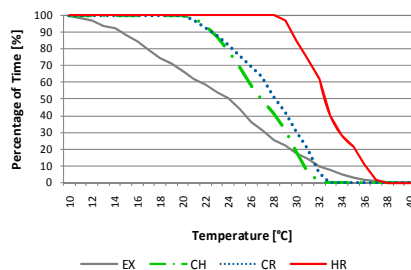


Figure 224 Cumulated Indoor Temperatures in the CH, CR, and HR in BAB from April 2006 till March 2007 including outdoor temperature.

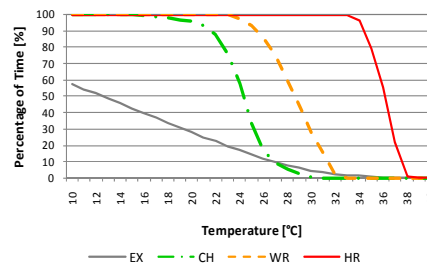


Figure 225 Cumulated Indoor Temperatures in the CH, WR, and HR in SEN (women section) from July 2006 till June 2007 including outdoor temperature.

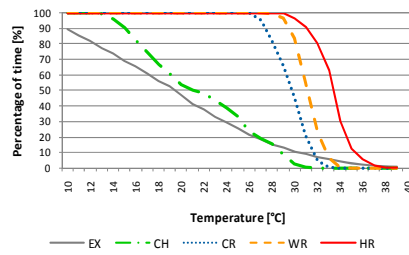


Figure 226 Cumulated Indoor Temperatures in the CH, CR, WR, and HR in SAF (women section) from October 2006 till September 2007 including corresponding outdoor temperature.

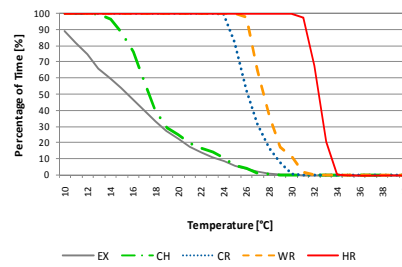


Figure 227 Cumulated Indoor Temperatures in the CH, CR, WR and HR in AMH from February 2007 till May 2007 including corresponding outdoor temperature.

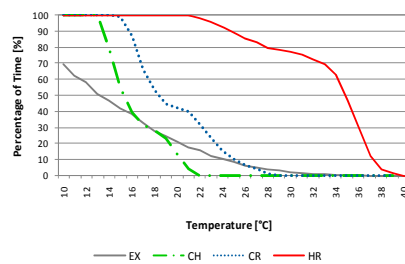


Figure 228 Cumulated Indoor Temperatures in the CH, CR, and HR in SAG from July 2007 till June 2008 including corresponding outdoor temperature from January 2008 till June 2008.

5.2.2. Thermal comfort

Psychometric charts with temperature and relative humidity were generated to further explore the widely fluctuating temperature ranges (and the thermal comfort ramifications) in the changing rooms of the hammams. These figures imply a relative good match between existing and desirable indoor conditions in BAB and SEN. Thermal conditions in changing room SAF and SAG are, however, problematic, especially during the winter period, when they remain unheated (Mahdavi and Orehounig 2009).

A highly interesting outcome of the thermal comfort study in the hammams was the relevance of the adaptive thermal comfort theory. If, for example, one simply compares the hygro-thermal conditions in the changing room of the hammam Bab al Bahr with the recommended range by the conventional thermal comfort theory (see Figure 229), one must conclude that the occupants in this space must always feel uncomfortable. A comparison of the existing conditions with the requirements of the adaptive thermal comfort theory shows, in contrast,

a much better match between existing and desirable conditions. This observation applies, to a certain degree, also to the other hammams studied.

A fully documented and conclusive explanation for this circumstance cannot be provided here. However, certain speculations are in order. Firstly, the aforementioned high thermal mass of the buildings provides with a thermal stability and long-term coupling of indoor and outdoor temperature conditions. This is consistent with the indoor-outdoor temperature coupling implied in the adaptive thermal comfort theory. Secondly, most hammams embody an interesting human-based feedback system regarding thermal operation. Hammam users in many countries are known to be quite vocal should water or indoor air temperatures decrease below certain thresholds. The manager of the hammam is thus provided with "real time" feedback concerning the users' thermal sensation, which itself is coupled – according to the adaptive thermal comfort theory – to the long-term (monthly) fluctuations of the external temperatures.

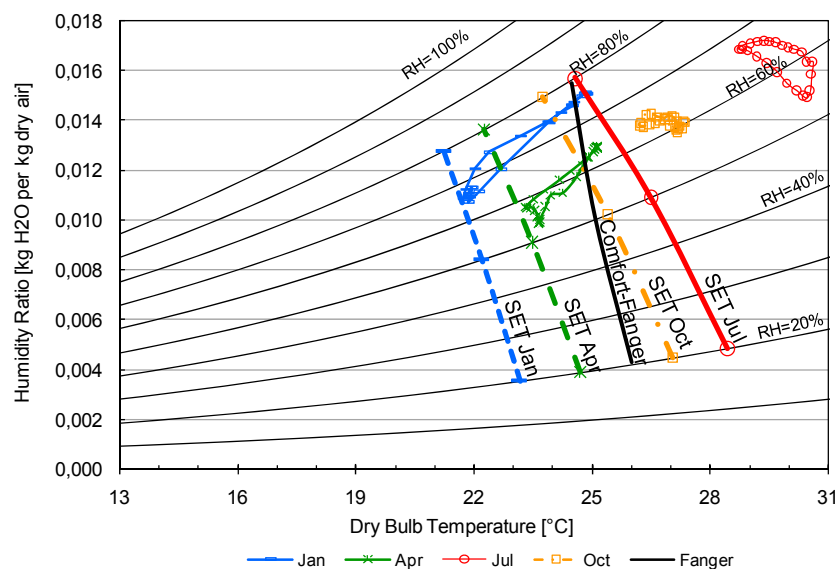


Figure 229 Comfort temperature after Fanger and SET in changing room of BAB

5.2.3. Thermal transition

Gradual temperature progression (i.e., increasing ambient temperature as one moves from changing room to hot room) in spaces of hammams has been regarded as an important feature of the thermal environment in these buildings. Consequentially, monitored data have been examined to see if, and to which extent, such transition is evident. Clear evidence for such transition could be found in the Hammams BAB and SEN (see Figures 230 and 231). In SAF (see Figure 232), a gradual transition can be

observed only within a rather narrow thermal range: the major temperature gradient exists between the changing room and the heated spaces. A real transitional pattern is de facto absent in SAG (see Figure 233), as no noteworthy difference in temperature between the changing room and the cold room can be observed (Mahdavi and Orehounig 2009).

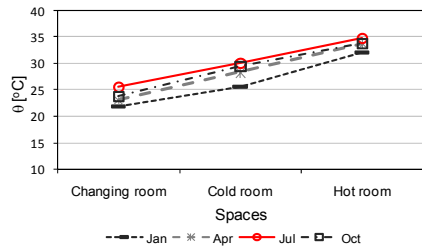


Figure 230 Temperature transition between spaces in BAB (mean monthly values during opening hours)

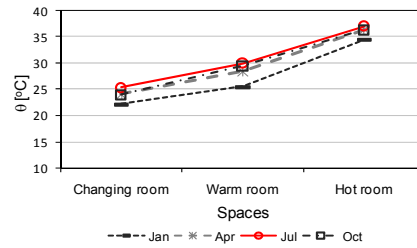


Figure 231 Temperature transition between spaces in SEN (mean monthly values during opening hours)

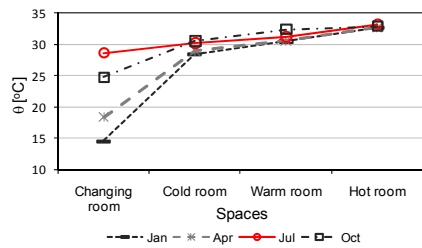


Figure 232 Temperature transition between spaces in SAF (mean monthly values during opening hours)

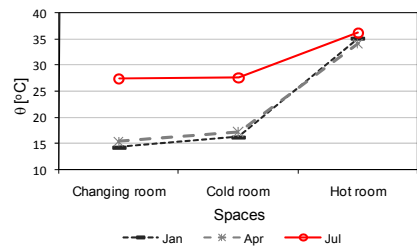


Figure 233 Temperature transition between spaces in SAG (mean monthly values during opening hours)

5.2.4. Hidden thermal patterns

Information visualization and data mining techniques can support the interpretation of measured data through identification of influence factors and hidden patterns. For example, Figure 234 shows the course of measured indoor temperature over a typical day in July 2006 in five locations in a hammam in Cairo. This Figure shows the differences in the temperatures of various hammam zones, but does not reveal, at the first glance, a distinctive pattern. However, a different visualization of the same information can, as Figure 235 illustrates, reveal a regularity that can be both of explanatory and predictive utility. Specifically, a distinct dependency pattern concerning indoor and outdoor temperature is revealed, which could facilitate the derivation of indoor temperatures in different hammam zones based on known outdoor temperatures. In this case, instead of plotting actual room temperature values against time, simply the relative indoor-outdoor temperature difference values – i.e. $\Delta\theta_{rel}$ as per Eq. (1) – are plotted against time.

The coupling between indoor and outdoor temperature as implied in the above mentioned hidden thermal patterns is consistent with the high thermal mass of the buildings and the previously discussed speculation regarding the users' feed back in terms of their thermal sensation.

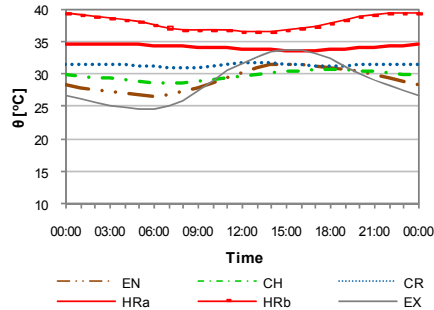


Figure 234 Temperature θ_{i+e} [°C] Cairo July 2006

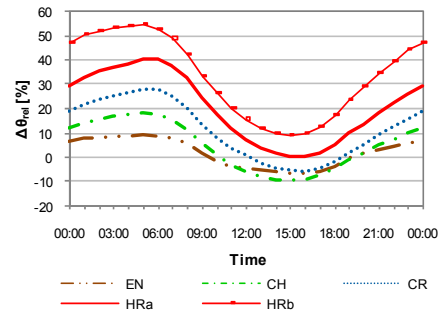


Figure 235 Relative Temperature [%] of July 2006

5.3. Acoustics

The spaces studied make a predominantly reverberant and – when occupied – loud impression. The measured reverberation times are drastically longer than assumed target values (particularly in the lower frequency range). Note that this conclusion is valid despite the fact that the reverberation time measurements were conducted in empty conditions: the sound absorption effect of unclothed occupants is rather small. The perception of loudness is corroborated by the snapshot measurements of ambient sound levels (see Table 26 and Figure 168).

Acoustically hard room enclosure surfaces and relatively large (sparsely furnished) volumes represent the main reasons for these conditions. Smooth and hard surfaces have been naturally applied in highly humid spaces as they can withstand water and moisture impact and are relatively easy to cleanse. However, they typically possess low absorption coefficients and are thus highly reflective acoustically. Even though special types of acoustically more effective plasters can increase the absorption the overall result may still not be satisfactory, if the absorption effectiveness is not broadband and occurs only selectively for certain – in this case higher – frequencies (Mahdavi et al. 2008b).

5.4. Visual Aspects

Illuminance and daylight factor measurement results imply rather low light levels in the selected objects (see Figures 171 to 176). It has been argued, that mild and dampened light levels are an intrinsic feature of indoor spaces in hammams and are to provide a welcome contrast to the typically harsh outdoor lighting circumstances in many countries where hammams were constructed. However, some of the currently prevailing low daylight levels do not seem to be the result of original design intentions. In fact, our observations revealed that in some hammams the original roof apertures (openings) for daylight were occasionally blocked ex post facto. This means that in some hammams the originally planned daylight penetration (and in certain cases the ventilation possibility) were compromised later on (see, for example, Figure 236, for a view of the HR of a hammam in Fez (Morocco) with almost entirely blocked daylight apertures). The addition of the "modern" electrical lighting components – necessary for the night operation of the hammams – are in all objects we studied neither sensitive architecturally, nor appropriate from the illuminating engineering point of view (see, as an example, Figure 237 with the view of CH in hammam BAB) (Mahdavi and Orehounig 2008).



Figure 236 Deterioration of daylight and fresh air supply to the interior spaces of a hammam in Fez (Morocco) due to the blockage of roof apertures



Figure 237 Electrical lighting in the changing room in hammam in Cairo, Egypt
(picture by A. Mahdavi)

5.5. Simulation

The results warrant a number of conclusions (Orehounig and Mahdavi 2009):

1. Generation of calibrated simulation models both in the thermal and acoustical domains was shown to be feasible and useful. However, calibrated thermal simulation models require rather long-term empirical data (both on indoor and outdoor environmental conditions). Such measurements allow to critically re-examine assumptions pertaining to the properties of construction materials and components, as well as energy systems' operation and efficiency.
2. Improvement of the thermal insulation of the roof construction (S2) was – as expected – more effective in the colder climates of SEN and SAG (approximately 26% and 38% respectively, versus 10% for BAB) (see Table 28, S2).
3. The additional improvement of the thermal properties of the glazing (S3) did not further reduce the heating loads in a noteworthy manner (see Figure 220). This is mainly due to the rather low percentage of glazing in the overall building envelope area.
4. As Table 28 and Figure 220 demonstrate, the heating load associated with these hammams' HRs could be effectively reduced for SEN (38%)

and SAG (53%), given the required high indoor air temperatures in these rooms.

5. Simulations confirm the starting point assumption regarding thermal mass. Traditional hammams with their considerable thermal mass appear to have a lower heating load (relevant for all hammam spaces) and a lower overheating tendency (relevant only for CHs) as compared to configurationally comparable buildings with lower thermal mass. Specifically, heating loads computed for the high thermal mass models of BAB, SEN, and SAG was found to be respectively 25%, 50%, and 40% less than the low thermal mass variations of these buildings (see Figure 222). Likewise, the mean overheating in the CHs of the original (high thermal mass) models of the hammams BAB, SEN, and SAG was shown to be 2.4 K, 0.9 K, and 0.5 K less than those of their low thermal mass counterparts (see Figure 221).
6. The spaces studied make a predominantly reverberant and – when occupied – loud impression. The measured reverberation times are drastically longer than assumed target values (particularly in the lower frequency range). The perception of loudness is corroborated by the measurements of ambient sound levels (see Mahdavi et al. 2008b). Acoustically hard room enclosure surfaces and relatively large (sparsely furnished) volumes represent the main reasons for these conditions. Smooth and hard surfaces have been naturally applied in highly humid spaces as they can withstand water and moisture impact and are relatively easy to cleanse. However, they typically possess low absorption coefficients and are thus highly reflective acoustically. Even though special types of acoustically more effective plasters can increase the absorption (see, for example, case C2 in Table 25 and Figure 223), the overall result may still not be satisfactory, if the absorption effectiveness is not broadband and occurs only selectively for certain – in this case higher – frequencies. The application of a broad-band absorber system (see Table 25, case C3) has a better potential to provide acoustically preferable conditions (see Figure 223).

6. Conclusions

6.1. Contributions

Most appraisals of the presumed strengths of traditional buildings are typically based on qualitative descriptions of some design strategies and features. In few instances, such appraisals are based on solid empirical data. Within this study the performance of traditional hammams was empirically monitored, indoor and outdoor climate data for five such buildings were collected leading to a comprehensive and high-resolution database with approximately 15 000 000 data points.

The monitoring results allow for an objective assessment of the actual performance of these buildings and evaluation of their strengths and weaknesses.

There is a concern that traditional hammam buildings in the Islamic countries are in decline. To explore the possibilities for sensible conservation of these buildings and their continued use in terms of their original functionality requires careful study of the status quo and analysis of appropriate preservation and renovation measures. In this context, the present contribution provided a summary of monitoring results pertaining to the thermal, acoustical and visual conditions in a number of traditional hammams.

In addition to analyzing the measurements, the potential of the application of digital performance simulation models toward the evaluation of possible thermal retrofit measures were explored. It was demonstrated that measured data could be used to calibrate such digital simulation models in order to increase the reliability of their predictions.

6.2. Future research

The application of digital performance simulation models as presented in this research gives a detailed understanding of the performance of these buildings. Furthermore, it allows for the possibility to compare, evaluate and optimize proposals for improvement and renovation. Future efforts can involve a consistent use of such calibrated simulation models of other types of objects with similar potentials and problems such as residential or educational buildings.

Moreover, a detailed survey of a specific building type showed efficient ways in the exploration and understanding of traditional systems and methods. For example traditional plasters used in hot rooms showed a remarkable good permeability and longevity under humid conditions. Whereas plaster systems applied at the moment during renovation of hammam buildings don't use these features and therefore cause major problems with mould growth especially in the humid spaces. Such outcome can significantly contribute to the development of modern techniques and practices.

From a technical point of view it can be stated that data collection with manual downloading of sensors caused data assessment difficulties. Access to the building was not always easily possible, consequently some data were lost. In future, the use of wireless sensors and remote data collection and management may provide a more efficient alternative to the data monitoring infrastructure used in the course of the present dissertation.

6.3. Publications

As of this writing, various portions and reports on earlier stages of this work have been published in the following articles:

Mahdavi, A. and Orehounig K. 2007. Understanding traditional architecture via building diagnostics and computational performance modelling. *Vienna Symposium: "The islamic Hammam and its Sustainable Future"*. Vienna, Austria.

Mahdavi, A., Orehounig, K., and Mikats, N. 2007. A tale of two hammams: Indoor environmenal conditions in traditional bath buildings. *PLEA 2007, Sun, Wind and Architecture*. Singapore. 185-192.

Mahdavi, A. Orehounig, K., Mikats, N., Lambeva, L., and El-Habashi, A. 2007. Analyzing Traditional Buildings Via Empirically Calibrated Building Performance Models. *Proceedings of the 10th International Building Performance Simulation Association Conference and Exhibition*. Beijing, China.

Mahdavi, A., Kainrath, B., Orehounig, K., and Lechleitner, J. 2008. A comparative study of room acoustics in highly humid spaces. *The 11th International Conference on indoor Air Quality and Climate*. Copenhagen, Denmark. ID 180.

Mahdavi, A., Kainrath, B., Orehounig, K., and Lechleitner, J. 2008. Measurement and Simulation of room Acoustics Parameters in Traditional

and Modern Bath Buildings. *Building Simulation Volume 1 Number 3*, 2008.

Mahdavi, A. and Orehounig, K. 2008. An inquiry into the thermal, acoustical and visual aspects of indoor environment in traditional hammams. *The traditional Hammam: A gift from the past for the future*. Damascus, Syria.

Mahdavi, A. and Orehounig K. 2008. An inquiry into the thermal, acoustical, and visual aspects of indoor environment in traditional hammams. *archnet-IJAR-International Journal of Architectural Research Vol 2 Issue 3*.

Mahdavi, A. Orehounig, K., and Kainrath, B. 2008. Assessment and evaluation of the thermal and acoustical conditions in traditional bath buildings. *Plea 2008 - 25th Conference on Passive and Low Energy Architecture*. Dublin, Ireland.

Mahdavi, A. and Orehounig K. 2009. On indoor environmental conditions in traditional hammams. *IFPO. Damascus, Syria*.

Orehounig, K. and Mahdavi, A. 2009. Thermal performance of traditional bath buildings. *4th International Building Physics Conference*. Istanbul, Turkey.

Orehounig, K. and Mahdavi, A. 2009. Application of calibrated simulation models toward performance assessment of traditional buildings. *to be published in Proceedings of IBPSA 2009 (11th International Building Performance Simulation Association Conference and Exhibition)*. Glasgow, Scotland.

7. References

7.1. Literature

Christensen, C. L. 2005. *ODEON Room Acoustics Program Version 8.0 Use manual*. Industrial, Auditorium and Combined Editions.

Dow, M. 1996. *The Islamic Baths of Palestine*. Oxford University Press. Jerusalem, Israel.

Driesen and Kern Company. February 20, 2009. <http://www.driesen-kern.de/>.

Écochard, M. and Le Coeur, C.1942. *Les bains de Damas*. Institut français de Damas, Beyrouth

E+E Elektronik Ges.m.b.H. February 20, 2009. <http://www.epluse.com/de/>.

EDSL 2007. A-Tas Theory Manual. EDSL Documentation.

EDSL 2009. *EDSL A-Tas*. February 20, 2009. <http://www.edsl.net/>.

Fanger, P. O. 1970. *Thermal Comfort-Analysis and Applications in environmental engeneering*. Danish Technical Press. Copenhagen, Denmark.

Fasold, W. and Veres E. 2003. *Schallschutz und Raumakustik in der Praxis*. Huss Medien GmbH. Berlin, Germany.

Grotzfeld, H. 1970. *Das Bad im arabisch-islamischen Mittelalter, Eine kulturgeschichtliche Studie*. Otto Harrassowitz Verlag. Wiesbaden, Germany.

HAMMAM 2006a. Background Information of the Hammam in Ankara. Deliverable EU-Project, Vienna.

HAMMAM 2006b. Background Information of the Hammam in Cairo. Deliverable EU-Project, Vienna.

HAMMAM 2006c. Background Information of the Hammam in Constantine. Deliverable EU-Project, Vienna.

HAMMAM 2006d. Background Information of the Hammam in Damascus. Deliverable EU-Project, Vienna.

HAMMAM 2006e. Background Information of the Hammam in Fez. Deliverable EU-Project, Vienna.

HAMMAM 2006f. Data Report of the Hammam in Ankara. Deliverable EU-Project, Vienna.

HAMMAM 2006g. Data Report of the Hammam in Cairo. Deliverable EU-Project, Vienna.

HAMMAM 2007a. Data Report of the Hammam in Constantine. Deliverable EU-Project, Vienna.

HAMMAM 2007b. Data Report of the Hammam in Damascus. Deliverable EU-Project, Vienna.

HAMMAM 2007c. Data Report of the Hammam in Fez. Deliverable EU-Project, Vienna.

Hammam Project. December 2008. www.hammams.org.

Kainrath, B. 2008. *Raumakustische Zustände in Feuchträumen am Beispiel traditioneller Bäder und moderner Thermen*. Diplomarbeit, TU Wien. Vienna, Austria.

Kiby, U. 1995. *Bäder und Badekultur in Orient und Okzident*. DuMont. Köln, Germany.

Konica Minolta. February 20, 2009. <http://www.konicaminolta.com/instruments/products/light/illuminance-meter/t10/index.html>.

Mahdavi, A 2007. Learning from traditional architecture through building diagnostics and performance modeling. *Proceedings of the 12th Symposium for Building Physics*. Dresden, Germany, p11-p22.

Mahdavi, A., Orehounig, K., Mikats, N., Lambeva, L., and El-Habashi, A. 2007. Analyzing Traditional Buildings Via Empirically Calibrated Building Performance Models. *Proceedings of the 10th International Building Performance Simulation Association Conference and Exhibition*. Beijing, China.

Mahdavi, A. and Orehounig K. 2008. An inquiry into the thermal, acoustical, and visual aspects of indoor environment in traditional hammams. *archnet-IJAR-International Journal of Architectural Research Vol 2 Issue 3*.

Mahdavi, A., Kainrath B., Orehounig K., and Lechleitner J. 2008a. A comparative study of room acoustics in highly humid spaces. *The 11th International Conference on indoor Air Quality and Climate*. Copenhagen, Denmark, ID 180.

Mahdavi, A., Kainrath, B., Orehounig, K., and Lechleitner J. 2008b. Measurement and Simulation of room Acoustics Parameters in Traditional and Modern Bath Buildings. *Building Simulation Volume 1 Number 3*.

- Mahdavi, A. and Orehounig K. 2009. On indoor environmental conditions in traditional hammams. *IFPO*. Damascus, Syria.
- Mikats, N. 2007. *Erfassung und Visualisierung der thermischen Performance eines traditionellen Hammams in Cairo*. Diplomarbeit, Technische Universität Wien. Vienna, Austria.
- Musil, A. 1907. *Ḳuṣejr Amra*. k.k. Hof- u. Staatsdruckerei. Vienna, Austria.
- Onset Company. February 20, 2009. <http://www.onsetcomp.com/>.
- Orehounig, K. and Mahdavi A. 2009. Application of calibrated simulation models toward performance assessment of traditional buildings. *to be published in Proceedings of IBPSA 2009 (11th International Building Performance Simulation Association Conference and Exhibition)*. Glasgow, Scotland.
- Pauty, E. 1933. *Les Hammams du Caire*. L'institut francais d'archeologie orientale du Caire. Cairo, Egypt.
- Rion. February 20, 2009. <http://www.rion.co.jp/english/>.
- Shedayeb, D. 2006. Hammam Activity pattern. Hammam Report, Cairo, Egypt.
- Sibley, M. 2006 The Historic Hammams of Damascus and Fez: Lessons of Sustainability and Future Developments. *The 23rd Conference on Passive and Low Energy Architecture*. Geneva, Switzerland.
- Szokolay, S. 2004. *Introduction to Architectural Science the basis of sustainable design*. Architectural Press, 2004. Oxford, Great Britain.

7.2. Tables

Table 1 Summarized parameters of Hammams.....	17
Table 2 Breakdown of the total annual delivered energy consumption for Hammam Bab al-Bahr (HAMMAM 2006g, 51)	21
Table 3 Breakdown of the total annual delivered energy consumption for Hammam Şengül (HAMMAM 2006f, 70)	25
Table 4 Breakdown of the total annual delivered energy consumption for Hammam Saffarin (HAMMAM 2007c, 91)	29
Table 5 Breakdown of the total annual delivered energy consumption for Hammam Ammouneh (HAMMAM 2007b, 79)	33
Table 6 Breakdown of the total annual delivered energy consumption for Hammam Suq al Ghazal (HAMMAM 2007a, 66)	37
Table 7 Overview of the external weather data collection period for the five buildings	38
Table 8 Overview of the internal hygro-thermal data collection period for the five buildings	42
Table 9 Overview of the performed acoustical measurements	46
Table 10 Assumed appropriate (target) reverberation times (in seconds) for the selected spaces.....	49
Table 11 Modeled Zones.....	52
Table 12 Simulation assumption regarding construction data (U-value, mass, g-value).....	53
Table 13 Simulation assumption regarding internal gains (people, lights), air change rate	53
Table 14 Modeled Zones of SEN	55
Table 15 Simulation assumption regarding construction data (U-value, mass, g-value).....	55
Table 16 Summarized air change rates and internal gains	56
Table 17 Modeled Zones.....	58
Table 18 Simulation assumption regarding construction data (U-value, mass, g-value).....	58

Table 19 Assumptions regarding air change rate and internal gains.....	58
Table 20 U-value and g-value assumptions regarding the pertinent building components for thermal simulation scenarios S1 to S3	61
Table 21 Assumptions pertaining to air change rates (ACH in h^{-1}), internal gains (W.m^{-2}), and heating set point ($^{\circ}\text{C}$) for the study of thermal mass impact on overheating in hammams (CH)	62
Table 22 Assumptions pertaining to air change rates (ACH in h^{-1}), internal gains (W.m^{-2}), and heating set point ($^{\circ}\text{C}$) for the study of thermal mass impact on the hammams' heating loads.....	62
Table 23 Model input assumptions regarding surface percentage (%), area (m^2), and scattering factor (Scat) of materials used in SAG, BEL, and BOU (Kainrath 2008).....	65
Table 24 used materials and there respecting sound absorption coefficients (Kainrath 2008)	65
Table 25 used materials and there respecting sound absorption coefficients	65
Table 26 A-weighted ambient sound levels (spot measurements)	103
Table 27 deviation of measured reverberation time values from desirable values (%)	104
Table 28 Simulated space heating demand ($\text{kWh.m}^{-2}.\text{a}^{-1}$) for BAB, SEN, and SAG (scenarios S1 to S3 as per Table 20)	119
Table 29 Reverberation time of simulated improvement scenarios of BOU	121

7.3. Figures

Figure 1 Basins in hot room of Hammam Ammouneh.....	5
Figure 2 Bucket system in Hammam Saffarin (HAMMAM 2007c).....	5
Figure 3 Mashlah, fountain in Hammam Fairouzi.....	7
Figure 4 Hot room of a hammam in Isfahan, Iran.....	8
Figure 5 Massive walls in Hammam Tambali, Cairo Egypt (picture by A. Mahdavi)	11
Figure 6 Floor in Hammam Fairouzi (Damascus, Syria).....	11
Figure 7 Typical openings in domes of hammam (Hammam Fairouzi).....	12
Figure 8 Typical openings in domes of hammam, outside view (Hammam Fairouzi)	12
Figure 9 Blocked apertures of Hammam Suq al Ghazal, Algeria.....	13
Figure 10 Section showing typical heating arrangements at Hammam al-Basha (Dow 1996)	14
Figure 11 Furnace of Hammam Saffarin (picture by Aisha Darwish)	14
Figure 12 Locations of selected cities	16
Figure 13 Entrance of Hammam Bab al-Bahr (picture by A. Mahdavi).....	18
Figure 14 Interior view of hot room in Hammam Bab al-Bahr (picture by A. Mahdavi)	19
Figure 16 Section of Hammam Bab al-Bahr	20
Figure 15 Floor plan of Hammam Bab al-Bahr.....	20
Figure 17 Outside view of Hammam Şengül (picture by A. Mahdavi)	22
Figure 18 Interior view of hot room in Hammam Şengül (HAMMAM 2006f)	22
Figure 19 Floor plan of Hammam Şengül.....	24
Figure 20 Section of Hammam Şengül	24
Figure 21 Outside view of Hammam Saffarin	26
Figure 22 Inside dome in changing room in Hammam Saffarin.....	26

Figure 23 Floor plan of Hammam Saffarin	28
Figure 24 Section of Hammam Saffarin	28
Figure 25 Hammam Ammouneh outside view	30
Figure 26 Changing Room of Hammam Ammouneh	30
Figure 27 Floor plan of Hammam Ammouneh	32
Figure 28 Section of Hammam Ammouneh.....	32
Figure 29 Entrance of hammam Suq al-Ghazal	34
Figure 30 connection changing room and cold room	34
Figure 31 Internal view cold room	35
Figure 32 Internal view hot room	36
Figure 33 Floor plan of Hammam Suq al Ghazal	36
Figure 34 Section of Hammam Suq al Ghazal	37
Figure 35 weather station in Cairo.....	39
Figure 36 weather station in Ankara.....	39
Figure 37 weather station in Fez.....	40
Figure 38 weather station in Damascus.....	40
Figure 39 weather station in Constantine (picture by Samira Debache) ...	41
Figure 40 Sensor locations in Hammam Bab al-Bahr	43
Figure 41 Sensor locations in Hammam Şengül.....	43
Figure 42 Sensor locations in Hammam Saffarin	44
Figure 43 Sensor locations in Hammam Ammouneh.....	44
Figure 44 Sensor locations of Hammam Suq al-Ghazal	45
Figure 45 Illustrative depiction of the process of simulation model generation, calibration, and application (Mahdavi et al. 2007).....	51
Figure 46 Example of a geometry model (Hammam Şengül) in Tas	52
Figure 47 Space heating assumptions ($W.m^{-2}$) for BAB	54
Figure 48 Space heating assumptions ($W.m^{-2}$) for SEN.....	57

Figure 49 Heating load of hammam SAG calculated based on energy use data and simulated based on measured indoor temperature values.....	60
Figure 50 Heating power assumptions for the simulation model (SAG) ...	60
Figure 51 Odeon-model of SAG, BEL, and BOU (Kainrath 2008).....	64
Figure 52 Indoor air temperature [°C] in CH of BAB for the observation period March 2006 to February 2007	67
Figure 53 Indoor air temperature [°C] in CR of BAB for the observation period March 2006 to February 2007	67
Figure 54 Indoor air temperature [°C] in HRa of BAB for the observation period March 2006 to February 2007	68
Figure 55 Indoor air temperature [°C] in HRb of BAB for the observation period March 2006 to February 2007	68
Figure 56 Outside air temperature [°C] of BAB for the observation period March 2006 to February 2007.....	69
Figure 57 Temperature θ_{i+e} [°C] Cairo July 2006	69
Figure 58 Relative Humidity RH [%] Cairo July 2006.....	69
Figure 59 Temperature θ_{i+e} [°C] Cairo October 2006.....	70
Figure 60 Relative Humidity RH [%] Cairo October 2006.....	70
Figure 61 Temperature θ_{i+e} [°C] Cairo January 2007.....	70
Figure 62 Relative Humidity RH [%] Cairo January 2007	70
Figure 63 Relative Temperature [%] in July 2006	70
Figure 64 Relative Temperature [%] in January 2007	70
Figure 65 Temperature distribution in changing room of BAB during opening hours	71
Figure 66 Temperature distribution in cold room of BAB during opening hours	71
Figure 67 Temperature distribution in main hot room of BAB during opening hours	71
Figure 68 Temperature distribution in pool room of BAB during opening hours	71

Figure 69 Temperature distribution of External temperature.....	71
Figure 70 Depiction of indoor climate conditions in the changing room in BAB for July and October 2006, January and April 2007, compared to Standardized Effective Temperature SET for each month.....	72
Figure 71 Indoor air temperature [°C] in CH of women section in SEN for the observation period July 2006 to June 2007	73
Figure 72 Indoor air temperature [°C] in CH of men section in SEN for the observation period July 2006 to June 2007	74
Figure 73 Indoor air temperature [°C] in WR of women section in SEN for the observation period July 2006 to June 2007	74
Figure 74 Indoor air temperature [°C] in HR of women section in SEN for the observation period July 2006 to June 2007	75
Figure 75 Indoor air temperature [°C] in HR of men section in SEN for the observation period July 2006 to June 2007	75
Figure 76 Outside air temperature [°C] of SEN for the observation period July 2006 to June 2007	76
Figure 77 Temperature θ_{i+e} [°C] Ankara female-part August 2006.....	76
Figure 78 Relative Humidity RH [%] Ankara female-part August 2006.....	76
Figure 79 Temperature θ_{i+e} [°C] Ankara female-part December 2006	77
Figure 80 Relative Humidity RH [%] Ankara female-part December 2006	77
Figure 81 Temperature θ_{i+e} [°C] Ankara female-part April 2007	77
Figure 82 Relative Humidity RH [%] Ankara female-part April 2007	77
Figure 83 Temperature θ_{i+e} [°C] Ankara male-part August 2006	77
Figure 84 Relative Humidity RH [%] Ankara male-part August 2006	77
Figure 85 Temperature θ_{i+e} [°C] Ankara male-part December 2006	78
Figure 86 Relative Humidity RH [%] Ankara male-part December 2006 ...	78
Figure 87 Temperature θ_{i+e} [°C] Ankara male-part April 2007.....	78
Figure 88 Relative Humidity RH [%] Ankara male-part April 2007.....	78
Figure 89 Relative Temperature [%] of August 2006.....	78
Figure 90 Relative Temperature [%] of April 2007.....	78

Figure 91 Temperature distribution in women changing room of SEN	79
Figure 92 Temperature distribution in women warm room of SEN	79
Figure 93 Temperature distribution in women hot room of SEN	79
Figure 94 Temperature distribution in men changing room of SEN	79
Figure 95 Temperature distribution in men hot room of SEN	79
Figure 96 Temperature distribution of external temperature.....	79
Figure 97 Depiction of the indoor climate conditions in the changing room in SEN for July and October 2006, January and March 2007, compared to Standardized Effective Temperature SET for each month	80
Figure 98 Indoor air temperature [°C] in CH of women section in SAF for the observation period October 2006 to September 2007	81
Figure 99 Indoor air temperature [°C] in CH of men section in SAF for the observation period October 2006 to September 2007	82
Figure 100 Indoor air temperature [°C] in CR of women section in SAF for the observation period October 2006 to September 2007	82
Figure 101 Indoor air temperature [°C] in CR of men section in SAF for five months during observation period	83
Figure 102 Indoor air temperature [°C] in WR of women section in SAF for the observation period October 2006 to September 2007	83
Figure 103 Indoor air temperature [°C] in WR of men section in SAF for two months during observation period	84
Figure 104 Indoor air temperature [°C] in HR of women section in SAF for the observation period October 2006 to September 2007	84
Figure 105 Indoor air temperature [°C] in HR of men section in SAF for the observation period October 2006 to September 2007	85
Figure 106 Outside air temperature [°C] of SAF for the observation period October 2006 to September 2007	85
Figure 107 Temperature θ_{i+e} [°C] Fez female-part November 2006	86
Figure 108 Relative Humidity RH [%] Fez female-part November 2006....	86
Figure 109 Temperature θ_{i+e} [°C] Fez female-part April 2007.....	86
Figure 110 Relative Humidity RH [%] Fez female-part April 2007	86

Figure 111 Temperature θ_{i+e} [°C] Fez female-part July 2007	86
Figure 112 Relative Humidity RH [%] Fez female-part July 2007	86
Figure 113 Temperature θ_{i+e} [°C] Fez male-part November 2006	87
Figure 114 Relative Humidity RH [%] Fez male-part November 2006	87
Figure 115 Temperature θ_{i+e} [°C] Fez male-part April 2007	87
Figure 116 Relative Humidity RH [%] Fez male-part April 2007	87
Figure 117 Temperature θ_{i+e} [°C] Fez male-part July 2007	87
Figure 118 Relative Humidity RH [%] Fez male-part July 2007	87
Figure 119 Relative Temperature [%] of November 2006	88
Figure 120 Relative Temperature [%] of April 2007	88
Figure 121 Temperature distribution in women changing room of SAF ..	88
Figure 122 Temperature distribution in men changing room of SAF	88
Figure 123 Temperature distribution in women cold room of SAF	89
Figure 124 Temperature distribution in men cold room of SAF	89
Figure 125 Temperature distribution in women warm room of SAF	89
Figure 126 Temperature distribution in men warm room of SAF	89
Figure 127 Temperature distribution in women hot room of SAF	89
Figure 128 Temperature distribution in men hot room of SAF	89
Figure 129 Temperature distribution of external temperature	89
Figure 130 Depiction of the indoor climate conditions in the changing room in SAF for October 2006, January, April and July 2007, compared to Standardized Effective Temperature SET for each month	90
Figure 131 Indoor air temperature [°C] in CH of AMH for the observation period February 2007 to May 2007	91
Figure 132 Indoor air temperature [°C] in CR of AMH for the observation period February 2007 to May 2007	92
Figure 133 Indoor air temperature [°C] in WR of AMH for the observation period February 2007 to May 2007	92

Figure 134 Indoor air temperature [°C] in HR of AMH for the observation period February 2007 to May 2007	93
Figure 135 Outside air temperature [°C] of AMH for the observation period February 2007 to May 2007	93
Figure 136 Temperature θ_{i+e} [°C] Damascus February 2007	94
Figure 137 Relative Humidity RH [%] Damascus February 2007	94
Figure 138 Temperature θ_{i+e} [°C] Damascus March 2007	94
Figure 139 Relative Humidity RH [%] Damascus March 2007	94
Figure 140 Temperature θ_{i+e} [°C] Damascus April 2007	94
Figure 141 Relative Humidity RH [%] Damascus April 2007	94
Figure 142 Temperature θ_{i+e} [°C] Damascus May 2007	95
Figure 143 Relative Humidity RH [%] Damascus May 2007	95
Figure 144 Relative Temperature [%] of February 2007	95
Figure 145 Relative Temperature [%] of April 2007	95
Figure 146 Temperature distribution in changing room of AMH	96
Figure 147 Temperature distribution in cold room of AMH	96
Figure 148 Temperature distribution in warm room of AMH	96
Figure 149 Temperature distribution in hot room of AMH	96
Figure 150 Temperature distribution of External Temperature	96
Figure 151 Indoor air temperature [°C] in CH of SAG for the observation period July 2007 to June 2008	97
Figure 152 Indoor air temperature [°C] in CR of SAG for seven months during the observation period	98
Figure 153 Indoor air temperature [°C] in HR of SAG for the observation period from July 2007 to June 2008	98
Figure 154 Outside air temperature [°C] of SAG for the observation period July 2007 to June 2008	99
Figure 155 Temperature θ_{i+e} [°C] Constantine January 2008	99
Figure 156 Relative Humidity RH [%] Constantine January 2008	99

Figure 157 Temperature θ_{i+e} [°C] Constantine April 2008	100
Figure 158 Relative Humidity RH [%] Constantine April 2008	100
Figure 159 Temperature θ_{i+e} [°C] Constantine June 2008.....	100
Figure 160 Relative Humidity RH [%] Constantine June 2008	100
Figure 161 Relative Temperature January 2008	100
Figure 162 Relative Temperature June 2008	100
Figure 163 Temperature distribution in CH of SAG	101
Figure 164 Temperature distribution in CR of SAG.....	101
Figure 165 Temperature distribution in HR of SAG	101
Figure 166 Temperature distribution of External Temperature of SAG ..	101
Figure 167 Depiction of the indoor climate conditions in the changing room in SAG for July and October 2007, January and April 2008, compared to Standardized Effective Temperature SET for each month .	102
Figure 168 Frequency dependent ambient sound levels for Hammam Saffarin and Hammam Ammouneh.....	103
Figure 169 Measured reverberation times in SAG, BEL, BOU.....	104
Figure 170 Deviation of measured reverberation time values from desirable values (%).....	104
Figure 171 Results of horizontal illuminance measurements in Hammam Bab al-Bahr, March 2006 11:50 (in lx).....	105
Figure 172 Results of horizontal illuminance measurements (lx) and daylight factors (%) in Hammam Şengül July 2006	106
Figure 173 Results of horizontal illuminance measurements in Hammam Saffarin November 2006 9:00 (in lx)	106
Figure 174 Results of horizontal illuminance measurements in Hammam Ammouneh February 2007 10:30 (in lx)	107
Figure 175 Results of horizontal illuminance measurements (daylight and electrical light) in Hammam Suq al Ghazal May 2007 7:30 (in lx).....	107
Figure 176 Results of daylight factor measurements in Hammam Suq al Ghazal May 2007 7:30 (in %).....	108

Figure 177 Summary of compared locations: CH, CR, HRa, and HRb	109
Figure 178 Simulated versus measured indoor air temperature in CH for a reference day (mean hourly values, April 2006)	109
Figure 179 Simulated versus measured indoor air temperature in CH for a reference day (mean hourly values, July 2006).....	109
Figure 180 Simulated versus measured indoor air temperature in CH for a reference day (mean hourly values, October 2006)	110
Figure 181 Simulated versus measured indoor air temperature in CH for a reference day (mean hourly values, January 2007)	110
Figure 182 Simulated versus measured indoor air temperature in CR for a reference day (mean hourly values, April 2006)	110
Figure 183 Simulated versus measured indoor air temperature in CR for a reference day (mean hourly values, July 2006).....	110
Figure 184 Simulated versus measured indoor air temperature in CR for a reference day (mean hourly values, October 2006)	110
Figure 185 Simulated versus measured indoor air temperature in CR for a reference day (mean hourly values, January 2007)	110
Figure 186 Simulated versus measured indoor air temperature in HRa for a reference day (mean hourly values, April 2006)	111
Figure 187 Simulated versus measured indoor air temperature in HRa for a reference day (mean hourly values, July 2006).....	111
Figure 188 Simulated versus measured indoor air temperature in HRa for a reference day (mean hourly values, October 2006).....	111
Figure 189 Simulated versus measured indoor air temperature in HRa for a reference day (mean hourly values, January 2007)	111
Figure 190 Simulated versus measured indoor air temperature in HRb for a reference day (mean hourly values, April 2006)	111
Figure 191 Simulated versus measured indoor air temperature in HRb for a reference day (mean hourly values, July 2006).....	111
Figure 192 Simulated versus measured indoor air temperature in HRb for a reference day (mean hourly values, October 2006).....	112
Figure 193 Simulated versus measured indoor air temperature in HRb for a reference day (mean hourly values, January 2007)	112

Figure 194 Summary of compared locations: CH, WR, and HR	113
Figure 195 Simulated versus measured indoor air temperature in CH for a reference day (mean hourly values, July 2006).....	113
Figure 196 Simulated versus measured indoor air temperature in CH for a reference day (mean hourly values, October 2006)	113
Figure 197 Simulated versus measured indoor air temperature in CH for a reference day (mean hourly values, January 2007)	114
Figure 198 Simulated versus measured indoor air temperature in CH for a reference day (mean hourly values, April 2007)	114
Figure 199 Simulated versus measured indoor air temperature in WR for a reference day (mean hourly values, July 2006).....	114
Figure 200 Simulated versus measured indoor air temperature in WR for a reference day (mean hourly values, October 2006)	114
Figure 201 Simulated versus measured indoor air temperature in WR for a reference day (mean hourly values, January 2007)	114
Figure 202 Simulated versus measured indoor air temperature in WR for a reference day (mean hourly values, April 2007)	114
Figure 203 Simulated versus measured indoor air temperature in HR for a reference day (mean hourly values, July 2006).....	115
Figure 204 Simulated versus measured indoor air temperature in HR for a reference day (mean hourly values, October 2006)	115
Figure 205 Simulated versus measured indoor air temperature in HR for a reference day (mean hourly values, January 2007)	115
Figure 206 Simulated versus measured indoor air temperature in HR for a reference day (mean hourly values, April 2007)	115
Figure 207 Summary of compared locations: CH, CR, and HR.....	116
Figure 208 Simulated versus measured indoor air temperature in CH for a reference day (mean hourly values, January 2008)	116
Figure 209 Simulated versus measured indoor air temperature in CH for a reference day (mean hourly values, March 2008)	116
Figure 210 Simulated versus measured indoor air temperature in CH for a reference day (mean hourly values, May 2008)	116

Figure 211 Simulated versus measured indoor air temperature in CR for a reference day (mean hourly values, January 2008)	116
Figure 212 Simulated versus measured indoor air temperature in CR for a reference day (mean hourly values, March 2008)	117
Figure 213 Simulated versus measured indoor air temperature in CR for a reference day (mean hourly values, May 2008)	117
Figure 214 Simulated versus measured indoor air temperature in HR for a reference day (mean hourly values, January 2008)	117
Figure 215 Simulated versus measured indoor air temperature in HR for a reference day (mean hourly values, March 2008)	117
Figure 216 Simulated versus measured indoor air temperature in HR for a reference day (mean hourly values, May 2008)	117
Figure 217 Simulated versus measured reverberation times in SAG	118
Figure 218 Simulated versus measured reverberation times in BEL	118
Figure 219 Simulated versus measured reverberation times in BOU.....	118
Figure 220 Heating load reduction for all 3 buildings for Scenario 3.....	120
Figure 221 Mean overheating (in K) for the existing (high thermal mass) and alternative (low thermal mass) scenarios	120
Figure 222 Heating loads (in kWh.m ⁻² .a ⁻¹) for the existing (high thermal mass) and alternative (low thermal mass) scenarios.....	121
Figure 223 Reverberation time of simulated scenarios for BOU including measured values	122
Figure 224 Cumulated Indoor Temperatures in the CH, CR, and HR in BAB from April 2006 till March 2007 including outdoor temperature.....	123
Figure 225 Cumulated Indoor Temperatures in the CH, WR, and HR in SEN (women section) from July 2006 till June 2007 including outdoor temperature.	123
Figure 226 Cumulated Indoor Temperatures in the CH, CR, WR, and HR in SAF (women section) from October 2006 till September 2007 including corresponding outdoor temperature.....	124
Figure 227 Cumulated Indoor Temperatures in the CH, CR, WR and HR in AMH from February 2007 till May 2007 including corresponding outdoor temperature.	124

Figure 228 Cumulated Indoor Temperatures in the CH, CR, and HR in SAG from July 2007 till June 2008 including corresponding outdoor temperature from January 2008 till June 2008.....	124
Figure 229 Comfort temperature after Fanger and SET in changing room of BAB	125
Figure 230 Temperature transition between spaces in BAB (mean monthly values during opening hours)	126
Figure 231 Temperature transition between spaces in SEN (mean monthly values during opening hours).....	126
Figure 232 Temperature transition between spaces in SAF (mean monthly values during opening hours).....	126
Figure 233 Temperature transition between spaces in SAG (mean monthly values during opening hours)	126
Figure 234 Temperature θ_{t+e} [°C] Cairo July 2006	127
Figure 235 Relative Temperature [%] of July 2006	127
Figure 236 Deterioration of daylight and fresh air supply to the interior spaces of a hammam in Fez (Morocco) due to the blockage of roof apertures	128
Figure 237 Electrical lighting in the changing room in hammam in Cairo, Egypt (picture by A. Mahdavi)	129

7.4. Equations

$$\Delta\theta_{rel} = \theta_i - \theta_{e\theta e} \cdot 100 [\%] \quad \text{Eq. 1} \quad \dots\dots\dots 48$$

$$T_n = 17.6 + 0.31 \cdot T_{o,av} \quad \text{Eq. 2} \quad \dots\dots\dots 48$$

$$OH_m = \sum_{i=1}^n \frac{\theta_i - \theta_r}{n} \quad \text{Eq. 3} \quad \dots\dots\dots 62$$

8. Appendix

8.1. Measurement Equipment

8.1.1. External

8.1.1.1. Onset weather station

The weather station has an operating range between -20°C and $+50^{\circ}\text{C}$ with alkaline batteries and -40°C to $+70^{\circ}\text{C}$ with the power of lithium batteries. Logging intervals can be set from 1 second up to 18 hours with time accuracy of 0 to 2 seconds for the first data point and up to ± 5 seconds per week up to 25°C . The data logger has a capacity from 500 000 data points. Table A.1 shows details about the measured parameters together with the measuring range and accuracy of the sensors.

Table A 1 Monitored external climate parameters together with sensor information (Onset Company 2009)

Parameter	Symbol	Unit	Sensor Range		Accuracy of Sensor
Outdoor air temperature	θ_e	$^{\circ}\text{C}$	-40°C	$+70^{\circ}\text{C}$	$\pm 0.7^{\circ}\text{C}$
Outdoor air relative humidity	RH	%	0%	100%	$\pm 3\%$
Global horizontal radiation	$E_{e, \text{glob, hor}}$	$\text{W}\cdot\text{m}^{-2}$	0 $\text{W}\cdot\text{m}^{-2}$	1280 $\text{W}\cdot\text{m}^{-2}$	$\pm 10 \text{ W}\cdot\text{m}^{-2}$
Wind speed	v	$\text{m}\cdot\text{s}^{-1}$	0 $\text{m}\cdot\text{s}^{-1}$	44 $\text{m}\cdot\text{s}^{-1}$	$\pm 0.5 \text{ m}\cdot\text{s}^{-1}$
Wind direction	WD	$^{\circ}$	0°	358° (2° dead band)	$\pm 5^{\circ}$

8.1.1.2. Driesen and Kern weather station

This weather station is suitable for temperature ranges from -20°C to $+70^{\circ}\text{C}$ and can store up to 256 000 data points. Logging intervals can be set from 2 seconds to up to 24 hours. Table A2 shows details about the measured parameters together with sensor ranges and accuracy.

Table A 2 Monitored external climate parameters together with sensor information (Driesen and Kern Company 2009)

Parameter	Symbol	Unit	Sensor Range		Accuracy of Sensor
Outdoor air temperature	θ_e	°C	-30°C	+80°C	± 0.5°C
Outdoor air relative humidity	RH	%	0%	100%	±2 % <90°C ±4 % >90°C
Global horizontal radiation	$E_{e, glob, hor}$	W.m ⁻²	0 W.m ⁻²	5000 W.m ⁻²	< 5%
Wind speed	v	m.s ⁻¹	0 m.s ⁻¹	75 m.s ⁻¹	1%

8.1.2. Internal sensors

8.1.2.1. Dataloggers from Onset

Hobo data loggers run on CR-2032 lithium batteries and have a storage capacity from 64 kB which enables them to store up to 43000 measurements. For launching and downloading data the accompanying software Hoboware was used. Table A3 shows details about measured parameters and sensor information.

Table A 3 Monitored internal climate parameters together with sensor information (Onset Company 2009)

Parameter	Symbol	Unit	Sensor Range		Accuracy of Sensor
Air temperature	θ_i	°C	-20°C	+70°C	± 0.35°C
Relative humidity	RH	%	5%	95%	± 2.5%
Illuminance	E	lx	ca. 10 lx	30000 lx	-

8.1.2.2. Dataloggers from E+E

Dataloggers (Humlogs) measure temperature and relative humidity, and have a storage capacity from up to 120 000 measurements. Humlogs run on 3.6V lithium batteries. Table A4 summarizes the according sensor information.

Table A 4 Monitored internal climate parameters together with sensor information (E+E Elektronik Ges.m.b.H 2009)

Parameter	Symbol	Unit	Sensor Range		Accuracy of Sensor
Air temperature	θ_i	°C	-40°C	+100°C	± 0.2°C
Relative humidity	RH	%	0 %	100 %	± 2 %



Figure A 1 Picture of internal sensor 1 (Onset Company 2009)



Figure A 2 Picture of internal sensor 2 (E+E Elektronik Ges.m.b.H 2009)

8.2. Further Results

8.2.1. Cairo

8.2.1.1. Hygro-thermal indoor conditions

Hourly values for reference days

Following figures show the hourly temperature and relative humidity values (for the reference months from March 2006 to February 2007) for the entrance area (EN), the changing room (CH), the cold room (CR) the main hot room (HRa), and the Pool room (HRb). Note that these figures include also the average outside temperature (EX).

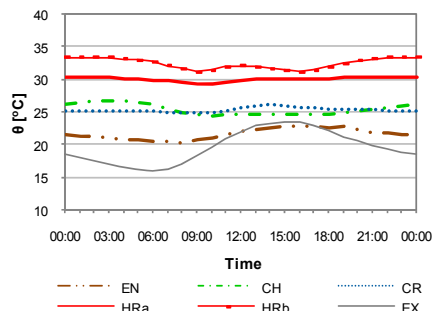


Figure A 3 Temperature θ_{i+e} [°C] Cairo March 2006

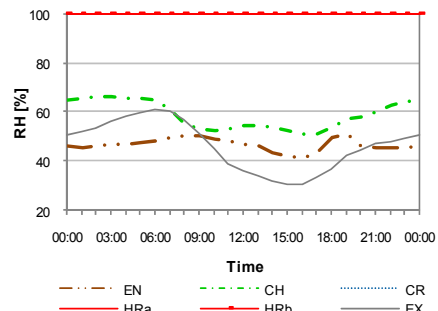


Figure A 4 Relative Humidity RH [%] Cairo March 2006

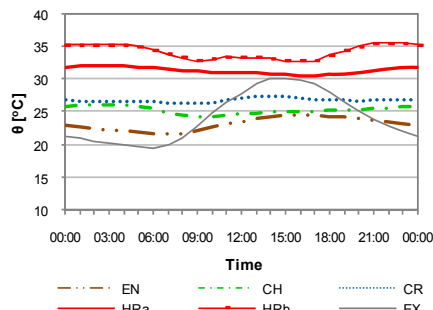


Figure A 5 Temperature θ_{i+e} [°C] Cairo April 2006

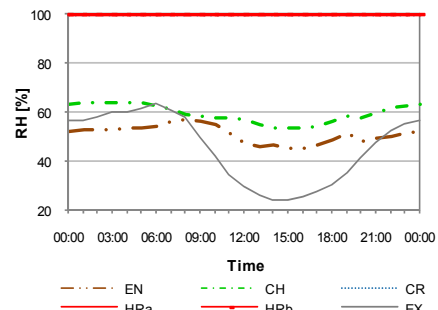


Figure A 6 Relative Humidity RH [%] Cairo April 2006

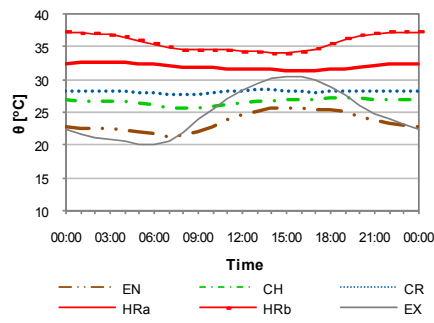


Figure A 7 Temperature θ_{i+e} [°C] Cairo May 2006

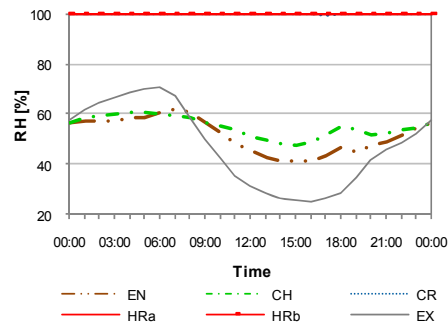


Figure A 8 Relative Humidity RH [%] Cairo May 2006

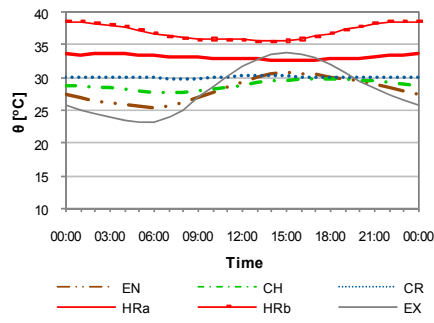


Figure A 9 Temperature θ_{i+e} [°C] Cairo June 2006

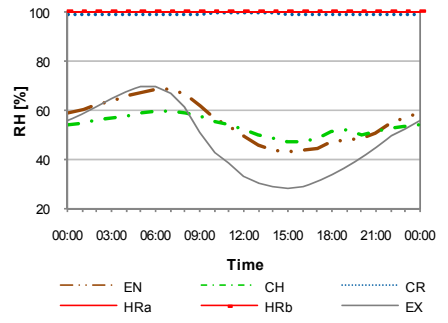


Figure A 10 Relative Humidity RH [%] Cairo June 2006

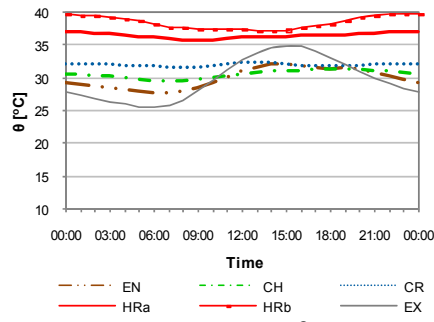


Figure A 11 Temperature θ_{i+e} [°C] Cairo August 2006

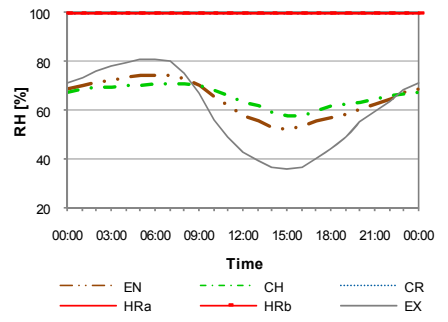


Figure A 12 Relative Humidity RH [%] Cairo August 2006

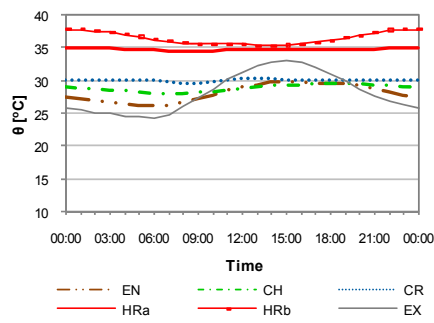


Figure A 13 Temperature θ_{i+e} [°C] Cairo September 2006

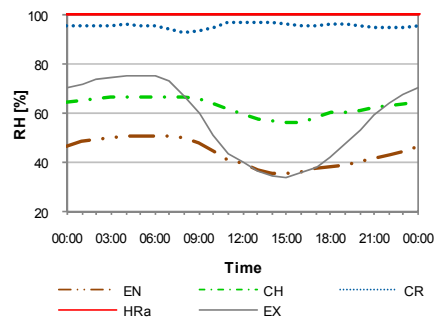


Figure A 14 Relative Humidity RH [%] Cairo September 2006

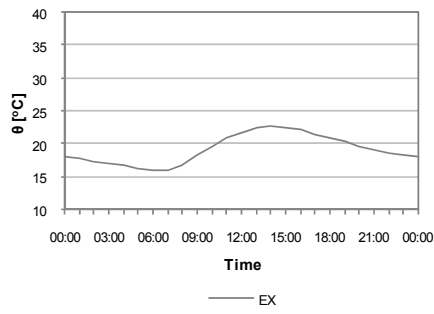


Figure A 15 Temperature θ_{i+e} [°C] Cairo November 2006

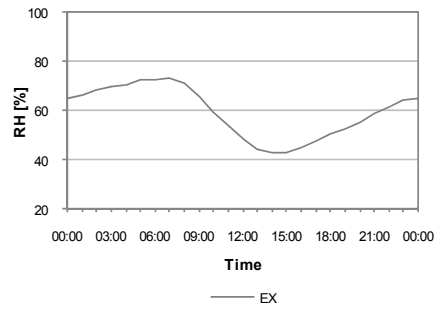


Figure A 16 Relative Humidity RH [%] Cairo November 2006

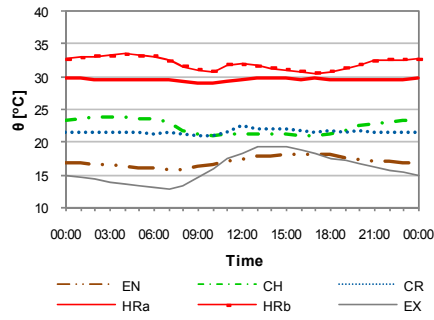


Figure A 17 Temperature θ_{i+e} [°C] Cairo December 2006

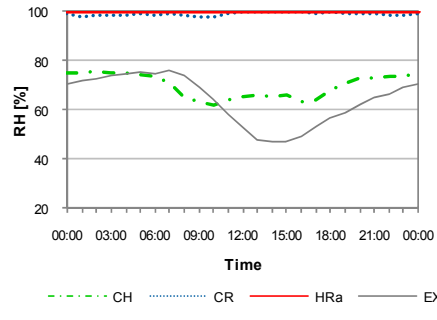


Figure A 18 Relative Humidity RH [%] Cairo December 2006

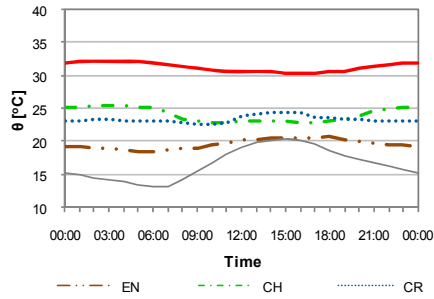


Figure A 19 Temperature θ_{i+e} [°C] Cairo February 2007

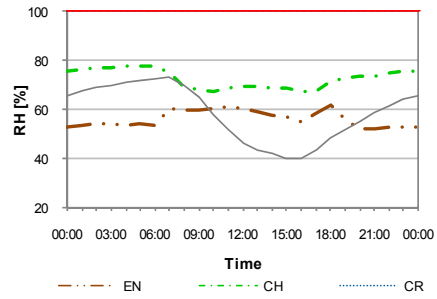


Figure A 20 Relative Humidity RH [%] Cairo February 2007

8.2.2. Ankara

8.2.2.1. Hygro-thermal indoor conditions

Hourly values for reference days

Following figures show the hourly temperature and relative humidity values (for the reference months from July 2006 to June 2007) for the female section of the Ankara Hammam. Data are given for the entrance area (EN), the changing room (CH), the warm room (WR), and the hot room (HR). Note that these figures include also the average outside temperature (EX). Note that these figures include also the average outside temperature (EX).

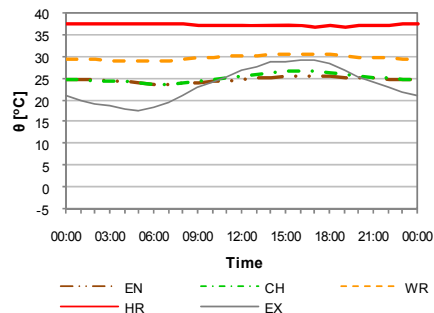


Figure A 21 Temperature θ_{i+e} [°C] Ankara female-part July 2006

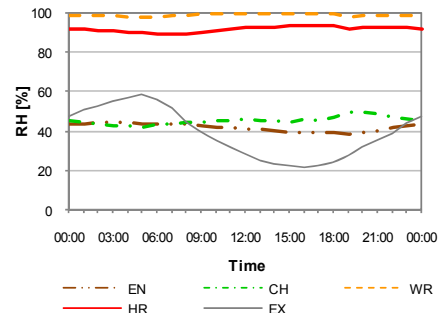


Figure A 22 Relative Humidity RH [%] Ankara female-part July 2006

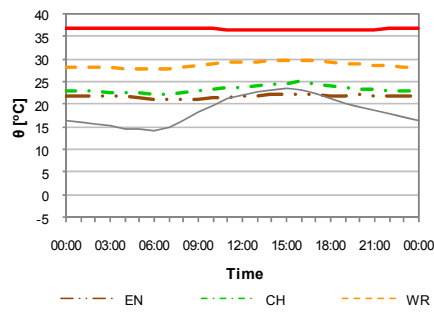


Figure A 23 Temperature θ_{i+e} [°C] Ankara female-part September 2006

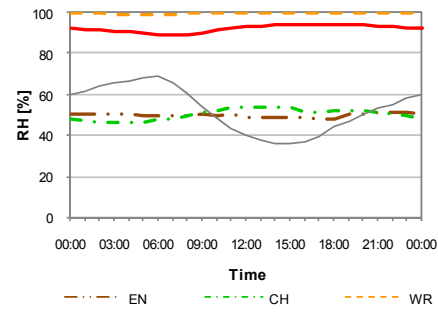


Figure A 24 Relative Humidity RH [%] Ankara female-part September 2006

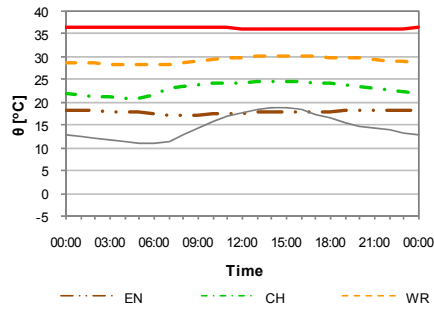


Figure A 25 Temperature θ_{i+e} [°C] Ankara female-part October 2006

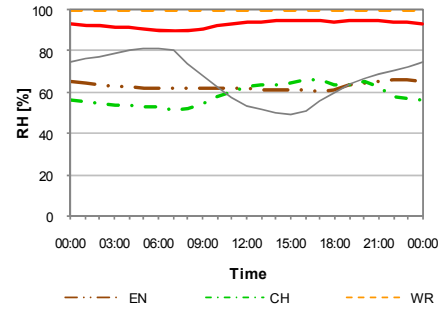


Figure A 26 Relative Humidity RH [%] Ankara female-part October 2006

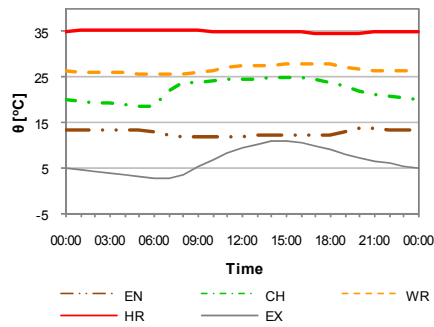


Figure A 27 Temperature θ_{i+e} [°C] Ankara female-part November 2006

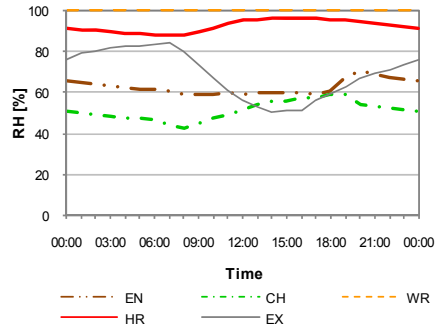


Figure A 28 Relative Humidity RH [%] Ankara female-part November 2006

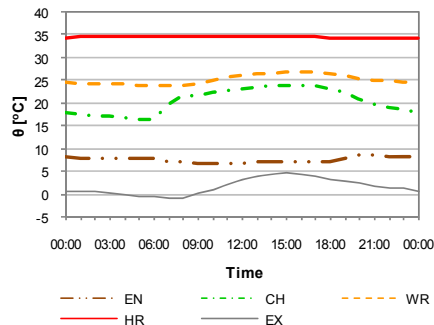


Figure A 29 Temperature θ_{i+e} [°C] Ankara female-part January 2007

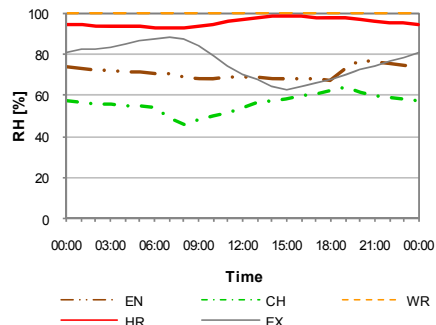


Figure A 30 Relative Humidity RH [%] Ankara female-part January 2007

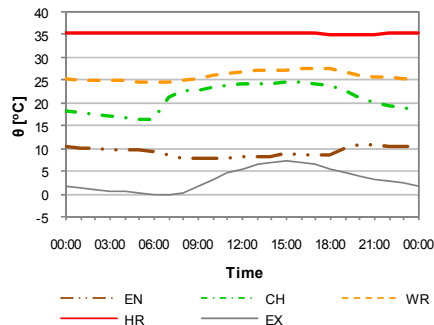


Figure A 31 Temperature θ_{i+e} [°C] Ankara female-part February 2007

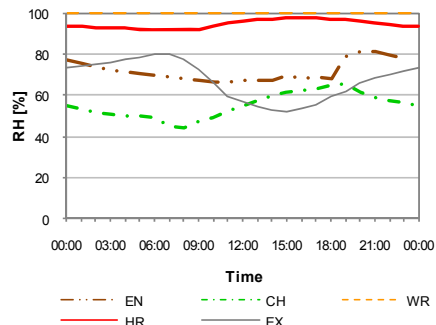


Figure A 32 Relative Humidity RH [%] Ankara female-part February 2007

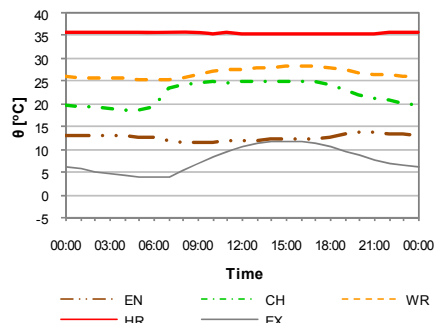


Figure A 33 Temperature θ_{i+e} [°C] Ankara female-part March 2007

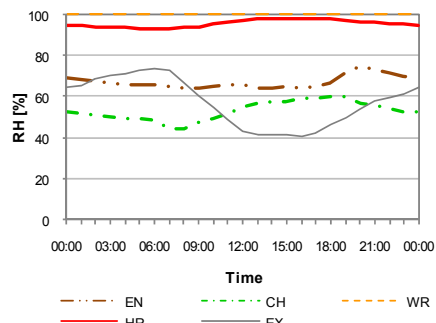


Figure A 34 Relative Humidity RH [%] Ankara female-part March 2007

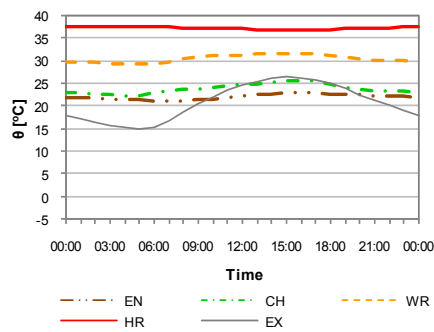


Figure A 35 Temperature θ_{i+e} [°C] Ankara female-part May 2007

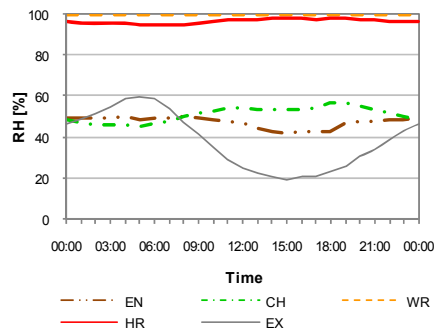


Figure A 36 Relative Humidity RH [%] Ankara female-part May 2007

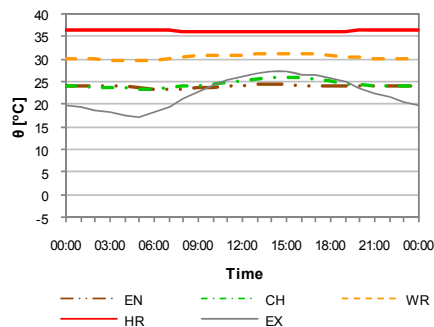


Figure A 37 Temperature θ_{i+e} [°C] Ankara female-part June 2007

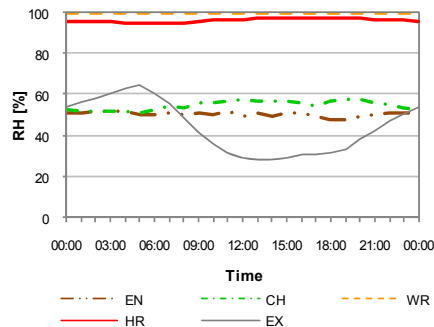


Figure A 38 Relative Humidity RH [%] Ankara female-part June 2007

Following figures show the hourly temperature and relative humidity values (for the reference months from July 2006 to June 2007) for the male section of the Ankara Hammam. Data are given for the changing room (CH), and the hot room (HR). Note that these figures include also the respective average outside temperature (EX).

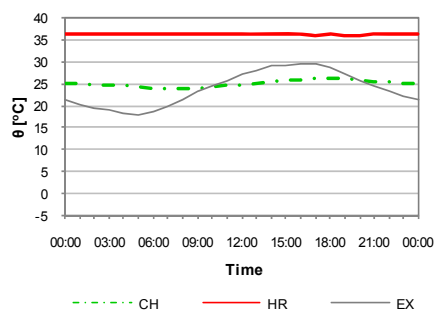


Figure A 39 Temperature θ_{i+e} [°C] Ankara male-part July 2006

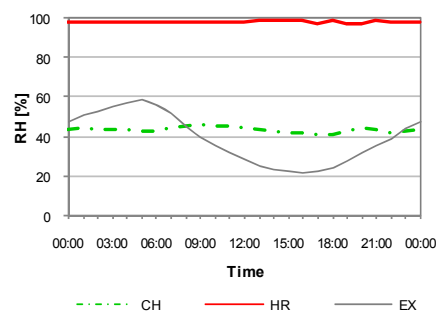


Figure A 40 Relative Humidity RH [%] Ankara male-part July 2006

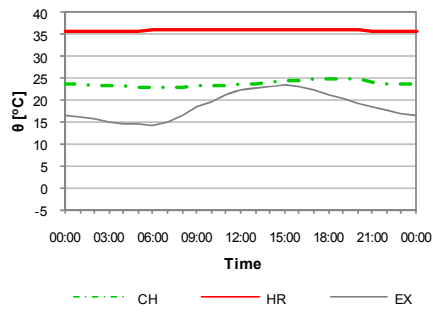


Figure A 41 Temperature θ_{t+e} [°C] Ankara male-part September 2006

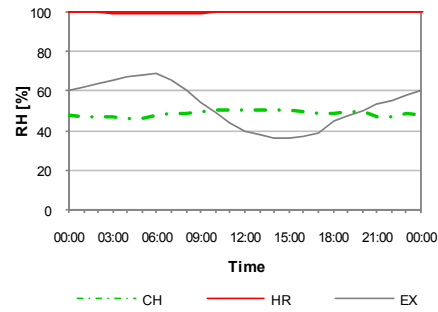


Figure A 42 Relative Humidity RH [%] Ankara male-part September 2006

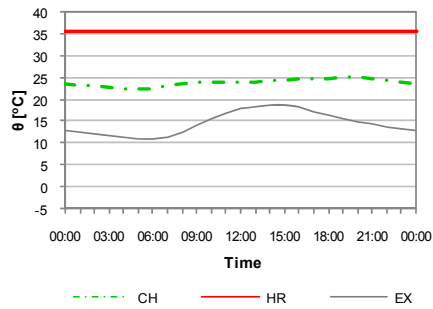


Figure A 43 Temperature θ_{t+e} [°C] Ankara male-part October 2006

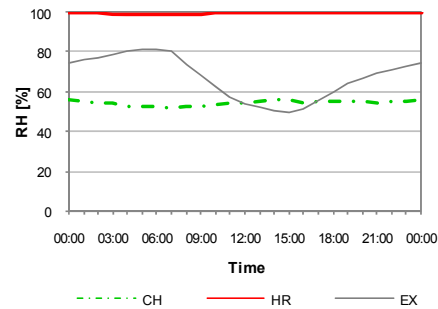


Figure A 44 Relative Humidity RH [%] Ankara male-part October 2006

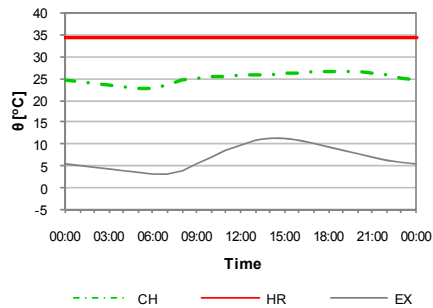


Figure A 45 Temperature θ_{t+e} [°C] Ankara male-part November 2006

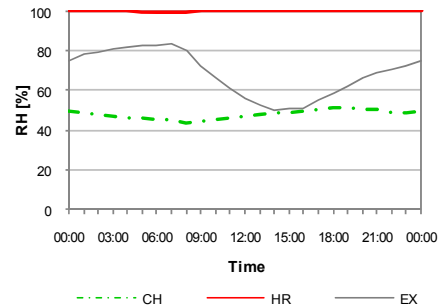


Figure A 46 Relative Humidity RH [%] Ankara male-part November 2006

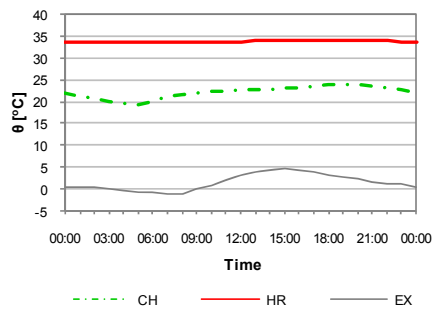


Figure A 47 Temperature θ_{t+e} [°C] Ankara male-part January 2007

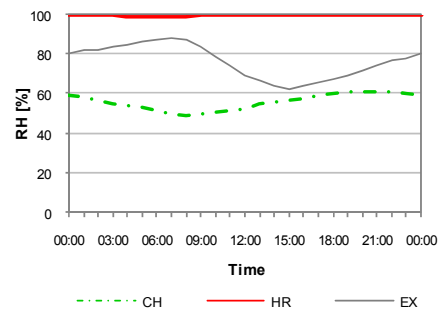


Figure A 48 Relative Humidity RH [%] Ankara male-part January 2007

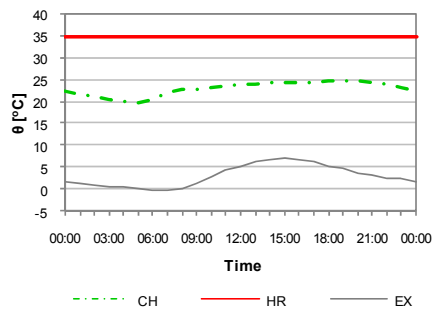


Figure A 49 Temperature θ_{t+e} [°C] Ankara male-part February 2007

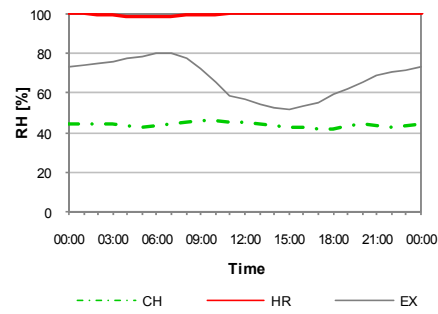


Figure A 50 Relative Humidity RH [%] Ankara male-part February 2007

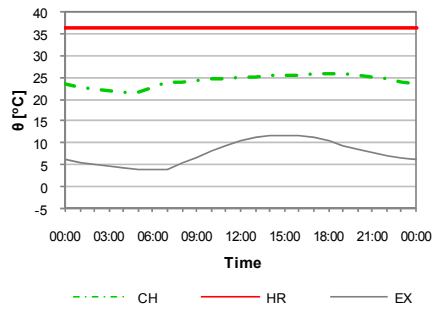


Figure A 51 Temperature θ_{t+e} [°C] Ankara male-part March 2007

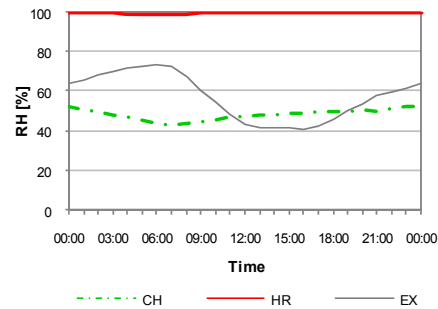


Figure A 52 Relative Humidity RH [%] Ankara male-part March 2007

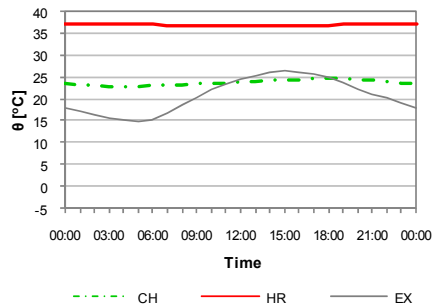


Figure A 53 Temperature θ_{t+e} [°C] Ankara male-part May 2007

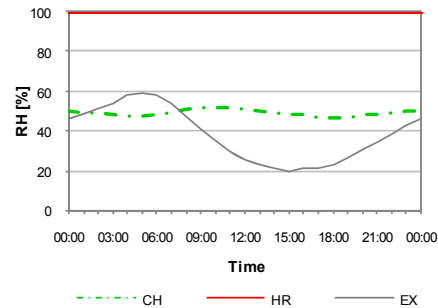


Figure A 54 Relative Humidity RH [%] Ankara male-part May 2007

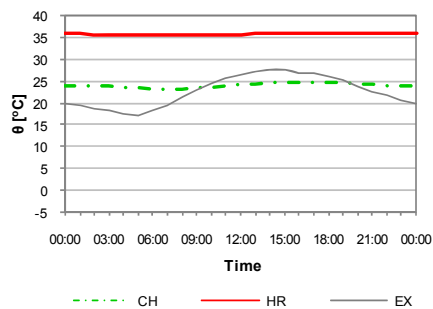


Figure A 55 Temperature θ_{t+e} [°C] Ankara male-part June 2007

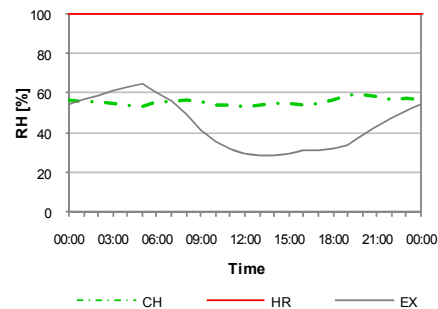


Figure A 56 Relative Humidity RH [%] Ankara male-part June 2007

8.2.3. Fez

8.2.3.1. Hygro-thermal indoor conditions

Hourly values for reference days

Following figures show the hourly temperature and relative humidity values (for the reference months from October 2006 to September 2007) for the female section of the Fez Hammam. Data are given for the entrance area (EN), the changing room (CH), the cold room (CR), the warm room (WR), and the hot room (HR). Note that these figures include also the respective average outside temperature (EX).

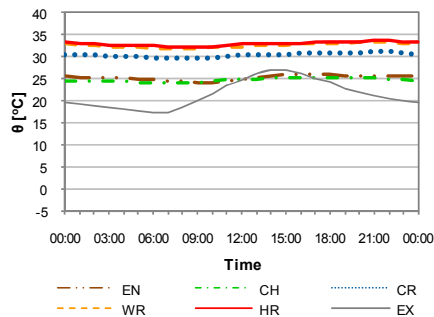


Figure A 57 Temperature θ_{i+e} [°C] Fez female-part October 2006

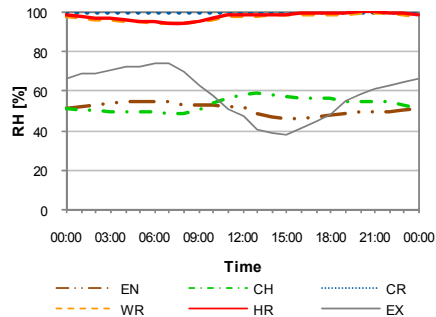


Figure A 58 Relative Humidity RH [%] Fez female-part October 2006

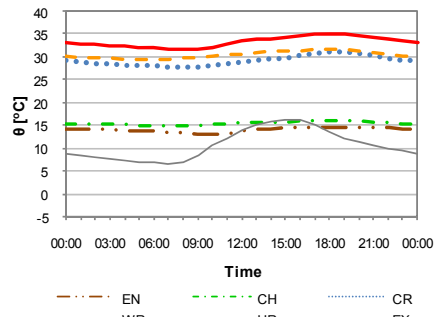


Figure A 59 Temperature θ_{i+e} [°C] Fez female-part December 2006

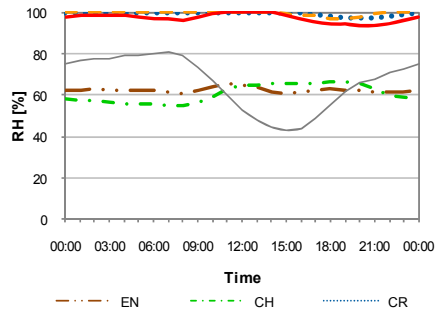


Figure A 60 Relative Humidity RH [%] Fez female-part December 2006

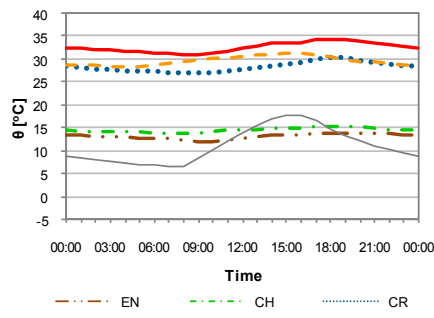


Figure A 61 Temperature θ_{i+e} [°C] Fez female-part January 2007

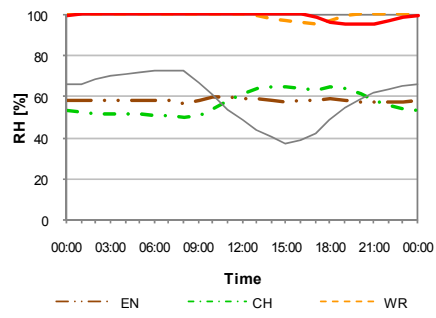


Figure A 62 Relative Humidity RH [%] Fez female-part January 2007

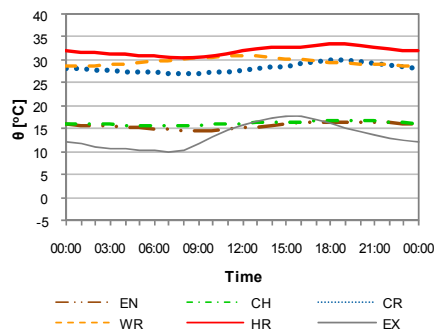


Figure A 63 Temperature θ_{i+e} [°C] Fez female-part February 2007

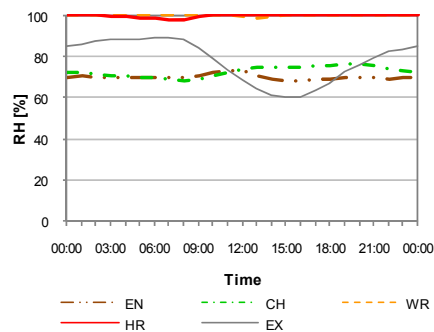


Figure A 64 Relative Humidity RH [%] Fez female-part February 2007

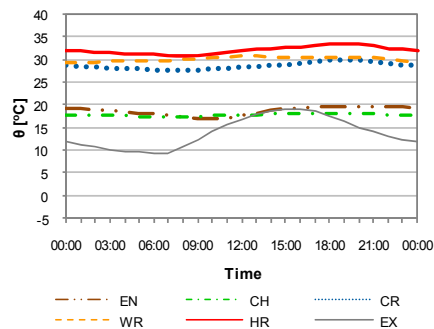


Figure A 65 Temperature θ_{i+e} [°C] Fez female-part March 2007

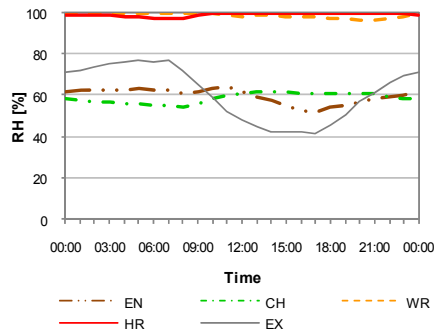


Figure A 66 Relative Humidity RH [%] Fez female-part March 2007

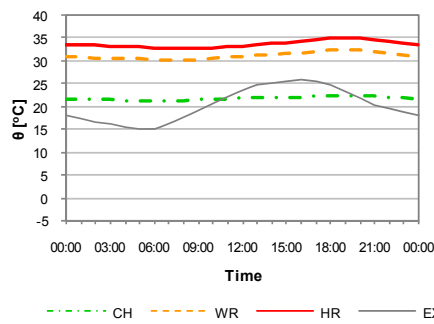


Figure A 67 Temperature θ_{i+e} [°C] Fez female-part May 2007

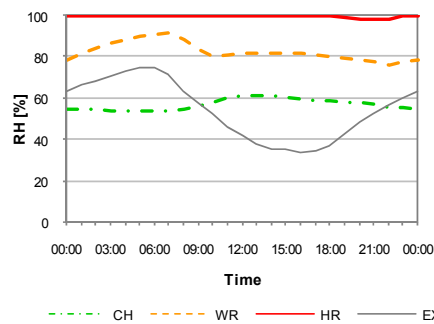


Figure A 68 Relative Humidity RH [%] Fez female-part May 2007

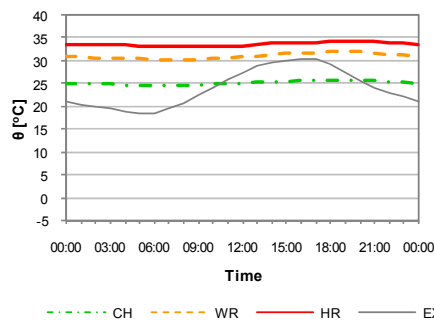


Figure A 69 Temperature θ_{i+e} [°C] Fez female-part June 2007

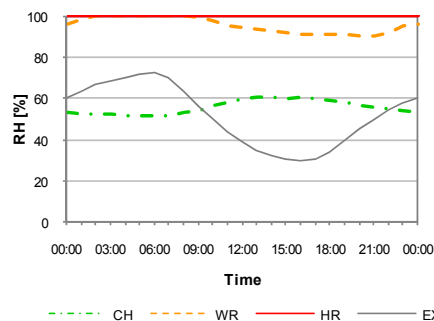


Figure A 70 Relative Humidity RH [%] Fez female-part June 2007

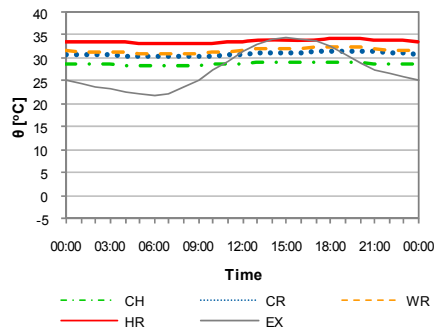


Figure A 71 Temperature θ_{i+e} [°C] Fez female-part August 2007

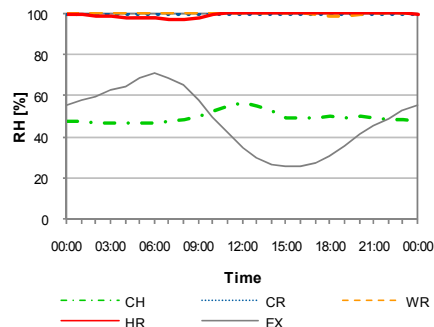


Figure A 72 Relative Humidity RH [%] Fez female-part August 2007

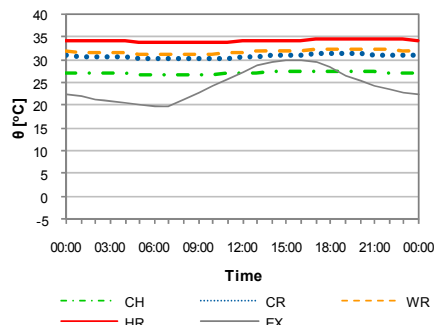


Figure A 73 Temperature θ_{i+e} [°C] Fez female-part September 2007

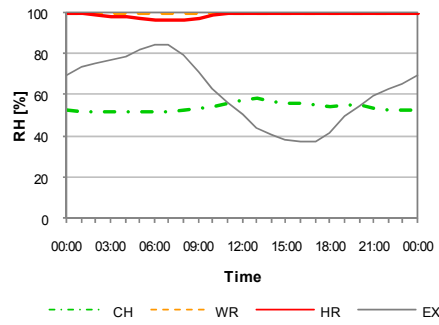


Figure A 74 Relative Humidity RH [%] Fez female-part September 2007

Following figures show the hourly temperature and relative humidity values (for the reference months from October 2006 to September 2007) for the male section of the Fez Hammam. Data are given for the entrance area (EN), the changing room (CH), the cold room (CR), the warm room (WR), and the hot room (HR). Note that these figures include also the respective average outside temperature (EX).

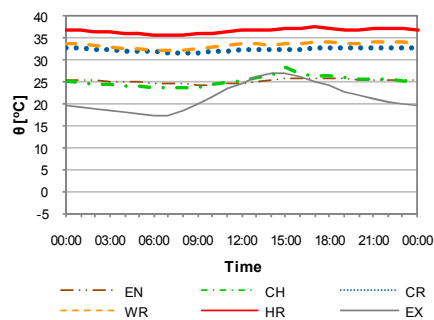


Figure A 75 Temperature θ_{i+e} [°C] Fez male-part October 2006

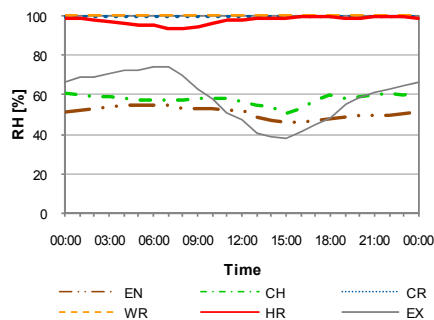


Figure A 76 Relative Humidity RH [%] Fez male-part October 2006

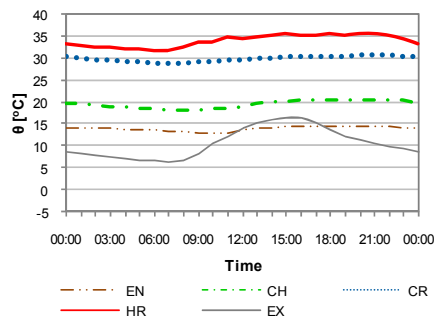


Figure A 77 Temperature θ_{i+e} [°C] Fez male-part December 2006

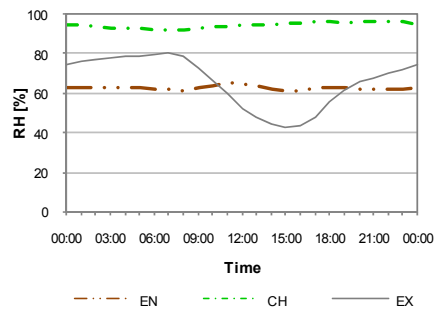


Figure A 78 Relative Humidity RH [%] Fez male-part December 2006

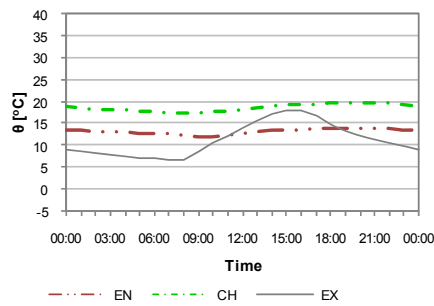


Figure A 79 Temperature θ_{i+e} [°C] Fez male-part January 2007

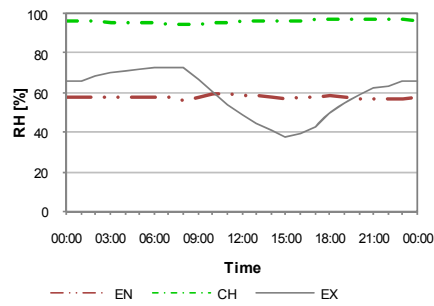


Figure A 80 Relative Humidity RH [%] Fez male-part January 2007

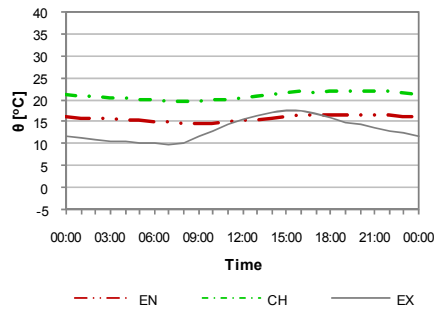


Figure A 81 Temperature θ_{i+e} [°C] Fez male-part February 2007

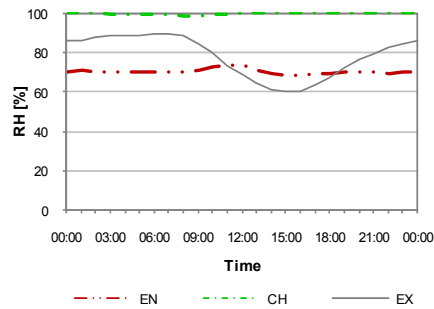


Figure A 82 Relative Humidity RH [%] Fez male-part February 2007

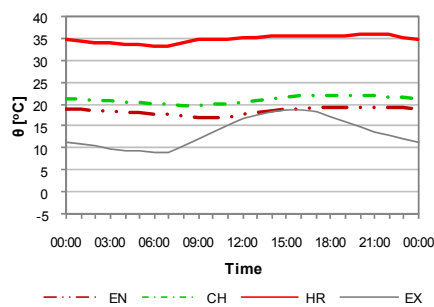


Figure A 83 Temperature θ_{i+e} [°C] Fez male-part March 2007

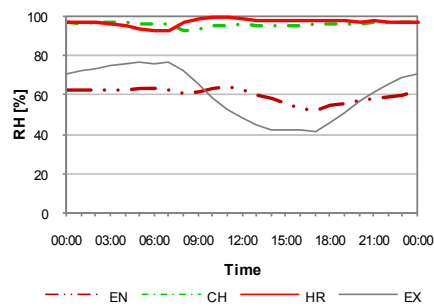


Figure A 84 Relative Humidity RH [%] Fez male-part March 2007

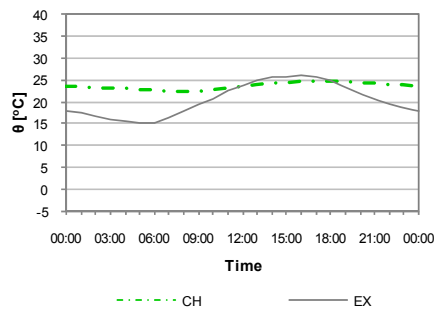


Figure A 85 Temperature θ_{i+e} [°C] Fez male-part May2007

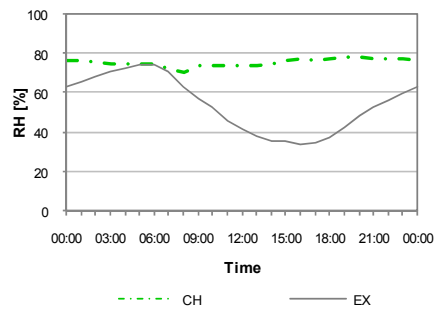


Figure A 86 Relative Humidity RH [%] Fez male-part May 2007

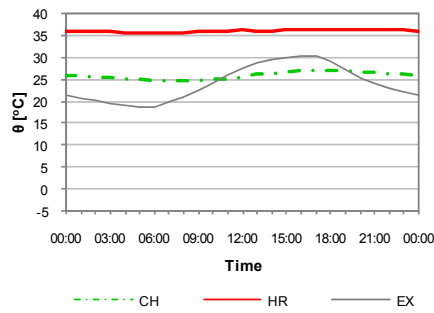


Figure A 87 Temperature θ_{i+e} [°C] Fez male-part June 2007

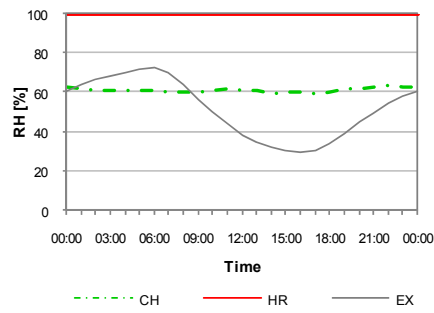


Figure A 88 Relative Humidity RH [%] Fez male-part June 2007

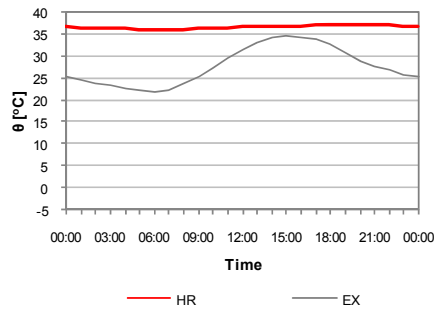


Figure A 89 Temperature θ_{i+e} [°C] Fez male-part August 2007

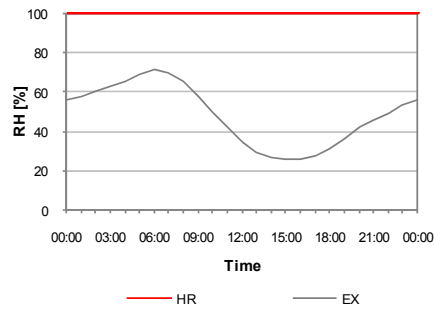


Figure A 90 Relative Humidity RH [%] Fez male-part August 2007

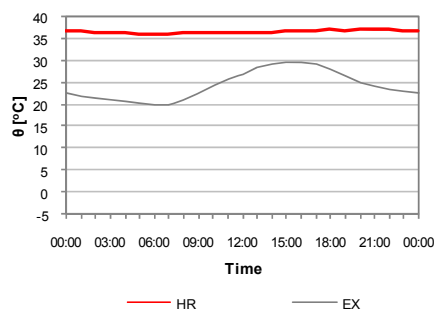


Figure A 91 Temperature θ_{i+e} [°C] Fez male-part September 2007

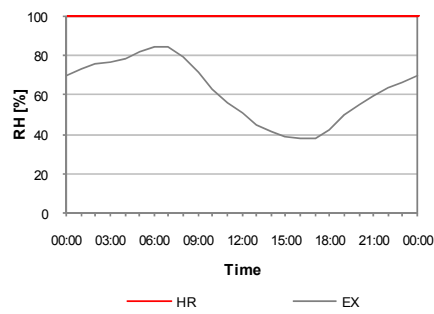


Figure A 92 Relative Humidity RH [%] Fez male-part September 2007

8.2.4. Constantine

8.2.4.1. Hygro-thermal indoor conditions

Hourly values for reference days

Following figures show the hourly temperature and relative humidity values for reference months from July 2007 to June 2008. Data are given for the changing room (CH), the cold room (CR), and the hot room (HR) including the respective outside temperature (EX). Note that the dedicated weather station was installed in January 2008. Previous outside conditions were monitored via a data logger mounted on the roof of the hammam.

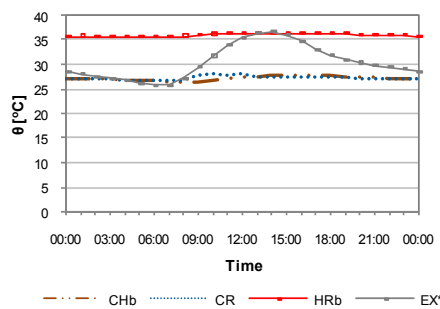


Figure A 93 Temperature θ_{i+e} [°C]
Constantine July 2007

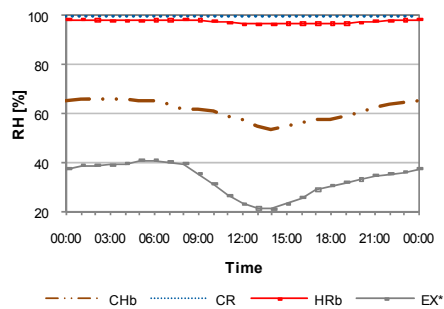


Figure A 94 Relative Humidity RH [%]
Constantine July 2007

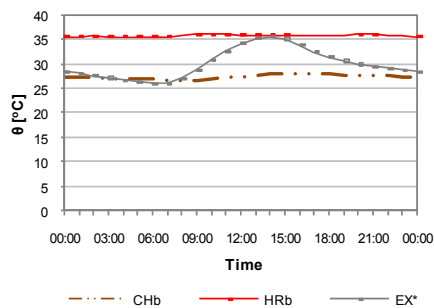


Figure A 95 Temperature θ_{i+e} [°C]
Constantine August 2007

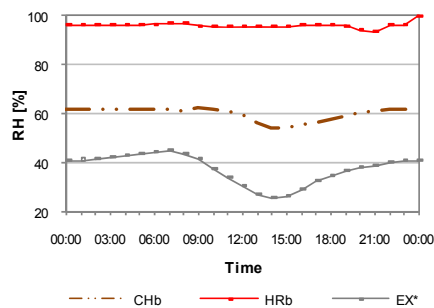


Figure A 96 Relative Humidity RH [%]
Constantine August 2007

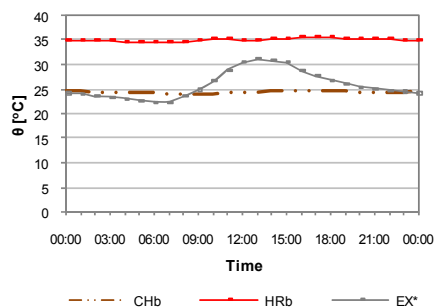


Figure A 97 Temperature θ_{i+e} [°C]
Constantine September 2007

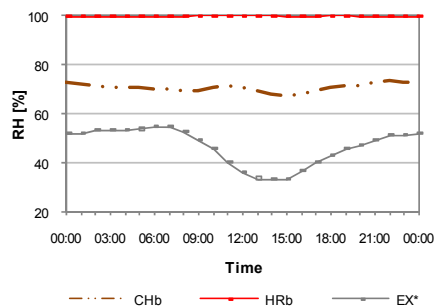


Figure A 98 Relative Humidity RH [%]
Constantine September 2007

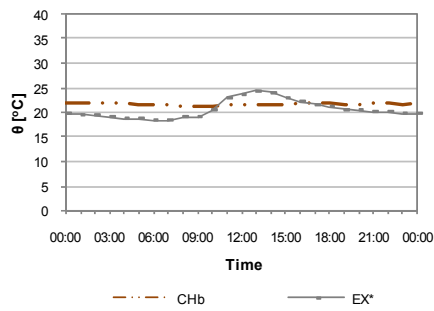


Figure A 99 Temperature $\theta_{it,e}$ [°C]
Constantine October 2007

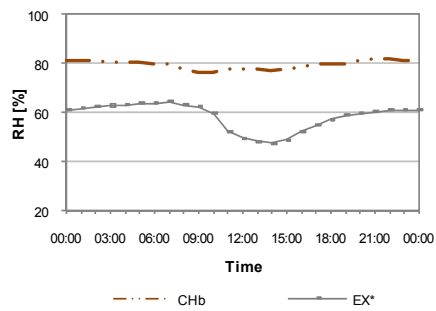


Figure A 100 Relative Humidity RH [%]
Constantine October 2007

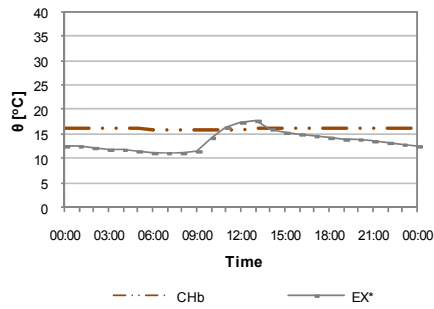


Figure A 101 Temperature $\theta_{it,e}$ [°C]
Constantine November 2007

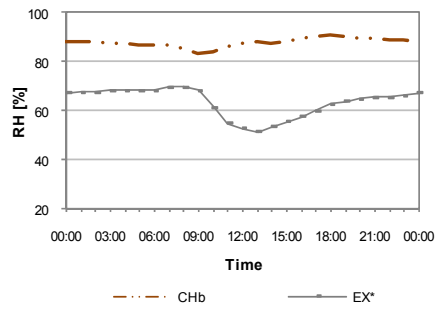


Figure A 102 Relative Humidity RH [%]
Constantine November 2007

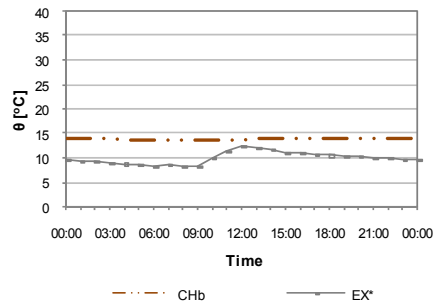


Figure A 103 Temperature $\theta_{it,e}$ [°C]
Constantine December 2007

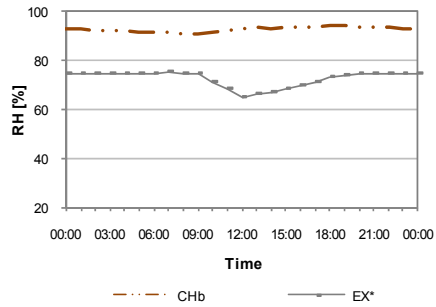


Figure A 104 Relative Humidity RH [%]
Constantine December 2007

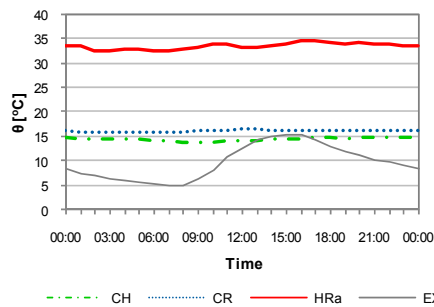


Figure A 105 Temperature $\theta_{it,e}$ [°C]
Constantine February 2008

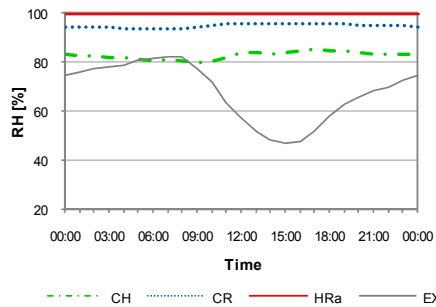


Figure A 106 Relative Humidity RH [%]
Constantine February 2008

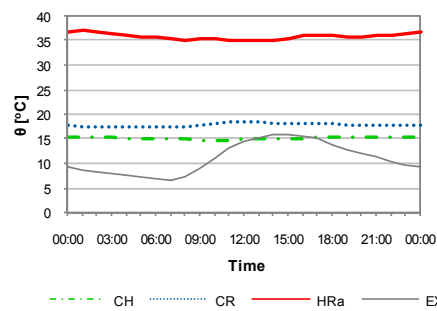


Figure A 107 Temperature θ_{i+e} [°C]
Constantine March 2008

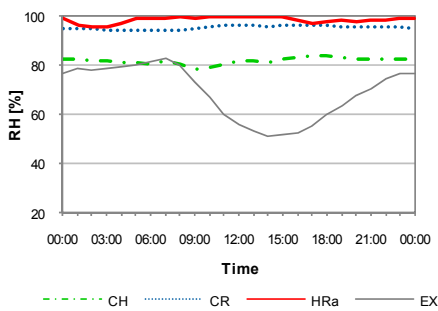


Figure A 108 Relative Humidity RH [%]
Constantine March 2008

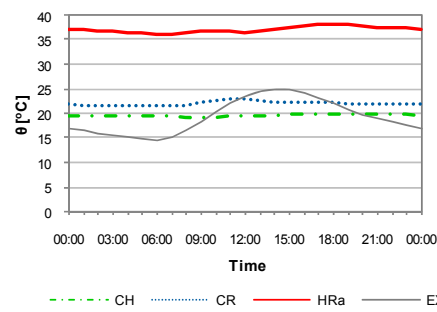


Figure A 109 Temperature θ_{i+e} [°C]
Constantine May 2008

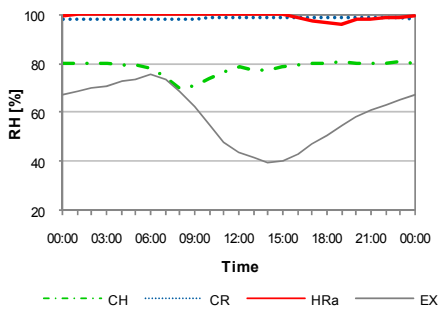


Figure A 110 Relative Humidity RH [%]
Constantine May 2008

CV Kristina Orehounig

Working Experience

- 2007 - University Assistant,
Department of Building Physics and Building Ecology,
Vienna University of Technology, Austria
- 2006 - 2007 Project Assistant,
Department of Building Physics and Building Ecology,
Vienna University of Technology, Austria
- 2004 - Architecture office T. Wagensommerer
Mödling, Austria
- 2002-2006 Student-assistant, Vienna University of Technology

Research area

Building physics, computational building performance simulation,
sustainable architecture

Education

- Since 2006 Doctoral studies,
Vienna University of Technology, Austria
- 2006 MSc. Arch. (Dipl.-Ing.),
Vienna University of Technology, Austria
- 2004 Erasmus
Università degli Studi Roma Tre, Italy
- 2000 A-levels Industrial Engineering,
Technical College Mödling, Austria

Awards, and scholarships

- Wirtschaftskammer (chamber of commerce) Award 2008
- Archdiploma 2007, Vienna University of Technology,
First price in research category
- Scholarship, Vienna University of Technology, 2007
for doctoral studies
- Der österreichische Baupreis 2006
Master thesis category
- Scholarship of the international summer academy Salzburg
2003